



# **UNIVERSIDAD DE INVESTIGACIÓN DE TECNOLOGÍA EXPERIMENTAL YACHAY**

**Escuela de Ciencias Físicas y Nanotecnología**

## **TÍTULO: Temporal Causality in Quantum Teleportation**

Trabajo de integración curricular presentado como  
requisito para la obtención del título de Físico

**Autor:**

Pineda Jimenez Jonnathan Sebastian

**Tutor:**

Dr. Guevara Granizo Marco Vinicio

**Co-Tutor:**

Dr. Svozilík Jiří

Urcuquí, agosto 2022

SECRETARÍA GENERAL  
ESCUELA DE CIENCIAS FÍSICAS Y NANOTECNOLOGÍA  
CARRERA DE FÍSICA  
ACTA DE DEFENSA No. UITEY-PHY-2022-00018-AD

En la ciudad de San Miguel de Urququí, Provincia de Imbabura, a los 24 días del mes de agosto de 2022, a las 09:00 horas, en el Aula S\_CAN de la Universidad de Investigación de Tecnología Experimental Yachay y ante el Tribunal Calificador, integrado por los docentes:

<b>Presidente Tribunal de Defensa</b>	Dra. ROJAS CELY CLARA INES , Ph.D.
<b>Miembro No Tutor</b>	Dr. PINTO ESPARZA, HENRY PAUL , Ph.D.
<b>Tutor</b>	Dr. GUEVARA GRANIZO, MARCO VINICIO , Ph.D.

Se presenta el(la) señor(ita) estudiante PINEDA JIMENEZ, JONNATHAN SEBASTIAN, con cédula de identidad No. 0105715064, de la ESCUELA DE CIENCIAS FÍSICAS Y NANOTECNOLOGÍA, de la Carrera de FÍSICA, aprobada por el Consejo de Educación Superior (CES), mediante Resolución RPC-SO-39-No.456-2014, con el objeto de rendir la sustentación de su trabajo de titulación denominado: **Temporal Causality in Quantum Teleportation**, previa a la obtención del título de FÍSICO/A.

El citado trabajo de titulación, fue debidamente aprobado por el(los) docente(s):

**Tutor** Dr. GUEVARA GRANIZO, MARCO VINICIO , Ph.D.

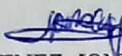
Y recibió las observaciones de los otros miembros del Tribunal Calificador, las mismas que han sido incorporadas por el(la) estudiante.

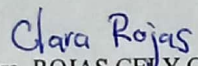
Previamente cumplidos los requisitos legales y reglamentarios, el trabajo de titulación fue sustentado por el(la) estudiante y examinado por los miembros del Tribunal Calificador. Escuchada la sustentación del trabajo de titulación, que integró la exposición de el(la) estudiante sobre el contenido de la misma y las preguntas formuladas por los miembros del Tribunal, se califica la sustentación del trabajo de titulación con las siguientes calificaciones:

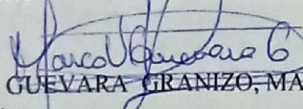
Tipo	Docente	Calificación
Tutor	Dr. GUEVARA GRANIZO, MARCO VINICIO , Ph.D.	10,0
Miembro Tribunal De Defensa	Dr. PINTO ESPARZA, HENRY PAUL , Ph.D.	9,8
Presidente Tribunal De Defensa	Dra. ROJAS CELY CLARA INES , Ph.D.	10,0

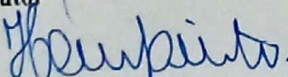
Lo que da un promedio de: **9.9 (Nueve punto Nueve)**, sobre 10 (diez), equivalente a: **APROBADO**

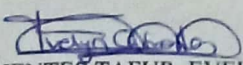
Para constancia de lo actuado, firman los miembros del Tribunal Calificador, el/la estudiante y el/la secretario ad-hoc.

  
PINEDA JIMENEZ, JONNATHAN SEBASTIAN  
Estudiante

  
Dra. ROJAS CELY CLARA INES , Ph.D.  
Presidente Tribunal de Defensa

  
Dr. GUEVARA GRANIZO, MARCO VINICIO , Ph.D.  
Tutor

  
Dr. PINTO ESPARZA, HENRY PAUL , Ph.D.  
Miembro No Tutor

  
CIFUENTES TAFUR, EVELYN CAROLINA  
Secretario Ad-hoc

## AUTORÍA

Yo, **Jonnathan Sebastian Pineda Jimenez**, con cédula de identidad 0105715064, declaro que las ideas, juicios, valoraciones, interpretaciones, consultas bibliográficas, definiciones y conceptualizaciones expuestas en el presente trabajo; así cómo, los procedimientos y herramientas utilizadas en la investigación, son de absoluta responsabilidad de el/la autora (a) del trabajo de integración curricular. Así mismo, me acojo a los reglamentos internos de la Universidad de Investigación de Tecnología Experimental Yachay.

Urcuquí, agosto 2022.



---

Jonnathan Sebastian Pineda Jimenez  
CI: 0105715064

## AUTORIZACIÓN DE PUBLICACIÓN

Yo, **Jonnathan Sebastian Pineda Jimenez**, con cédula de identidad 0105715064, cedo a la Universidad de Investigación de Tecnología Experimental Yachay, los derechos de publicación de la presente obra, sin que deba haber un reconocimiento económico por este concepto. Declaro además que el texto del presente trabajo de titulación no podrá ser cedido a ninguna empresa editorial para su publicación u otros fines, sin contar previamente con la autorización escrita de la Universidad.

Asimismo, autorizo a la Universidad que realice la digitalización y publicación de este trabajo de integración curricular en el repositorio virtual, de conformidad a lo dispuesto en el Art. 144 de la Ley Orgánica de Educación Superior

Urcuquí, agosto 2022.



---

Jonnathan Sebastian Pineda Jimenez  
CI: 0105715064

## **Dedicatoria**

*Para mi abuelo Victor Manuel Pineda Ochoa con polvos de Soto y de Solano.*

*Jonnathan Sebastian Pineda Jimenez*

## Agradecimiento

To start, I would like to thank my whole family for their support along my development since a child. Special thanks to my mother Lilia Jimenez, my father Wilson Pineda, my brother Andres Pineda, my sister Karen Pineda, my niece Amelia Pineda, and my grandfather Victor Pineda, who as co-authors have accompanied me to write each line of my life book. Thank you very much to my family for being my support under all this dream, all the achievements in my life are and will be yours. // *Para comenzar, me gustaría agradecer a toda mi familia por su apoyo a lo largo de mi desarrollo desde que soy un niño. Un agradecimiento especial a mi madre Lilia Jimenez, a mi padre Wilson Pineda, a mi hermano Andres Pineda, a mi hermana Karen Pineda, a mi sobrina Amelia Pineda y a mi abuelo Víctor Pineda, quienes como co autores me han acompañado a escribir cada línea del libro de mi vida. Muchas gracias familia por darme su apoyo en este sueño, todo aquello que alcance en esta vida es y será para ustedes.*

To continue, I want to say thanks to my advisor Jiří Svozilík Ph.D, to whom I am deeply indebted for all his support during my research learning, and for not abandoning me and this research thesis even in front of unfair circumstances. You have taught me what light is, and I assure you that it will always shine for you. Thanks for sharing with me your vision of science and life. // *Luego, quiero agradecer a mi tutor Jiří Svozilík Ph.D, con quien estoy profundamente en deuda por todo su apoyo durante mi aprendizaje de investigación, y por no abandonarme a mí y a esta tesis de investigación incluso en frente de circunstancias injustas. Me has enseñado lo que es la luz, y estoy seguro de que ella siempre brillará para ti. Muchas gracias por compartir conmigo tu visión de la ciencia y de la vida.*

To conclude, I would like to say thanks to all my YT friends, especially Alex, Jereme, Andre, Emil, Marlon, Xavier, Mishel, Cynthia and Andy for sharing with me such a huge moment of our lives. Also, a special thank to Maria Lorena for all her support in my life and as a math consultant. Finally, thank to all the people whom I interacted in YT, specially to my professors, that have provided my enough potential energy to conclude this life stage. A quick final recognition to the IBM Corporation for their opened contribution, breaking barriers in a quantum research. Additionally, thanks to arXiv. // *Para concluir, me gustaría agradecer a mis compañeros de YT, especialmente a Alex, Jean, Jereme, Andre, Emil, Marlon, Xavier, Mishel y Andy por compartir conmigo este momento tan grande en nuestras vidas. También, un agradecimiento especial a Maria Lorena por su apoyo en la vida y como consultora matemática. Para terminar, me gustaría agradecer a toda la gente con la que interactúe en YT, especialmente a mis profesores, que me han dado la energía potencial suficiente para concluir esta etapa de la vida. Un rápido reconocimiento a IBM Corporation por su abierta contribución para la investigación cuántica. Adicionalmente, gracias a arXiv.*

*Jonnathan Sebastian Pineda Jimenez*

## Resumen

Con el objetivo de estudiar los efectos temporales de fuentes que producen ruido sobre la fidelidad promedio relacionada con diferentes protocolos de teletransportación, nosotros hemos preparado dos escenarios. El primero, la teletransportación cuántica estándar (SQT) y la teletransportación cuántica controlada (CQT). Los correspondientes circuitos cuánticos que definen cada uno de estos protocolos son construidos y todas las compuertas cuánticas necesarias para transmitir el estado inicial son evaluadas. Haciendo uso de operaciones controladas, nosotros creamos entrelazamiento entre el qubit controlador y qubits auxiliares, así implementando una fuente que produce ruido. Nosotros insertamos este nuevo miembro en todos los diferentes qubits que son parte de los protocolos de teletransportación, en las diferentes etapas de los mismos, calculando la fidelidad cuántica de teletransportación al final. Esto es lo que define la causalidad temporal, dado que nosotros estudiamos como la posición temporal del ruido insertado con respecto a todas las otras operaciones cuánticas afecta el rendimiento de dichos protocolos. Inicialmente, nosotros enfocamos nuestro estudio en simulaciones cuánticas utilizando el paquete de python QISKIT, y con la finalidad de testear nuestros modelos teóricos, ejecutamos nuestros circuitos en computadoras cuánticas de acceso público de la empresa IBM. Finalmente, para probar esta ventaja cuántica, debida a la presencia del entrelazamiento cuántico, nosotros producimos correcciones que mejoran los cálculos que provienen de estos sistemas reales, usando el procedimiento de mitigación de errores de medición, que demuestra tener una alta relevancia al procesar esta información experimental.

### Palabras Clave:

Teletransportación cuántica, computadoras cuánticas, simuladores cuánticos, entrelazamiento cuántico, fidelidad de estados.

## **Abstract**

In order to study the temporal effects of noisy sources on the average fidelity in the protocols of quantum teleportation, we prepare two scenarios. The Standard Quantum Teleportation (SQT) and the Controlled quantum teleportation (CQT). Corresponding quantum circuits defining each protocol are constructed and all necessary stages, in order to transmit initial quantum state, are evaluated. By making use of controlled operations, we create entanglement between the target qubit and auxiliary qubit within a noisy source. We insert this additional party into all different qubit members of the teleportation protocols in different stages of the protocol, computing the teleportation fidelity at the end. This is what defines Temporal Causality as we are studying how the temporal position of inserted noise with respect to all other quantum operations affects the overall performance of examined protocols. Initially, we focus our study on quantum simulations by using the QISKIT python package, and then we test our protocols by running them on the IBM's public quantum computers to compare our theoretical models. Finally, in order to probe quantum advantage due to the presence of entanglement, we produce corrections to improve the calculations coming from real devices by using the Measurement Error Mitigation (MEM). With this process, we demonstrate the high importance of post-correction of processed experimental data.

### **Key Words:**

Quantum teleportation, quantum computers, simulators, entanglement, fidelity of states.

# Contents

<b>List of Figures</b>	<b>xiv</b>
<b>List of Tables</b>	<b>xvii</b>
<b>1 Introduction</b>	<b>1</b>
1.1 Problem Statement . . . . .	2
1.2 General and Specific Objectives . . . . .	2
1.3 Overview . . . . .	2
<b>2 Theoretical Background</b>	<b>3</b>
2.1 Fundamentals of Quantum Information . . . . .	3
2.1.1 Principle of Superposition and Quantum Bits . . . . .	3
2.1.2 Quantum Entanglement . . . . .	6
2.1.3 Computational Models . . . . .	8
2.1.4 Quantum Processors: physical implementation . . . . .	12
2.2 Standard Quantum Teleportation . . . . .	23
2.3 Controlled Quantum Teleportation . . . . .	25
2.4 Fidelity of States - Quantifier of Efficiency and its Bounds for Quantum Teleportation . . . . .	27
2.5 Causality Problem . . . . .	30
2.6 Problem Statement . . . . .	33
<b>3 Methodology</b>	<b>35</b>
3.1 Standard Quantum Teleportation . . . . .	35
3.2 Controlled Quantum Teleportation . . . . .	44
3.3 Quantum State Tomography . . . . .	49
3.4 Calibration . . . . .	51
<b>4 Results &amp; Discussion</b>	<b>55</b>
4.1 Standard Quantum Teleportation . . . . .	55
4.1.1 Simulated Implementation - Qiskit Simulators . . . . .	55
4.1.2 Experimental Implementation - IBM's Quantum Devices. . . . .	57
4.2 Controlled Quantum Teleportation . . . . .	62
4.2.1 Simulated Implementation - Qiskit Simulators . . . . .	62
4.2.2 Experimental Implementation - IBM's Quantum Devices . . . . .	68

<b>5 Conclusions &amp; Outlook</b>	<b>71</b>
<b>Bibliography</b>	<b>73</b>
<b>Abbreviations</b>	<b>75</b>

# List of Figures

2.1	Bloch Sphere Representation. . . . .	5
2.2	Turing Machine scheme. . . . .	9
2.3	Digital logical gate. . . . .	9
2.4	Digital NOT gate representation. . . . .	10
2.5	Quantum measurement circuit. . . . .	11
2.6	Discrete quantum Fourier transform circuit on three qubits. . . . .	11
2.7	Quantum gates representation. . . . .	11
2.8	Xanadu’s physical implementation of photonic quantum processor. . . . .	14
2.9	Optical cavity QED scheme of implementations. . . . .	15
2.10	Ion trap implemented by NIST. . . . .	16
2.11	NMR bases quantum computer. . . . .	17
2.12	Energy levels of harmonic oscillator. . . . .	18
2.13	Potential and wavefunctions of Charge qubits - basis states. . . . .	18
2.14	Charge qubit circuit. . . . .	19
2.15	Potential and wavefunctions of flux qubits - basis states. . . . .	19
2.16	Flux qubit circuit. . . . .	19
2.17	Potential and wavefunction of phase qubits - basis states. . . . .	20
2.18	Phase qubits circuit. . . . .	20
2.19	QHO vs Anharmonic energy levels. . . . .	20
2.20	Transmon qubit circuit and physical implementation scheme. . . . .	21
2.21	Energy levels of a transmon qubits. . . . .	22
2.22	IBM’s quantum processor. . . . .	22
2.23	IBM’s quantum computer chip. . . . .	23
2.24	SQT scheme representation. . . . .	23
3.1	Initial circuit with quantum and classical registers. Classical registers are used to store the results of BSM. . . . .	36
3.2	First step of SQT. . . . .	36
3.3	Second step of SQT. . . . .	37
3.4	Third step of SQT. . . . .	37
3.5	SQT circuit with deferred measurement applied. . . . .	38
3.6	Fiducial state representation using Bloch spheres. . . . .	38
3.7	First step of SQT representation using Bloch spheres. . . . .	39
3.8	Second step of SQT representation using Bloch spheres. $\hat{C}\hat{X}$ operation. . . . .	39

3.9	Second step of SQT representation using Bloch spheres. $\hat{H}$ operation. . . . .	39
3.10	Third step of SQT representation using Bloch spheres. $\hat{H}$ operation. . . . .	39
3.11	Final step of SQT representation using Bloch spheres. $\hat{H}$ gate operation. . . . .	40
3.12	Evolution of single state under $\hat{R}_x$ gate. . . . .	41
3.13	Noise action on first party after first step of SQT. . . . .	41
3.14	Noise action on first party after second step of SQT. . . . .	42
3.15	Noise action on second party after first step of SQT. . . . .	42
3.16	Noise action on second party after second step of SQT. . . . .	43
3.17	Noise action on third party after first step of SQT. . . . .	43
3.18	Noise action on third party after second step of SQT. . . . .	44
3.19	First step of CQT. . . . .	45
3.20	Second step of CQT. . . . .	45
3.21	Non-conditioned teleportation circuit. . . . .	46
3.22	Conditioned Controlled teleportation circuit. . . . .	47
3.23	CQT with the deferred measurements applied on it. . . . .	47
3.24	Noise action on first party after first step of CQT. . . . .	48
3.25	Noise action on second party after second step of CQT. . . . .	48
3.26	Noise action on third party after second step of CQT. . . . .	49
3.27	Noise action on fourth party after the third step of CQT. . . . .	49
3.28	Density matrix plot (real and imaginary parts) of the $ +\rangle$ state. . . . .	50
3.29	Circuit calibration of the $\hat{H}$ gate, using $ 0\rangle$ state. . . . .	53
3.30	Circuit calibration of the $\hat{H}$ gate, using $ 1\rangle$ state. . . . .	53
3.31	Calibration matrix of a single qubit. . . . .	53
3.32	Calibration circuit of the SQT circuit gates. . . . .	54
4.1	Average fidelity of SQT dependence on the number of shots. . . . .	55
4.2	Average fidelity dependence on temporal causality of noisy affection on Alice parties, SQT. . . . .	56
4.3	Average fidelity dependence on temporal causality of noisy affection on Bob party, SQT. . . . .	57
4.4	Average fidelity behavior on temporal causality of complete noisy affection on Alice parties. . . . .	57
4.5	Calibration matrix of a five qubits processor. . . . .	58
4.6	Experimental temporal causality behavior of SQT on first party after first step. . . . .	59
4.7	Experimental temporal causality behavior of SQT on first party after second step. . . . .	59
4.8	Experimental temporal causality behavior of SQT on second party after first step. . . . .	60
4.9	Experimental temporal causality behavior of SQT on second party after second step. . . . .	60
4.10	Experimental temporal causality behavior of SQT on third party after first step. . . . .	61
4.11	Experimental temporal causality behavior of SQT on third party after second step. . . . .	61
4.12	Ibmq_quito device's architecture. . . . .	62
4.13	Average fidelity of CQT dependence on the number of shots. . . . .	63
4.14	Conditioned average fidelity behavior of $U(\theta,\phi)$ . . . . .	63
4.15	Conditioned average fidelity behavior of $U(\theta,\lambda)$ . . . . .	64
4.16	Conditioned average fidelity behavior of $U(\phi,\lambda)$ . . . . .	64
4.17	Conditioned average fidelity behavior of $U(\theta,\phi)$ . . . . .	65
4.18	Conditioned average fidelity behavior of $U(\theta,\lambda)$ . . . . .	65

4.19 Conditioned average fidelity behavior of  $(\phi, \lambda)$ . . . . . 66

4.20 Overlap between the regions where the control power works with  $U(\phi, \lambda)$ . . . . . 66

4.21 Average fidelity dependence on temporal causality of noisy affection on *Alice*<sub>0</sub> party, CQT. . . . . 67

4.22 Average fidelity dependence on temporal causality of noisy affection on *Alice*<sub>1</sub> and *Bob*<sub>0</sub> parties, separately, CQT. . . . . 67

4.23 Average fidelity dependence on temporal causality of noisy affection on *Charlie*<sub>0</sub> party, CQT. . . . . 68

4.24 Experimental temporal causality behavior of CQT on first party after first step. . . . . 68

4.25 Experimental temporal causality behavior of CQT on second party after second step. . . . . 69

4.26 Experimental temporal causality behavior of CQT on third and fourth parties after third step. . . . . 69

4.27 Ibmq\_manilla device’s architecture. . . . . 70



# List of Tables

- 2.1 Coherence times (T1-T2) and its respective number of operations, for different physical realizations.  
Adapted from<sup>1</sup>. . . . . 13
- 2.2 Recovery Operations dependence on the BM for SQT. . . . . 25
- 2.3 Recovery Operations dependence on the BM for CQT using GHZ entangled state. . . . . 27
  
- 4.1 Coherence times (T1-T2) of ibmq\_quito quantum processor provided by Quantum Experience platform. 62
- 4.2 Coherence times (T1-T2) of ibmq\_manilla quantum processor provided by Quantum Experience platform. 70



# Chapter 1

## Introduction

Information processing in general posses a big range of branches, it appears from daily tasks, as cryptography and communications, to the theoretical study of the information kept by a Black Hole. On the other hand, the birth of quantum mechanics has intrigued generations of scientists, who have tried to search its analog in any area of the science. These two areas mixed have created what nowadays we know as "Quantum Information theory"<sup>1</sup>.

Moreover, quantum information theory has became necessary as an alternative theory to classical information theory, given that the classical computers posses a limitation in its architecture in order to achieve larger amounts of storage of information, but mainly because in the classical information theory there are some kind of problems, that by classical methods, the needed time to achieve a solution of them could become exponential, becoming the computation very inefficient.

It turns out that a quantum system could be the solution to some of these problems, and this is the main motivation to build quantum processors, which are the main motivation for studying Quantum Computing. Due to the quantum behavior that some systems exhibit, the computation of the information can be done in parallel, it means that we could work more than one problem at once, decreasing the computational time and perhaps the physical resources.

Luckily or unluckily for physicists and quantum engineers, quantum computers are very hard to be built, the main reason of this is the sensitivity of the quantum systems to the interactions with any other system, usually called, environment or noise. These interactions can produce variations in the information that the systems posses, so the final result of the computation could be incorrect, depending on how much the environment has affected the whole system.

Regarding information processing, quantum teleportation is one of the most striking applications of quantum information theory. It combines counter intuitive properties that the quantum description of nature presents. For example, the usage of the superposition principle of quantum states, which roughly states that an object does not posses a unique and defined description. This superposition of states is the main source for having entanglement between parties, which is connection that two or more systems keep after a interaction, without any kind of physical process. Entanglement is then used to implement successful protocols of quantum teleportation in order to transfer information.

The main idea of a protocol of quantum teleportation is the transference of an unknown quantum state<sup>2</sup>, from a sending station, commonly called Alice, to a receiving station, commonly called Bob, without revealing the state that is being teleported. The state is not revealed due to quantum mechanical properties which states that a quantum states cannot be directly observed without breaking its configuration.

On the other hand, in this quantum era, where every possible quantum advantage is being exploited and explored, the quantum computers provide a chance to experiment directly with protocols of teleportation. This is because each single unit of a quantum computer fit in the description of the mathematical formalism of quantum teleportation.

As quantum teleportation can be tested in quantum processors, noise affection is always present given extra sources or even systematic errors, which will alter the state of the teleportation. In this sense, temporal causality is developed in order to give a chance to the characterization of the noise<sup>3</sup>.

In this thesis, a beautiful combination between the theoretical behavior of quantum teleportation, quantum systems simulation, and an experimental testing using quantum processors is performed, trying to contrast the mathematical formalism treatment and the physical implementation of quantum teleportation protocols.

## **1.1 Problem Statement**

Quantum Teleportation has been studied in many different situations, and its behavior is very attractive in any application of information processing as quantum internet, quantum communication, and, even in quantum cryptography. In spite of the this fact, the randomness of the noisy sources is something that does not allow a perfect performance of the teleportation. It has resulted very complicated to create a quantum systems that could be perfectly isolated or that could be resistant to any source of noise. In this way, it is of full relevance to understand theoretically how the information is affected by the affection of known noise. Consequently, this theoretical knowledge gives way to experimental tests in order to prove with certainty the theoretical model.

## **1.2 General and Specific Objectives**

The main objective of this research thesis is to explore how the environment or noise can affect the output information of the selected protocols of teleportation, when a known source of noise is inserted after each step of the protocol of teleportation.

## **1.3 Overview**

This thesis is organized as follows: The chapter 2, called Theoretical Background, posses the definition of the necessary mathematical formalism to understand main elements that describe quantum computers, the protocols of the teleportation that we will test, and the temporal causality formalism. Additionally, a brief review of computational models and some physical implementations of quantum processors. In chapter 3, we develop the methodology we are going to approach to study the noise affection in protocols of teleportation, plus a brief explanation of how to reconstruct information by quantum state tomography and how to calibrate a quantum device. In chapter 4, named Results and Discussion, we present the results of the methodology section, of both simulations and experimental tests. Finally, in chapter 5, we discuss the results of the chapter 4, and provide the outlook of quantum computation and teleportation from our point of view.

# Chapter 2

## Theoretical Background

### 2.1 Fundamentals of Quantum Information

#### 2.1.1 Principle of Superposition and Quantum Bits

In order to be able to describe correctly the superposition principle of states, which actually will allow us to describe our qubit states, first we need to set the mathematical formalism which describes the quantum mechanical behavior of a discrete variables system, as it is going to be used for our purpose, and the same that is based mainly in elementary linear algebra.

According to the postulates of quantum mechanics, we need to know where our mathematical objects belong, for that purpose, we need to define our space and, the basis that expands it and its properties. Each quantum state, with the same properties of a physical system, is a unit vector in a finite Hilbert space ( $\mathcal{H}$ ), that is defined as an inner product, complete and complex vector space, where the inner product  $(\cdot, \cdot)$  satisfies these three requirements: linearity, the symmetric property and the positive definite property.

For our purpose, the state of each party will be an element of a 2 dimensional Hilbert space. Here the set of linearly independent vectors that form a basis for the space, using Dirac notation, are  $\{|n\rangle\}_{n \in \{0,1\}}$ , where each vector  $|n\rangle$ , commonly known as the computational bases, has components as shown in (2.1).

$$|0\rangle = \begin{bmatrix} 1 \\ 0 \end{bmatrix} \quad ; \quad |1\rangle = \begin{bmatrix} 0 \\ 1 \end{bmatrix}. \quad (2.1)$$

The orthogonality relation between these states can be expressed by the Kronecker delta, which is defined as:

$$\delta_{mn} = \begin{cases} 1, & m \neq n \\ 0, & m = n \end{cases}. \quad (2.2)$$

Additionally, these states are supposed to be normal to satisfy normalization condition,  $\| |n\rangle \| = \sqrt{\langle n|n \rangle} = 1$ , where  $\langle n|m \rangle = \delta_{nm}$ , and it is showed by the inner product, for example:

$$\langle 0|, |0 \rangle \rangle = \langle 0|0 \rangle = 1 \quad ; \quad \langle 0|, |1 \rangle \rangle = \langle 0|1 \rangle = 0 \quad ; \quad \langle 1|, |0 \rangle \rangle = \langle 1|0 \rangle = 0 \quad ; \quad \langle 1|, |1 \rangle \rangle = \langle 1|1 \rangle = 1. \quad (2.3)$$

In this way, any vector on the  $\mathbb{C}^2$  space can be written as a linear combination of these two vectors in the following way:

$$|\psi\rangle = \sum_{n=0}^{n=1} \alpha_n |n\rangle, \quad (2.4)$$

where  $\alpha_n$  are complex numbers, and each state needs to be normalized by  $|\psi\rangle/\|\psi\rangle\|$ . It can be seen that:

$$\|\psi\rangle\|^2 = \langle\psi|\psi\rangle = \alpha_0^* \alpha_0 + \alpha_1^* \alpha_1 = |\alpha_0|^2 + |\alpha_1|^2 = 1. \quad (2.5)$$

**Qubits:** Equations (2.4) and (2.5) are what we have been waiting for the description of a qubit, abbreviation of quantum bit, making an analogous comparison of a classical bit or just bit to the information unit of the quantum regime.

Therefore, a qubit state is a quantum state in superposition, or linear combination of two quantum bases, commonly referred to as two level states. Here these bases are commonly implemented by, for example, the polarization of a photon, or  $\frac{1}{2}$ -spin particles such as electrons. As we are dealing with quantum vectors or states, their superposition coefficients need to fit the requirements of equation (2.5) in order to be a probability distribution. What we then get is the probability  $|\alpha_n|^2$  of observing the state  $|n\rangle$  as outcome of a quantum measurement. So, in other words, it is said that before the qubit is observed, measured or collapsed, it is in a superposition of basis states. By applying some projective measurement the state collapses to the most probable state, according to its probability distribution. According to the *second postulate of quantum mechanics*, the evolution of a closed quantum system is going to be managed by an Unitary operation  $\hat{U}$  defined on the vectorial domain and codomain of the the Hilbert space, as a linear map from  $\mathcal{H}$  to itself, as  $\hat{U} : \mathcal{H} \rightarrow \mathcal{H}$ . This means that the resulting state is still an element of the same space. The  $\hat{U}$  operator obeys the condition of linearity if it can be linearly distributed to its inputs, by:  $\hat{U}(\alpha|\psi\rangle + \beta|\phi\rangle) = \alpha\hat{U}|\psi\rangle + \beta\hat{U}|\phi\rangle$ , where  $\alpha, \beta \in \mathbb{C}$ , and  $|\psi\rangle, |\phi\rangle \in \mathcal{H}$ .

In order to introduce the unitary condition, let's check briefly Hermitian operators, commonly used by physicist, defined on finite dimensional vector spaces or self adjoint operators on infinite dimensional vector spaces. Given the existence of a linear map  $\hat{U}$  on the Hilbert space, there exists a unique linear map  $\hat{U}^\dagger$  defined on  $\mathcal{H}$ , which satisfies that:

$$\forall |\psi\rangle, |\phi\rangle \in \mathcal{H} : \langle\psi|\hat{U}|\phi\rangle = \langle\hat{U}^\dagger|\psi\rangle, |\phi\rangle, \quad (2.6)$$

which indeed keeps the linearity of the inner product in second argument. If we notice, the relation of  $(\hat{U}^\dagger)^\dagger = \hat{U}$ , and we say that  $\hat{U}^\dagger$  is the Hermitian conjugate operator of  $\hat{U}$ , where the dagger operation is the transpose conjugate operation. If the operator satisfy that  $\hat{U}^\dagger = \hat{U}$ , then we say that  $\hat{U}$  is a hermitian operator. Also, we can say that  $\hat{U}$  is a normal operator if  $\hat{U}\hat{U}^\dagger = \hat{U}^\dagger\hat{U}$ . Finally, we say that a  $\hat{U}$  operator is unitary if  $\hat{U}^\dagger\hat{U} = \hat{U}\hat{U}^\dagger = \hat{I}$ , being also normal. The unitary condition of the operators becomes important when we try to conserve the normalization conditions of the quantum states, given that unitary operators preserve inner products between two vectors, as it can be seen using the same properties of inner product, as:

$$\langle\hat{U}|\psi\rangle, \hat{U}|\phi\rangle\rangle = \langle\psi|\hat{U}^\dagger\hat{U}|\phi\rangle = \langle\psi|\hat{I}|\phi\rangle = \langle\psi|\phi\rangle = \langle|\psi\rangle, |\phi\rangle\rangle. \quad (2.7)$$

**Quantum Gates:** Given that we have defined already the properties of the operators acting on the vectors defined in our Hilbert space, then, we can talk about quantum gates for single qubit states, which actually can be seen as  $2 \times 2$  matrices.

The most common quantum gates are the Pauli operators or Pauli Gates, which are indeed, unitary operators. It is useful to think about the unitary property that they posses in that if we apply once the gate on a quantum state, and then we apply its hermitian operator, we leave the state invariant under that kind of transformation.

We can see the matrix representation of some of the most used gates in equation 2.8. Their implementation on quantum computers is very important, and we can get a universal set of gates, which will help us to produce any kind of evolution to our single quantum states.

The Pauli operators are in quantum information denoted as  $\{\hat{X}, \hat{Y}, \hat{Z}\}$ , while in quantum optics  $\{\hat{\sigma}_x, \hat{\sigma}_y, \hat{\sigma}_z\}$ , and by adding to them the  $2 \times 2$  identity matrix ( $\hat{I} = \sigma_0$ ), generate the Pauli group  $G_1 = \{\pm\hat{I}, \pm i\hat{I}, \pm\hat{X}, \pm i\hat{X}, \pm\hat{Y}, \pm i\hat{Y}, \pm\hat{Z}, \pm i\hat{Z}\}$  on one qubit.

$$\hat{I} = \hat{\sigma}_0 \equiv \begin{bmatrix} 1 & 0 \\ 0 & 1 \end{bmatrix} ; \quad \hat{X} = \hat{\sigma}_x \equiv \begin{bmatrix} 0 & 1 \\ 1 & 0 \end{bmatrix} ; \quad \hat{Y} = \hat{\sigma}_y \equiv \begin{bmatrix} 0 & -i \\ i & 0 \end{bmatrix} ; \quad \hat{Z} = \hat{\sigma}_z \equiv \begin{bmatrix} 1 & 0 \\ 0 & -1 \end{bmatrix},$$

$$C\hat{N}OT = \begin{bmatrix} 1 & 0 & 0 & 0 \\ 0 & 1 & 0 & 0 \\ 0 & 0 & 0 & 1 \\ 0 & 0 & 1 & 0 \end{bmatrix} ; \quad \hat{H} = \frac{1}{\sqrt{2}} \begin{bmatrix} 1 & 1 \\ 1 & -1 \end{bmatrix} ; \quad \hat{U}(\theta, \phi, \lambda) = \begin{bmatrix} \cos(\frac{\theta}{2}) & -e^{i\lambda} \sin(\frac{\theta}{2}) \\ e^{i\phi} \sin(\frac{\theta}{2}) & e^{i(\phi+\lambda)} \cos(\frac{\theta}{2}) \end{bmatrix}. \quad (2.8)$$

Until now, we have just seen the formalism for single qubit states, but we can see in equation (2.8) that  $C\hat{N}OT$ -gate is a  $4 \times 4$  matrix. This is because it is a gate that acts on two qubit states, meaning that the Hilbert space grows, changing its dimension.

The  $\hat{H}$  denotes the Hadamard gate, used to create a superposition of states. The last gate  $\hat{U}(\theta, \phi, \lambda)$  can actually produce any kind of rotation just setting the values of the angles as needed. For example,  $\hat{U}(\pi, 0, \pi)$  is equivalent to the  $\hat{X}$  gate.

## Bloch Sphere

A very useful way to visualize single qubit states is using the Bloch Sphere (BS) representation, which is a 3D unitary sphere that has been parametrized by two angles,  $0 \leq \theta \leq \pi$  and  $0 \leq \phi \leq 2\pi$ , which are real numbers. This provides any possible single qubit representation, under:

$$|\psi\rangle = \alpha|0\rangle + \beta|1\rangle = e^{i\gamma} \left( \cos\left(\frac{\theta}{2}\right)|0\rangle + e^{i\phi} \sin\left(\frac{\theta}{2}\right)|1\rangle \right), \quad (2.9)$$

where  $\gamma$  is also a real number, called global phase, which can be ignored since it is not going to contribute to the associated observation in measurements.

The Bloch sphere, despite the fact it is very useful for representing single qubit states, lacks the ability to represent multiple qubit states, given the higher dimension of the combined system. In any case, the Bloch sphere has aligned to its poles, or what we used as the  $z$ -axis the  $|0\rangle$  and  $|1\rangle$  states, at the  $x$ -axis the  $|+\rangle$  and  $|-\rangle$  states and finally the  $|i\rangle$  and  $|-i\rangle$  state aligned to the  $y$ -axis.

It can be visualized as in figure 2.1, a single pure qubit state, which is an expansion of computational bases.

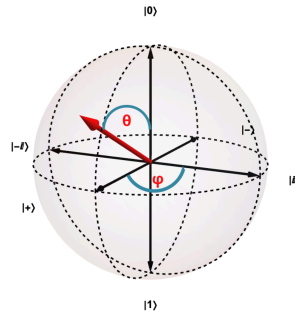


Figure 2.1: Bloch Sphere representation of a single qubit state. Adapted from<sup>1</sup>.

where  $|\pm\rangle = \frac{1}{\sqrt{2}}(|0\rangle \pm |1\rangle)$  and  $|\pm i\rangle = \frac{1}{\sqrt{2}}(|0\rangle \pm i|1\rangle)$ . Unit vectors, that follows the BS representation, will be evolved by any unitary operations preserving their magnitude. If vector states stop being unitary, their row becomes less than 1.

This means that this state is no longer a pure state and now is a mixed state, and it can be seen in the BS representation when a vector does not lie on its surface.

### 2.1.2 Quantum Entanglement

We already mentioned that the  $C\hat{N}OT$  operator is a gate acting on two different  $\mathcal{H}$  Hilbert spaces. In order to explain this growth in the dimension, we need to introduce a way of joining two or more vector spaces, each one preserving the already explained properties of a single qubit state. This operation is called the tensor product.

To start, let us consider a two qubit situation, where the first qubit state is an element of the complex vector space with inner product  $\mathcal{H}_1$  and the second is an element of the  $\mathcal{H}_2$ . Each space is a 2-dimensional, owing to its basis states  $\{|n\rangle_i\}_{n \in \{0,1\}}$ , where the sub index  $i$  labels the Hilbert space where the basis states  $|n\rangle_i$  belong.

Then, using the tensor product, the resulting space is the tensor product between each vector space  $\mathcal{H}_1 \otimes \mathcal{H}_2 = \mathcal{H}$ . Now, the bases on each space will also follow the tensor product relation, as  $|n\rangle_1 \otimes |n\rangle_2$ , and generate the orthonormal bases of the tensor Hilbert space  $\mathcal{H}$ , for our case, these bases are:  $|00\rangle, |01\rangle, |10\rangle, |11\rangle$ . It is important to notice that  $|0\rangle_1 \otimes |0\rangle_2 = |0\rangle|0\rangle = |00\rangle$ .

In addition, the tensor product needs to satisfy its properties of  $(|\psi\rangle + |\phi\rangle) \otimes |\chi\rangle = |\psi\chi\rangle + |\phi\chi\rangle$ , the same property of the linear combination is placed in the second argument, and with a scalar  $k \in \mathbb{C}$ ,  $k|\psi\rangle \otimes |\phi\rangle = |\psi\rangle \otimes k|\phi\rangle = k(|\psi\rangle \otimes |\phi\rangle)$ .

Now, let's see how the tensor product operates. Let us assume to have two parties, as above, then if a pure quantum state of a compound system can be taken by local operations of the form  $|\phi\rangle = |m, m'\rangle$  then it is called a separable or product state. Otherwise, it is called Entangled state<sup>4</sup>. Having two or more subsystems, to observe entanglement, an important condition is the superposition of states.

$$|00\rangle = \begin{bmatrix} 1 \\ 0 \end{bmatrix} \otimes \begin{bmatrix} 1 \\ 0 \end{bmatrix} = \begin{bmatrix} 1 \begin{bmatrix} 1 \\ 0 \end{bmatrix} \\ 0 \begin{bmatrix} 1 \\ 0 \end{bmatrix} \end{bmatrix} = \begin{bmatrix} 1 \\ 0 \\ 0 \\ 0 \end{bmatrix}, \quad (2.10)$$

where, it could be used the Kronecker product, to make it mechanical.

If we compute the tensor product for the four possible bases of two qubits, we will see that each resulting vector has an entry of 1 in different positions, and it is how they become orthogonal to each other, becoming bases for this 4-dimensional tensor product space. With each basis defined in our space, as with single qubit states, we can write each vector residing in this joint space as a linear combination of basis states. Without forgetting the normalization of our vector states,

$$|\psi\rangle = \sum_n \sum_{n'} \alpha_{nn'} |n\rangle_1 \otimes |n'\rangle_2 = \sum_{nn'} \alpha_{nn'} |nn'\rangle. \quad (2.11)$$

An important property of the tensor product space appears, when we write the superposition of the vector states. To see this, we can start with separable states, that means you can write a state by tensor product of its single basis. For example, the state  $|00\rangle = |0\rangle \otimes |0\rangle$ , and is commonly known as the product state.

Another example can be state  $\frac{1}{\sqrt{2}}(|00\rangle + |01\rangle) = |0\rangle \otimes \frac{1}{\sqrt{2}}(|0\rangle + |1\rangle)$ , where the second  $\mathcal{H}$  space is in a superposition of states, with  $\frac{1}{\sqrt{2}}$  as a normalization factor, and the first  $\mathcal{H}$  space is in  $|0\rangle$  state. This is a valid state on the joint Hilbert space, and also can be written as a product of its corresponding bases.

On the other hand, the non-separable states cannot be written as a product of separable states, and are called entangled states. These kinds of state are of interest given that they are responsible for quantum teleportation.

Some very important examples of these kinds of vectors are the Bell states, which are maximally entangled bipartite quantum states, and are written in the following way:

$$\begin{aligned} |\Phi^+\rangle &= \frac{1}{\sqrt{2}}(|00\rangle + |11\rangle) & ; & & |\Phi^-\rangle &= \frac{1}{\sqrt{2}}(|00\rangle - |11\rangle), \\ |\Psi^+\rangle &= \frac{1}{\sqrt{2}}(|01\rangle + |10\rangle) & ; & & |\Psi^-\rangle &= \frac{1}{\sqrt{2}}(|01\rangle - |10\rangle), \end{aligned} \quad (2.12)$$

which are the ones maximizing the violation of Bell inequalities<sup>56</sup>.

A very important property of these states, and the reason why they are so much important in information processing, is that just one of the qubit state provides information of the state of the other. Let's focus on the  $|\Phi^+\rangle$  state. If we perform a measurement on the first subsystem, and for example the outcome of the observation is  $|0\rangle$ , then that measurement induces a projection of the state of the second subsystem to be strictly in the  $|0\rangle$  state.

We can see that the projection of the first subsystem to the  $|0\rangle$  state breaks the superposition, turning the whole  $|\Phi\rangle$  state to the product state  $|0\rangle$ .

Let's define  $|0\rangle\langle 0| = \hat{M}_0$  and  $|1\rangle\langle 1| = \hat{M}_1$  as the set of measurement operators, according to the *postulate number 3* of quantum mechanics<sup>1</sup>. So, if the result of the measurement is  $|0\rangle$ , then the resulting state after this measurement is:  $\frac{\hat{M}_0}{\sqrt{p(0)}}|\Phi^+\rangle = \frac{\sqrt{2}}{\sqrt{2}}|0\rangle\langle 0|(|00\rangle + |11\rangle) = |0\rangle\langle 0|00\rangle + |0\rangle\langle 0|11\rangle = |00\rangle$ , where the probability  $p(0)$  to measure zero in the first subsystem is given by  $p(0) = \langle \Phi^+ | 0 \rangle \langle 0 | \Phi^+ \rangle = \frac{1}{2}$ .

This is due to an intricate relation to the purity and mixture of quantum states, where the pure states can be described by both vector and density matrix operator notation, but mixed states can only be written in density matrix representation. This is a property coming from the partial trace  $\text{Tr}_i$  of the whole system.

The partial trace helps us when we have a joint vector state and we want to have a description of the individual subsystem, so it means,  $|\psi\rangle_1 = \text{Tr}_2(\hat{\rho}_{12})$ , where  $\hat{\rho}_{12} = |\psi\rangle_{12}\langle\psi|$ . Additionally, using the trace operation, we can define pure states as  $p = \text{Tr}(\hat{\rho}^2) = 1$  and mixed states as  $p = \text{Tr}(\hat{\rho}^2) < 1$ . Then, if the state  $|\psi\rangle_{12}$  is a non-separable state, we will not be able to use Dirac notation to represent the state (so  $p < 1$ ).

**Operators Under Tensor Product Treatment:** We are now just missing the description of how operators act on the tensor product state. As vectors are joined by the tensor product, we will need to do the same with operators in order to respect the dimension of the Hilbert space, where we represent the joined operators as  $\hat{A}_1 \otimes \hat{B}_2$ .

Each operator maps its subsystem as,  $\hat{A}_1 : \mathcal{H}_1 \rightarrow \mathcal{H}'_1$ , and  $\hat{B}_2 : \mathcal{H}_2 \rightarrow \mathcal{H}'_2$ . Here the space is  $\mathcal{H}' = \mathcal{H}'_1 \otimes \mathcal{H}'_2$ , and we use the prime notation on the final space, where each operator acts on different Hilbert spaces. The tensor product works in the same way as was explained previously, and again can be used the Kronecker product. For example,

$$\hat{C}_{12} = \hat{X}_1 \otimes \hat{Z}_2 = \begin{bmatrix} 0 & 1 \\ 1 & 0 \end{bmatrix} \otimes \begin{bmatrix} 1 & 0 \\ 0 & -1 \end{bmatrix} = \begin{bmatrix} 0 \begin{bmatrix} 1 & 0 \\ 0 & -1 \end{bmatrix} \\ 1 \begin{bmatrix} 1 & 0 \\ 0 & -1 \end{bmatrix} \end{bmatrix} = \begin{bmatrix} 0 & 0 & 1 & 0 \\ 0 & 0 & 0 & -1 \\ 1 & 0 & 0 & 0 \\ 0 & -1 & 0 & 0 \end{bmatrix}. \quad (2.13)$$

As mentioned previously, the  $CNOT$  operator is defined to act on two qubits. Moreover, it is especially important in our context, because it is a quantum gate that can produce entanglement.

Some other examples of two qubit gates are the Controlled- $U$  and  $S\hat{W}AP$  gates, where  $U$  can be any single qubit operator including rotation operators. At the equation (2.14) we can see their matrix representation.

$$\hat{C}(\hat{U}) = \begin{bmatrix} 1 & 0 & 0 & 0 \\ 0 & e^{i\gamma} \cos(\frac{\theta}{2}) & 0 & -e^{i(\gamma+\lambda)} \sin(\frac{\theta}{2}) \\ 0 & 0 & 1 & 0 \\ 0 & e^{i(\gamma+\phi)} \sin(\frac{\theta}{2}) & 0 & -e^{i(\gamma+\phi+\lambda)} \cos(\frac{\theta}{2}) \end{bmatrix} ; \quad S\hat{W}AP = \begin{bmatrix} 1 & 0 & 0 & 0 \\ 0 & 0 & 1 & 0 \\ 0 & 1 & 0 & 0 \\ 0 & 0 & 0 & 1 \end{bmatrix} ; \quad (2.14)$$

where the ( $\hat{U}$ ) gate posses dependence on four parameters ( $\theta, \phi, \lambda, \gamma$ ), where they are bounded as:  $0 \leq \theta \leq \pi, 0 \leq \phi < 2\pi, 0 \leq \lambda < 2\pi$  and  $0 \leq \gamma \leq 2\pi$ . Also, it is the matrix representation when the action of the  $\hat{U}$  gate is controlled by the state  $|1\rangle$ . It also could be controlled by the  $|0\rangle$  state.

A gate commonly applied to three qubits is the Toffoli-gate, and we can see its matrix representation in equation 2.15.

$$\hat{U}_{Tof} = \begin{bmatrix} 1 & 0 & 0 & 0 & 0 & 0 & 0 & 0 \\ 0 & 1 & 0 & 0 & 0 & 0 & 0 & 0 \\ 0 & 0 & 1 & 0 & 0 & 0 & 0 & 0 \\ 0 & 0 & 0 & 0 & 0 & 0 & 0 & 1 \\ 0 & 0 & 0 & 0 & 1 & 0 & 0 & 0 \\ 0 & 0 & 0 & 0 & 0 & 1 & 0 & 0 \\ 0 & 0 & 0 & 0 & 0 & 0 & 1 & 0 \\ 0 & 0 & 0 & 1 & 0 & 0 & 0 & 0 \end{bmatrix} . \quad (2.15)$$

Some final important relation to this representation of the operators by tensor product is a super operator  $\hat{C} = \sum_i \alpha_i (\hat{A}(i)_1 \otimes \hat{B}(i)_2)$ , which is a linear combination of different operations defined by the index  $i$  under the subsystems one and two.

### 2.1.3 Computational Models

Before going directly to quantum circuits, first we are going to make some comments about classical computation models. We are then going to provide a broad idea of the most remarkable quantum computational model, here it is important to start mention the first days of classical computation and information theory, from which some models have been extended to the quantum realm. To conclude this section, we are going to focus on the quantum circuit model since we will be directly applying quantum circuits.

Alonzo Church and Alan Turing are perhaps the most influential scientists that pioneered the computation and information theory. They pushed the limits of computational knowledge in an effort to answer one of the most intriguing question of computational science.

This was asked by the famous David Hilbert, the same mathematician of Hilbert space ( $\mathcal{H}$ ) that we have been using to define our state space. Given that algorithms provide universal tools to face any kind of problem, Hilbert wanted to know if there exist some universal algorithm.

In this context universal means that it could work under any kind of situation, that could be able to solve any mathematical question in any scenario.

To answer this question, Alan Turing implemented what today we know as Turing Machines. In any case, finally and surprisingly, the answer was *no*. However, this question became the catapult to formalise the foundations of algorithm theory, which nowadays is one of the most useful tools that computational science inherited.

On the other hand, a secondary approach, to answer related questions is the Circuit Model, where the use of wires, electronic devices, and electrical currents can help to create logical scenarios. In this way, it becomes important to provide an open idea of what these computational models encompass, due to their relevance for the development of this thesis.

**Classical Computational Models**

**Turing Machines:** To introduce the Turing machine model, we need first to know its principal components. Given that Turing machines are directly thought to its physical implementation, we need: a) **Tape** that will work as the memory of the device, here the results of the program operation will be saved.

In some models, at the left most, there is a special symbol that implies the beginning of the tape, and it can be extended as much as needed to the right side. b) **Finite state control** that can be thought as a set of states which are predefined by the calculations that are going to be accomplished. These internal states will act as the processor given that they will be managing the operations of the Turing Machine. c) A **Program** that will codify the actions needed to carry out. d) The **Read/Write Tape-Head** will be used to point the position of tape where the operation is currently being done, and could be moved to the right, left, or stay, depending on the instructions of the program.

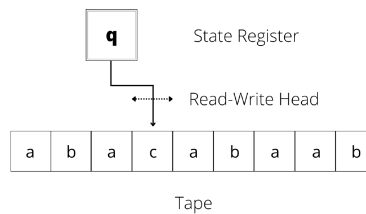


Figure 2.2: Turing Machine scheme. Adapted from<sup>1</sup>.

With the main elements recognized, what the machine will do is the following: it starts by reading the initial state (or input) that contains some characters at the beginning of the tape, and by using the tape-head, it follows the program, changing initial states, writing the result and moving the tape-head.

**Circuits:** Circuit model can accomplish the same tasks of Turing Machines, but in a more realistic approach. As mentioned previously, circuit models are of major importance and classical circuits have their quantum version. For this reason, we begin by defining the main elements of the classical circuit model.

Primarily we need necessary **wires** that through electrical voltage levels will create the common bit ('0' or '1') and its **gates** to recreate logical operations on desired bits.

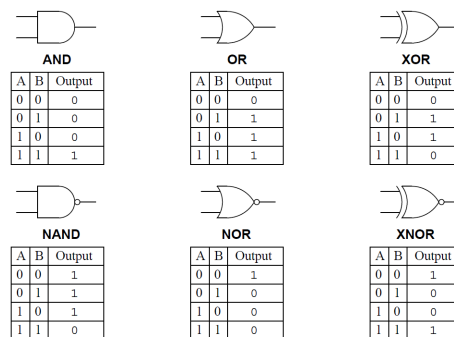


Figure 2.3: Digital Logic gates. Adapted from<sup>7</sup>.

As we see in figure 2.3, for a given bit, 0 or 1, as input to a logical gate and then we have specific outcomes. In this approach, information is encapsulated in bits, which cannot be taken in superposition.

Each gate can be physically implemented using, for example, semiconductors, where an energy gap, can be used as a switch to implement any of the operations shown in Figure 2.3.

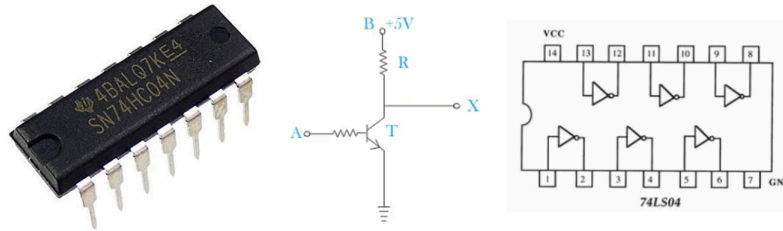


Figure 2.4: NOT gate physical device, circuit and internal connections inside the electronic chip. Adapted from<sup>8</sup>.

In figure 2.4 we can see a gate implemented by the Arduino company in a classical circuit. Finally, we see how the inside the device is connected to produce the NOT operation.

### Quantum Computational Models

We have many different approaches to realize algorithms in the quantum realm, and some of them actually do not possess a classical counterpart. As we saw, Turing machines and circuits models possess a quantum analog, as **Quantum Turing Machines**.

For example, we have: **Adiabatic Quantum Computing** that works under the adiabatic theorem. This basically tells the systems how to evolve in time but slow enough to give the wavefunction associated to the systems time to not change its properties. The most remarkable company that takes this principle to the functioning of their quantum devices is the D-Wave systems company.

Another example is the **One way Quantum Computing** or Measurements Based Quantum Computing (MBQC). It works under the principle of quantum entanglement, where at the initial state the whole system is entangled and then the execution is done by performing measurements and unitary operations on qubits. The application of measurements is why it is called "one-way".

### Quantum Circuit Model

To introduce quantum circuit model, let's check its main elements. We saw in the first section we have a well defined basis states, in our case the  $|0\rangle$  and  $|1\rangle$  states. They can be implemented with different physical implementations, as superconducting materials. This basis states in our schemes will be seen as horizontal lines, or wires, which indicate the temporal evolution of each qubit part of the system.

To continue we need necessary quantum gates to accomplish logical operations, as we will see the temporal evolution of the qubits. Then we see each gate applied on the circuit in some particular moment.

Finally, we need classical registers in order to save measurements of our qubits, given that the information carried by each qubit cannot be obtained without observing the state through quantum measurements, that project the state into one of the basis states.

If we realize sufficient number of experiments, we can reconstruct the state through its statistics, for example using quantum state tomography, as explained in following sections.

We may consider Figure 2.5, to be most simple circuit, where the initial state  $|\phi\rangle$  is measured, and the result saved in a classical bit. In reality, we can see the gate representation of the measurement action on the qubit, projecting the qubit states to only 0 or 1.

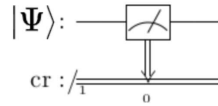


Figure 2.5: Quantum measurement is a process, which projects a qubit state to two orthogonal states  $|0\rangle$  and  $|1\rangle$ . Adapted from<sup>1</sup>.

For example, we can present the circuit of the discrete quantum Fourier transform on three qubits in the Figure 2.6.

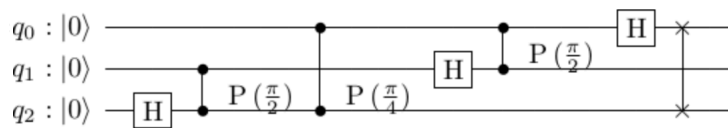


Figure 2.6: Circuit of discrete quantum Fourier transform on three qubits. Adapted from<sup>1</sup>.

In addition, Figure 2.7 adapted from the book of Quantum Computation and Information<sup>1</sup>, we have the representation of the quantum gates as boxes, with their corresponding matrix representations.

Quantum Gate	Symbol	Matrix Representation
Pauli X		$\begin{bmatrix} 0 & 1 \\ 1 & 0 \end{bmatrix}$
Pauli Y		$\begin{bmatrix} 0 & -i \\ i & 0 \end{bmatrix}$
Pauli Z		$\begin{bmatrix} 1 & 0 \\ 0 & -1 \end{bmatrix}$
Hadamard		$\frac{1}{\sqrt{2}} \begin{bmatrix} 1 & 1 \\ 1 & -1 \end{bmatrix}$
Controlled Not (CNOT)		$\begin{bmatrix} 1 & 0 & 0 & 0 \\ 0 & 1 & 0 & 0 \\ 0 & 0 & 0 & 1 \\ 0 & 0 & 1 & 0 \end{bmatrix}$
Controlled Z (CNOT)		$\begin{bmatrix} 1 & 0 & 0 & 0 \\ 0 & 1 & 0 & 0 \\ 0 & 0 & 1 & 0 \\ 0 & 0 & 0 & -1 \end{bmatrix}$
SWAP		$\begin{bmatrix} 1 & 0 & 0 & 0 \\ 0 & 0 & 1 & 0 \\ 0 & 1 & 0 & 0 \\ 0 & 0 & 0 & 1 \end{bmatrix}$

Figure 2.7: Quantum gates representation. Adapted from<sup>1</sup>.

### 2.1.4 Quantum Processors: physical implementation

In order to talk about any kind of physical implementation that has been realized to create a quantum processor, first we are to present the statements that the construction of a quantum processor requires in order to be sufficiently efficient. This is one of the most important parts of quantum computation, because computers need to recreate our mathematical formalism, where every state exist in a Hilbert space, that the quantum computer needs to reproduce. We will then discuss the criteria necessary for quantum computing.

#### DiVincenzo's Criteria

As already said, there exist the necessary criteria that a quantum computer needs to posses in order to recreate our mathematical formalism, and this could be thought of as the actual status of research by physicist, quantum engineers, and developers, where any research group is trying to reach a quantum advantage. We will then focus in detail on each criterion and then explain why each of these items are important:

- **1. Scalable Qubits:** A scalable physical system with well characterized qubits
- **2. Initialization:** The ability to initialize or prepare the state of the qubits to a simple, fiducial input state as  $|000\dots\rangle$ .
- **3. Measurement:** A qubit-specific measurement capability. The ability of measure a qubit state with enough high fidelity.
- **4. Universal Set of Quantum Gates:** Ability of perform a universal set of quantum gates with a enough high fidelity.
- **5. Coherence:** Long relevant coherence time. The coherence time of each qubit state needs to be longer than the operation time of each quantum gate. Here coherence means to maintain relative phases between basis states.

#### Additionally for Quantum Communication

- **6. Interconversion:** Ability to convert stationary and flying qubits. Where a flying qubit is a state that can be freely transmitted from one node or physical party to another.
- **7. Transmission:** Ability to faithfully transmit flying qubits between specified locations.

There exist many physical implementations of qubits and operations on them, but currently it is still a very complicated task for scientists. For this let's introduce Decoherence, which is the action of taking a quantum system to a classical state. In our context, decoherence also can be understood as the variations produce in the quantum state by affection of unknown sources. So, we can see that decoherence is a plague that spreads on any kind of implementation, which is exactly why we try to avoid it. We may then nicely summarize<sup>1</sup>, for some implementations, with their coherence times, the time that takes to a gate to operate on the states, and the maximum of operations of the physical system.

Physical Resource	$\tau_Q$	$\tau_{op}$	$n_{op} = \lambda^{-1}$
Electron spin	$10^{-3}$	$10^{-7}$	$10^4$
Nuclear spin	$10^{-2} - 10^8$	$10^{-3} - 10^{-6}$	$10^5 - 10^{14}$
Optical cavity	$10^{-5}$	$10^{-14}$	$10^9$
Ion trap (In <sup>+</sup> )	$10^{-1}$	$10^{-14}$	$10^{13}$
Quantum dot	$10^{-6}$	$10^{-9}$	$10^3$

Table 2.1: Coherence times (T1-T2) and its respective number of operations, for different physical realizations. Adapted from<sup>1</sup>.

The times of coherence T1 and T2 can be defined as: T1 time is called the relaxation time and it can be understood as the time that the systems is able to maintain itself in the first excited state, in our case the  $|1\rangle$  state. On the other side, the T2 time is known as dephasing time and is the time that after which a input state, let's say the  $|+\rangle$  state, evolves into its classical probabilistic mixture, in this case the  $|-\rangle$  state.

In addition,  $\lambda$  is the ratio between qubit coherence time and the gate operation time. We can see that there are many sources than can be used as qubits, and some examples can be found at the M. Nielsen and I. Chuang book "Quantum Computation and Quantum information"<sup>1</sup>.

The physical implementations, although there are a lot of possible systems, can be understood as qubits systems implemented by: charge, spin and photons.

Now that we have defined quantum computational models, some principles for quantum computer, additionally some physical sources used to implement qubits, we are going to mention some important realization of quantum computers with different sources, which are actually what will change the mathematical model, taking into account some of its advantages and disadvantages regarding their physical implementations.

### Optical Photon Quantum Computer

Light or its quanta, a photon, as the main source to create a single qubit, can have some interesting properties, given that it does interact very weakly with some other photon state and even weakly with a matter. Light has many degrees of freedom: polarization, momentum, direction, wavefront, frequency, intensity, OAM and can be used to implement qubits.

In light, a single photon, the quantization of light, gets a defined electric and magnetic vector field, the same that could be in superposition of states, and we call it polarization of the light. This quantization becomes important when we want to isolate a single photon. We could then represent each state as  $|n\rangle$ , where  $n$  is the number of photons in a given optical mode.

Then, the  $|0\rangle$  and  $|1\rangle$  states can be implemented, based on whether there is a photon present. These states are usually called Fock states. But it is not the only way a qubit can be implemented with light. We can use what we call coherent states<sup>1</sup>, which come from a superposition of Fock states as:

$$|\alpha\rangle = e^{-\frac{|\alpha|^2}{2}} \sum_{n=0}^{\infty} \frac{\alpha^n}{\sqrt{n!}} |n\rangle, \quad (2.16)$$

which can be used with  $|\alpha| \rightarrow 0$  to implement a two level system, with  $|0\rangle$  as vacuum state and  $|1\rangle$  with one photon. Optical states can be manipulated using basic optical components, nonlinear materials, and as well, implemented using integrated optics.

## Xanadu's Device

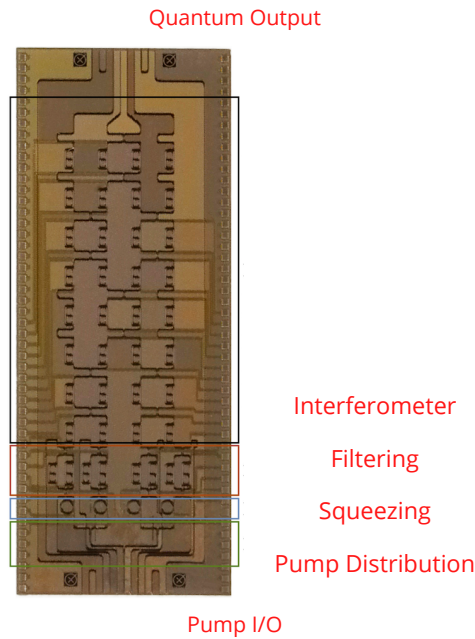


Figure 2.8: Xanadu's physical implementation of photonic quantum processor, where it can be appreciated its main components as: the interferometer, the filtering and the squeezing sections, and the pump distributor. Adapted from Arrazola (2021)<sup>9</sup>.

In Figure 2.8, adapted from Arrazola (2021)<sup>9</sup>, we can see a physical implementation of this kind of computation, where the Xanadu company has created this high quality optical chips.

### Optical Cavity Quantum Electrodynamics

Optical cavity Quantum Electrodynamics (QED) is a mixture of a single atom living in a cavity with high quality factor  $Q$ , which is the ratio of the resonant frequency to the bandwidth of the cavity resonance, and it could be some photon at some optical cavity modes. Without going into to much detail, we can visualize the behavior inside the cavity as the photon bouncing in the cavity and interacting the quantized energy levels of the atom.

Then, first, supposing that our system can be perfectly isolated, the photon will be able to produce a transference of the energetic levels of the atom at certain levels, already know, coming from the Schrodinger equation. Then, if the atom has absorbed the photon, it is in the excited energetic level, and non-photon will be detected. In the other way, we can know the state of the atom, if the photon has not been absorbed, then, it can be detected.

As mentioned, the system lives inside a cavity, which can be described a Fabry-Perot Cavity. Selecting monochromatic and single spatial mode of the light ( $\mathbf{K}$ ), the electric field  $\mathbf{E}$  becomes:

$$\mathbf{E}(\mathbf{r}) = i\mathbf{E}_0[\hat{\mathbf{a}}e^{i\mathbf{k}\cdot\mathbf{r}} - \hat{\mathbf{a}}^\dagger e^{-i\mathbf{k}\cdot\mathbf{r}}]\hat{\mathbf{n}}, \quad (2.17)$$

this appropriate and approximate description of the electric field inside the cavity gets a dependence on  $\mathbf{r}$ , to be the position of the field and strength  $E_0$ .

The Fabry-Perot cavity is basically formed of two plates, commonly of silver, as mirrors, with reflective and transmissive indices, that create the bounds of the oscillations of the electric fields. Finally, one of the most important definitions of the cavity is that it only supports fields with frequency matching the cavity resonance frequencies.

The model, which describes what is happening inside the cavity, will be the Jaynes-Cummings model, where the Hamiltonian describes the behavior explained before, as:

$$\hat{H} = \frac{\hbar\omega_0}{2}\hat{Z} + \hbar\omega\hat{a}^\dagger\hat{a} + g(\hat{a}^\dagger\sigma_- + \hat{a}\sigma_+), \quad (2.18)$$

where, the sigmas are the lowering and raising Pauli operators, acting on the states of the atom,  $\omega$  and  $\omega_0$  are the frequencies of the field and the atom, respectively. And, finally, the  $\hat{a}$  and  $\hat{a}^\dagger$  are the annihilation and creation operators for the photon description.

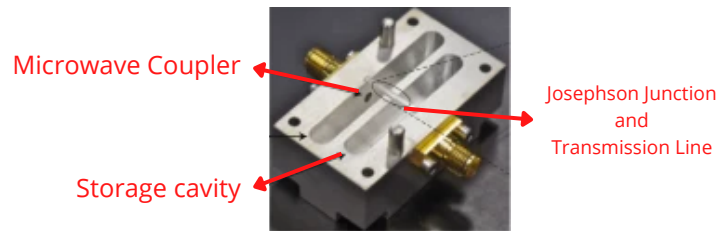


Figure 2.9: Optical cavity QED scheme of implementations, where it can be appreciated its main components as: the microwave coupler, the storage cavity, the Josephson junction and the transmission line. Adapted from Haroche (2020)<sup>10</sup>.

The figure 2.9 was adapted from<sup>10</sup> paper called "From cavity to circuit quantum electrodynamics", treating exactly this kind of physical implementation.

### Ion traps

Ions traps are used for the physical implementation of traps for charged particles. For the implementation of these kind of qubits, scientists have been trying to explore the spin properties of some particle, which in practice are more difficult to target, given that their potential energetic contribution is very much lower than the contribution, for example, of the kinetic energy of an atom.

On the other hand, the spin becomes more effective than other implementations, as it turns out to be manipulated. Then, one possibility is to cool the atom as much as the kinetic energy contribution until it is negligible compared to the energy of the spin of the ion. Then, the isolated spin-ion can be controlled by using electric fields, accomplishing what we need.

This behavior, by cooling, will be observed by lowering the temperature until the regime of  $\hbar\omega_z \gg k_B T$  which could be first implemented by Doppler Cooling, which makes use of lasers and knowledge of the atomic energies, and the trapped atoms can be cooled down to  $k_B T \approx \frac{\hbar\Gamma}{2}$ , where  $k_B$  is the Boltzmann's constant, which provides a relation of temperature and energy,  $T$  the temperature of the system and  $\Gamma$ , the inverse of the lifetime. And second, using the sideband cooling method, where using knowledge of phonon quasi-particles, experimental researchers can reach the desired regime of temperature.

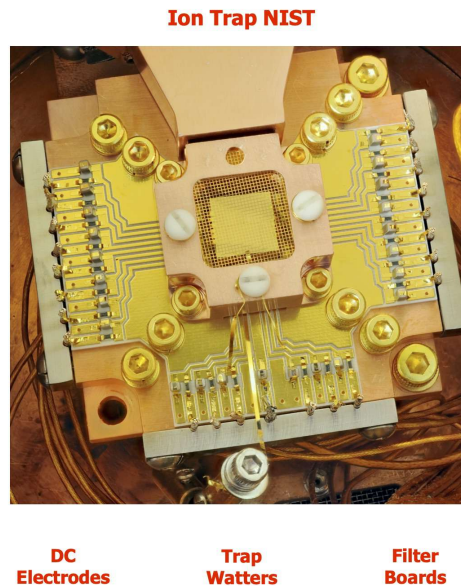


Figure 2.10: Ion trap implemented by NIST, where it can be appreciated its main components as: DC electrodes, the trap Watters and Filter boards. Adapted from Blakestad (2011)<sup>11</sup>.

Regarding the trap, which works by applying to some electrodes, a static electric field and creating a radio frequency potential, some ions being part of the electrodes, can be trapped in the axis of the the material, where now we can think of them, as dots, given that they have been bounded to a region of the space. This provides the quantization of these particles, which could be thought of as isolated from the rest of the world.

The noisy effects will have similar nature, given that anything in the device can produce fluctuations, changing the geometry of the trapped ions, or even changing the electric fields that trap the sample, and finally, changing the known dynamics, producing decoherence of our desired qubits, which happens when spins are coupled to another degree of freedom (like phonons). Then, our states in a superposition are going to be codified by the spin of our atoms and the their phononic configuration. Then, the lasers are going to work as operators, by tuning its frequency according the energetic levels of the ions. At figure 2.10 we can see a real implementation of NIST at 2011, where the ions are trapped in the middle of the whole square chip structure.

### Nuclear Magnetic Resonance

If we check in the table of lifetimes, the largest number of operations comes from nuclear spins, given that they are not very susceptible to the environment, but the problem is to control them. We need to be very accurate and the time that takes to operate make the computation very complicated.

There is a lot knowledge about manipulation of nuclear spin states, commonly known as the Nuclear magnetic Resonance (NMR). The problem arrives, given that the magnetic moment arriving emitted by the nucleus is very small, then huge number of molecules need to grouped in order to make it stronger. This produces many systematic problems in the computation.

On the other hand, the evolution of such nuclear states could be realized by magnetic field pulses, that target the

spin states in a strong magnetic field. The fiducial state preparation, which is one of the DiVincenzo's requirements for computations is problematic given that the physical apparatus at room temperature provides the equilibrium of the collection of molecules, making the initial state of computation random.

Then, if we try to remove some of the molecules, in order to reach a pure state, the readout turns out to be difficult by the insufficient signal produced by the sample, given that the measurement needs to be done by voltage signals coming from the magnetic moment.

## NMR Quantum Computer



Liquid Helium and Nitrogen      Superconducting Magnet

Figure 2.11: NMR based quantum computer, where it can be appreciated its main components as: the Liquid Helium and Nitrogen cavity and the superconducting magnet. Adapted from<sup>12</sup>.

At figure 2.11, we can see a real implementation of a quantum computer based on NMR developed by Professor Steffen Glaser and his group at the Technical University of Munich, at Germany.

### Superconducting Qubits

In order to introduce the superconducting qubits, we are going to make a brief review of the simplest case, the harmonic oscillator. However, it is almost impossible to have a quantum computer based on this behavior. There are many sources that correspond to a harmonic oscillator, as a mass attached to a spring, where the transitions comes given by the interchange of kinetic and potential energy. An important example is a L-C circuit, where the electric energy of the resonant circuit is being transmitted from an inductor and a capacitor defining the circuit.

The discrete set of eigenstates associated to the Hamiltonian of the system can be, by notation  $\{|n\rangle\}_{n \in \mathbb{N}}$ , associated to  $\hat{H} = \hbar\omega_0(\hat{a}^\dagger \hat{a} + \frac{1}{2}) + h.c.$ , where the annihilation and creation operators are defined by using position and momentum operators, finally if we wish to reach the two-level state, we run a serious problem, as the levels are equally separated and we will not be able to target a particular pair, like  $|0\rangle$  and  $|1\rangle$ , when sending photons with frequency  $\omega_0$ .

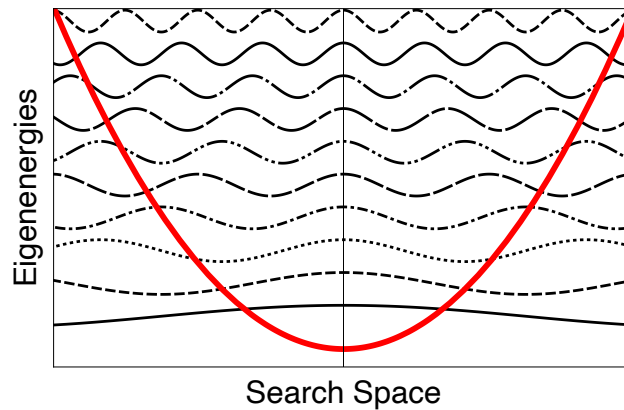


Figure 2.12: Energy levels of harmonic oscillator. Pictorial representation. Adapted from <sup>1</sup>.

Given already mentioned difficulties, to improve these kind of models, some extra elements should be inserted in order to reach an accurate readout of the energetic levels and manipulation of such elements are usually nonlinear, such as Josephson junctions <sup>13</sup>.

Inside of superconducting qubits, there are many variations from three main simple structures: charge, flux and phase superconducting qubit implementations. All of them make use of a non-linear element called Josephson Junction (JJ) which provides a differentiation of energy levels. Inside the superconductor the electrons are attractively bounded, possessing the same momentum but different spin, these are what we used to call the Cooper pairs, that additionally present integer spin behaving as bosons.

The charge-like qubits have dependence on the number of Cooper pairs, which will be located in a superconducting island opening the the concept of superposition of logical basis states.

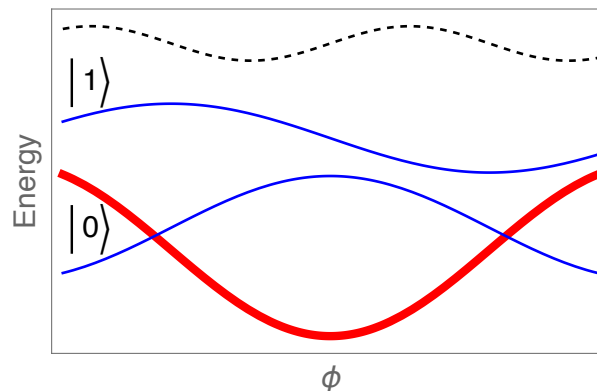


Figure 2.13: Potential and wavefunctions of Charge qubits - basis states. The red curve represents the potential and the blue curves represent the needed eigenenergies. Adapted from <sup>14</sup>.

In the Figure 2.13, we can see the isolated energy levels of a charge qubit, that will be used as a computational basis. A basic circuit scheme of this qubits is shown continuously, where the x-boxed gate represents the JJ.

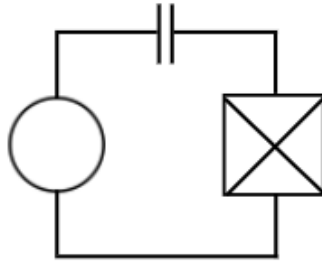


Figure 2.14: Charge qubit circuit scheme. Adapted from<sup>14</sup>.

Continuing, flux qubits make use of magnetic flux quanta reached in a superconducting ring loop and again the energy levels will be controlled by a JJ element. In this case, the basis states come given by a superposition of the direction of magnetic flux, caused by superconducting current going around the circuit.

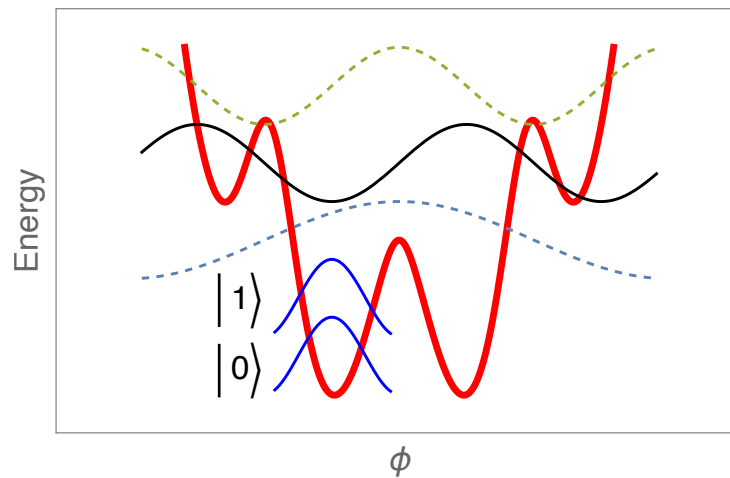


Figure 2.15: Potential and wavefunctions of flux qubits - basis states. The red curve represents the potential and the blue curves represent the needed eigenenergies. Adapted from<sup>14</sup>.

And like that, a basic circuit will be showed in following Figure, where  $\Phi$  is used to control the magnetic flux.

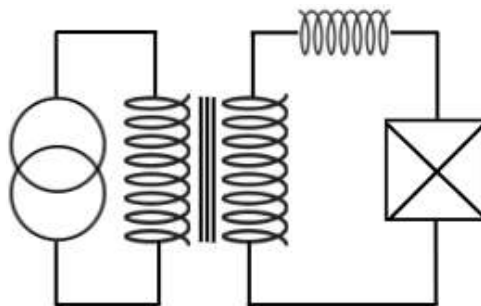


Figure 2.16: Flux qubit circuit scheme. Adapted from<sup>14</sup>.

To conclude, phase qubits produce energy levels that are distinguished by quantum charge oscillation amplitudes across the JJ, and it is used the commonly known washboard potential.

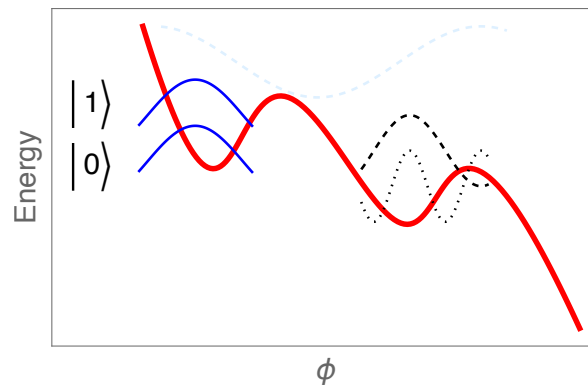


Figure 2.17: Potential and wavefunction of phase qubits - basis states. The red curve represents the potential and the blue curves represent the needed eigenenergies. Adapted from<sup>14</sup>.

The circuit that represent a systems like this is showed in the following Figure 2.18, where the promotion of the states and superposition, and respective measurements (using DC-SQUID magnetometer) will be given by a biased voltage. Additionally, all images were taken from the paper called "Superconducting qubits: A short review"<sup>14</sup>.

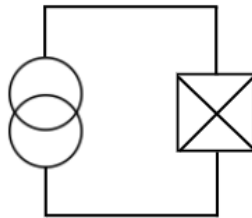


Figure 2.18: Phase qubits circuit scheme. Adapted from<sup>14</sup>.

The anharmonicity in the energy states produced by the Josephson-Junction can be seen the following figure, where the both scenarios are compared. The figure was obtained on qiskit textbook at "Introduction to Transmon Physics"<sup>15</sup>.

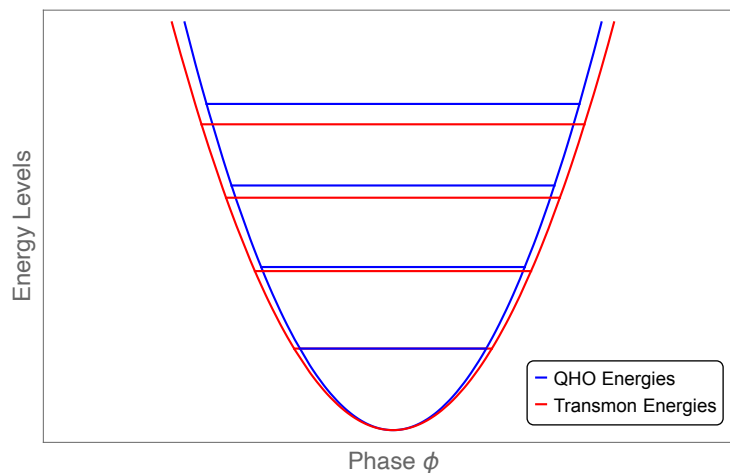


Figure 2.19: QHO vs Anharmonic energy levels. The red curve represents the deformed potential to get the anharmonic energies, and the blue curve represents the quantum harmonic oscillator potential and eigenenergies. Adapted from<sup>15</sup>.

**Transmon Qubits:** This kind of qubits are part of charge qubits, its name comes from "Transmission line shunted plasma oscillation (Transmon)" qubit<sup>16</sup>, which uses electrical properties of some materials to accomplish the requirements of a qubit state. Again, it is necessary the insertion of a JJ non-linear element in L-C circuits in order to differentiate the energy levels, and the advantage of this kind of qubits respect the three already mentioned is that its sensitivity to charge noise is very low.

The common Quantum Harmonic Oscillator (QHO) hamiltonian  $\hat{H} = \frac{\hat{Q}^2}{2C} + \frac{\hat{\Phi}^2}{2L}$  can be manipulated in order to arrive to a current description of Transmon qubits, both are the Charge and Flux operators, which in quantum mechanics follow the same conditions as in classical mechanics, where charge and flux can be found by integrating voltage and current.

Current and Flux operators obey the operator commutation relations, as  $[\hat{\Phi}, \hat{Q}] = i\hbar$ . This last relation between these two operations is pretty important in the implementation of transmon qubits, given that they obey the Heisenberg Uncertainty Principle, due to this fact they are not simultaneously observable, then they have some relative definition.

$$\hat{H} = 4E_C(\hat{n} - n_g)^2 - E_J \cos(\hat{\varphi}), \quad (2.19)$$

where, the operators  $\hat{n}$  and  $\hat{\varphi}$  are what denote the number of Cooper pairs transferred between islands in the J-junction, and the gauge invariant phase difference between the superconducting parts, respectively.

The  $E_C$  and  $E_J$  denote charge and Josephson-junction energies, and for this precise case, they need to operate in the regime where  $E_J \gg E_C$ .

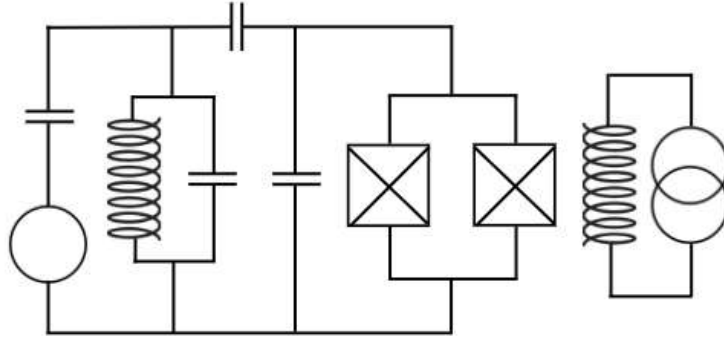


Figure 2.20: Transmon qubit circuit and physical implementation scheme, where it can be appreciated the connections of main components to get the desired energy levels. Adapted from<sup>16</sup>.

The previous Figure 2.20, we have the scheme of a Transmon like qubit circuit, by a combination of inductors, capacitances and JJ elements, biased by a desired voltage, and the most important, we can see the  $E_J$  and  $C_J$  dependence in the circuit. Finally, we can check how the energy levels are going to be achieved by manipulating the quality parameter of the JJ elements.

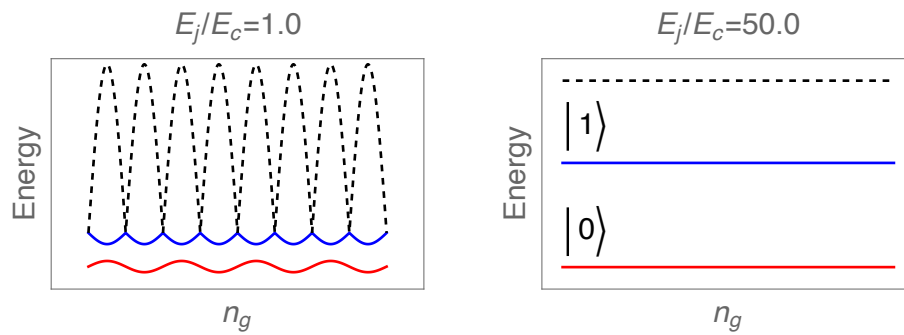


Figure 2.21: Energy levels of the transmon qubit. It can be appreciated the deformation the desired energies by controlling the  $E_j/E_c$  parameter. Adapted from<sup>16</sup>.

We have paid a little more attention to these kind of qubits given that IBM's Quantum Computer (QC)s use this superconducting property to construct their units for computation. Even though it remains a very challenging task to realize quantum computers with zero or with the lowest amount of noise.

The figures 2.20 and 2.21 were adapted from original proposal of transmon qubits paper<sup>16</sup>. As we are discussing IBM's implementations, we can check how a real processor looks like, and how it is managed.

### IBM's Quantum Computer

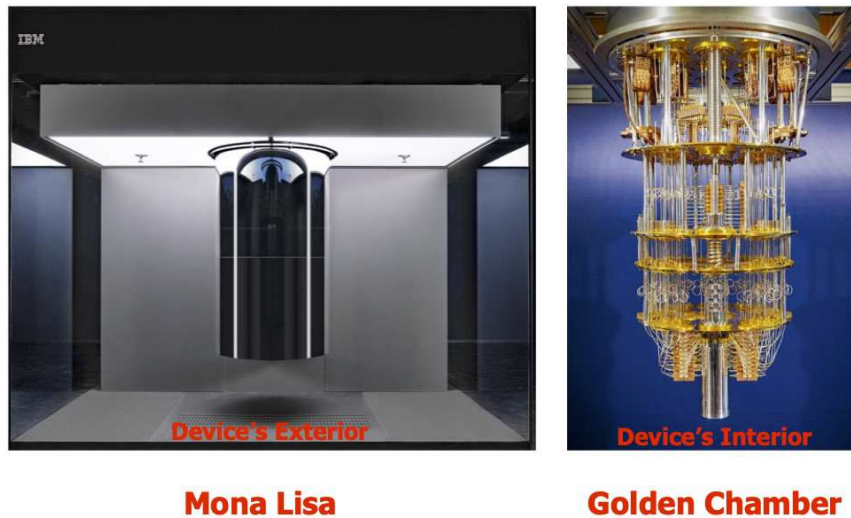


Figure 2.22: IBM's quantum processor. At the left side we can see the exterior of the device and at the right side its interior. Adapted from<sup>15</sup>.

The left part is how the whole system is ensemble, and is actually called the "Mona Lisa", and the right part is the inside of the Mona Lisa cavity, which is known as the Golden chamber, which indeed is build up of gold due to its thermal conductivity qualities. The chamber support the decrease of temperature from the upper level to the lowest level, going from 300 K to 0.015 K, where the Transmon based processors actually reaches its superconductive phase.

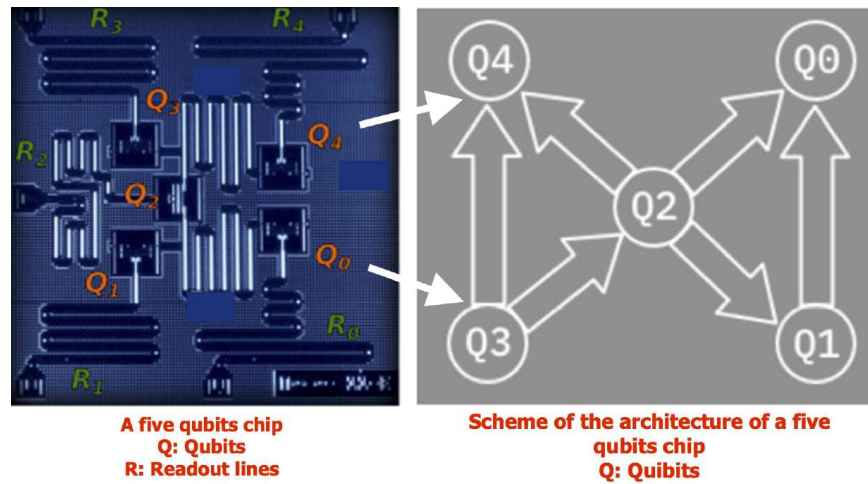


Figure 2.23: IBM's quantum computer chip. It can be appreciated the architecture of a chip of five qubits. Adapted from<sup>15</sup>.

Inside the golden chamber, in the lower part, the chip containing the qubits is placed. The chip is showed in the past Figure 2.23, where we can see how the five qubits are assembled, and multi-connected in order to accomplish computation.

Its architecture which is going to be important for example when the noise must be added due to local interactions. Additionally, we can see how the island that are part of the JJ element are place and how the entries for biased voltage and elements for state readouts are placed in the circuit in optimal scheme.

## 2.2 Standard Quantum Teleportation

The Standard Quantum Teleportation (SQT) is a simple protocol of quantum teleportation involving an input state and a bipartite entangled state<sup>2</sup>. We can see the scheme of SQT in Figure 2.24, where Alice sends a quantum state  $|\psi_{in}\rangle$  through a quantum channel to Bob. In order to introduce this protocol we need to define the main steps and components that are part of it:

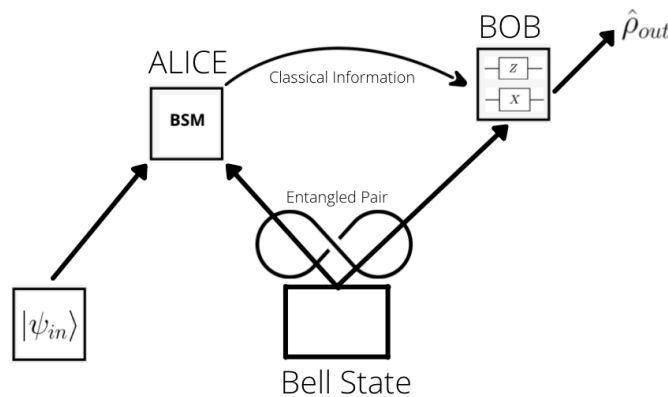


Figure 2.24: SQT scheme representation. It can be appreciated the main steps to accomplished a protocol of standard teleportation. Adapted from<sup>2</sup>.

**Step 1.** Preparation of states: In this initial step, we need to prepare the input unknown state, a vector on the surface of the BS, which is the state that is going to be teleported, and the channel, in this case a Bell state. The entangled channel, Einstein-Podolsky-Rosen (EPR) pair, can be prepared by applying Hadamard gate ( $\hat{H}$ ) on the first qubit and then a controlled not gate ( $C\hat{N}OT$ ) taking the first party as controller and the second party as the target state.

$$\begin{aligned}
 \text{init} : |0\rangle_{Alice} \otimes |0\rangle_{Bob} &= |00\rangle_{AB}. \\
 (\hat{U}_{CNOT} \otimes \hat{I})(\hat{H} \otimes \hat{I})|0\rangle|0\rangle &= (\hat{U}_{CNOT} \otimes \hat{I})\frac{1}{\sqrt{2}}(|0\rangle + |1\rangle)|0\rangle \\
 &= (\hat{U}_{CNOT} \otimes \hat{I})\frac{1}{\sqrt{2}}(|0\rangle|0\rangle + |1\rangle|0\rangle) \\
 &= \frac{1}{\sqrt{2}}(|00\rangle + |11\rangle).
 \end{aligned} \tag{2.20}$$

**Step 2.** The input state and one of the parties of the entangled channel are sent to Alice station, while the other half of the entangled channel is sent to the Bob Station. Alice with her two qubits performs a Bell State Measurement (BSM) which consist of a controlled not gate with the input state as controller and the target the member of the EPR pair, followed by a Hadarmard gate ( $\hat{H}$ ) on input qubit.

$$\begin{aligned}
 \text{init} : |\psi_{in}\rangle \otimes \frac{1}{\sqrt{2}}(|00\rangle + |11\rangle) &= (\alpha|0\rangle + \beta|1\rangle) \otimes \frac{1}{\sqrt{2}}(|00\rangle + |11\rangle) = \frac{1}{\sqrt{2}}(\alpha|000\rangle + \alpha|011\rangle + \beta|100\rangle + \beta|111\rangle). \\
 (\hat{H} \otimes \hat{I} \otimes \hat{I})(\hat{U}_{CNOT} \otimes \hat{I})\frac{1}{\sqrt{2}}(\alpha|000\rangle + \alpha|011\rangle + \beta|100\rangle + \beta|111\rangle) &= (\hat{H} \otimes \hat{I} \otimes \hat{I})\frac{1}{\sqrt{2}}(\alpha|000\rangle + \alpha|011\rangle + \beta|110\rangle + \beta|101\rangle) \\
 &= \frac{1}{2}(\alpha|000\rangle + \alpha|100\rangle + \alpha|011\rangle + \alpha|111\rangle + \beta|010\rangle - \beta|110\rangle + \beta|001\rangle - \beta|101\rangle) \\
 &= \frac{1}{2}(|00\rangle(\alpha|0\rangle + \beta|1\rangle) + |10\rangle(\alpha|0\rangle - \beta|1\rangle) + |01\rangle(\alpha|1\rangle + \beta|0\rangle) + |11\rangle(\alpha|1\rangle - \beta|0\rangle)).
 \end{aligned} \tag{2.21}$$

This expression can be reorganized using the following expressions:

$$\begin{aligned}
 |00\rangle &= \frac{1}{\sqrt{2}}(|\Phi^+\rangle + |\Phi^-\rangle), \\
 |01\rangle &= \frac{1}{\sqrt{2}}(|\Psi^+\rangle + |\Psi^-\rangle), \\
 |10\rangle &= \frac{1}{\sqrt{2}}(|\Psi^+\rangle - |\Psi^-\rangle), \\
 |11\rangle &= \frac{1}{\sqrt{2}}(|\Phi^+\rangle - |\Phi^-\rangle).
 \end{aligned} \tag{2.22}$$

Then, the equation 2.21, after  $\hat{U}_{CNOT}$  and  $\hat{H}$  operations, can be seen in the Bell bases, which help us to understand what is the purpose of BSM, which actually is to explore in which of the Bell states the Alice's parties are.

$$\frac{1}{2}(|\Phi^+\rangle(\alpha|0\rangle + \beta|1\rangle) + |\Phi^-\rangle(\alpha|0\rangle - \beta|1\rangle) + |\Psi^+\rangle(\alpha|1\rangle + \beta|0\rangle) + |\Psi^-\rangle(\alpha|1\rangle - \beta|0\rangle)). \tag{2.23}$$

At the end of equations 2.21 and 2.23 each part member of the sum posses the Bob party state in a superposition with the amplitudes of the input state, in some cases these coefficients are on the wrong basis or the state has a different phase, which is actually what opens the third step. Also, it is important to mention that each Bell state is equally probable, and as we notice they are four, each gets a  $p = \frac{1}{4}$ .

**Step 3.** As Bob already posses on his station the amplitudes of the superposition, he just needs to apply conditioned recovery operations on his parti in order to be able to obtain the input state. To accomplish this, Alice communicates her result (2 classical bits according to equation 2.21) of the BSM to Bob through any classical communication channel.

An alternative for this classical communication, which actually for our purpose of executing our code into QCs is the "Deferred Measurement Principle (DMP)", which works with controlled quantum operations, applying same recovery operation that Bob would do it. We use controlled conditioned operations, where the controllers (outputs from Alice) applies  $\hat{Z}$  and  $\hat{X}$ , respectively to target (Bob). For our current development, we have following conditioned operations:

Alice 1	Alice 2	Bob
0	0	$\hat{I}$
0	1	$\hat{Z}$
1	0	$\hat{X}$
1	1	$\hat{X}\hat{Z}$

Table 2.2: Recovery Operations dependence on the BM for SQT.

## 2.3 Controlled Quantum Teleportation

Controlled quantum teleportation (CQT) works in a very similar way that SQT, but now we have the appearance of the "Controller" which actually will be responsible for the correct transference of the input quantum state from Alice station to Bob station. The controller, commonly called Charlie, appears in this scenario due to our channel, which is tripartite, and if this station wants to allow the success of the protocol, he needs to apply and specific operation, and reveal the result of measurement into his qubit. The protocol consist of the following steps:

**Steps 1.** Preparations of the input state (or state to be teleported) and the quantum tripartite channel. As it has been mentioned, the channel now is tripartite and two tripartite maximal entangled quantum states are Greenberger-Horne-Zeilinger (GHZ) and W-states ( $|W\rangle$ ). The preparation of the states that will be used as channels will be explained in methodology section.

$$\begin{aligned}
 |GHZ\rangle &= \frac{1}{\sqrt{2}}(|000\rangle + |111\rangle), \\
 |W\rangle &= \frac{1}{\sqrt{3}}(|001\rangle + |010\rangle + |100\rangle).
 \end{aligned}
 \tag{2.24}$$

For simplicity, we will use  $|GHZ\rangle$  state to explained the basics of the protocol. Then, the systems at first is:

$$\begin{aligned}
 init : (|\psi_{in}\rangle)_I \otimes (|GHZ\rangle)_{ABC} &= (\alpha|0\rangle + \beta|1\rangle) \otimes \frac{1}{\sqrt{2}}(|000\rangle + |111\rangle) \\
 &= \frac{1}{\sqrt{2}}(\alpha|0000\rangle + \alpha|0111\rangle + \beta|1000\rangle + \beta|1111\rangle).
 \end{aligned}
 \tag{2.25}$$

**Step 2.** As previous step 2, the input state and the first qubit of GHZ state are sent to the Alice Station, while second parti is sent to the Bob station and the third parti to the Charlie (controller) station. Once Alice owns her two parties, she performs a Bell measurement, following the same operations as in SQT, controlled-not and Hadamard on input state. The whole system will look like:

$$\begin{aligned}
& (\hat{H} \otimes \hat{I} \otimes \hat{I} \otimes \hat{I})(\hat{U}_{CNOT} \otimes \hat{I} \otimes \hat{I}) \frac{1}{\sqrt{2}}(\alpha|0000\rangle + \alpha|0111\rangle + \beta|1000\rangle + \beta|1111\rangle) \\
&= (\hat{H} \otimes \hat{I} \otimes \hat{I} \otimes \hat{I}) \frac{1}{\sqrt{2}}(\alpha|0000\rangle + \alpha|0111\rangle + \beta|1100\rangle + \beta|1011\rangle) \\
&= \frac{1}{2}(\alpha|0000\rangle + \alpha|1000\rangle + \alpha|0111\rangle + \alpha|1111\rangle + \beta|0100\rangle - \beta|1100\rangle + \beta|0011\rangle - \beta|1011\rangle).
\end{aligned} \tag{2.26}$$

**Step 3.** If the controller decides to participate in the protocol and make the process successful, that is equal to apply a unitary operation on his qubit, for GHZ states, the operations is  $\hat{H}$ , or any other  $U(\lambda)$ :

$$\begin{aligned}
& (\hat{I} \otimes \hat{I} \otimes \hat{I} \otimes \hat{H}) \frac{1}{\sqrt{2}}(\alpha|0000\rangle + \alpha|1000\rangle + \alpha|0111\rangle + \alpha|1111\rangle + \beta|0100\rangle - \beta|1100\rangle + \beta|0011\rangle - \beta|1011\rangle) \\
&= \frac{1}{2\sqrt{2}}(\alpha|0000\rangle + \alpha|0001\rangle + \alpha|1000\rangle + \alpha|1001\rangle + \alpha|0110\rangle - \alpha|0111\rangle + \alpha|1110\rangle - \alpha|1111\rangle \\
&\quad + \beta|0100\rangle + \beta|0101\rangle - \beta|1100\rangle - \beta|1101\rangle + \beta|0010\rangle - \beta|0011\rangle - \beta|1010\rangle + \beta|1011\rangle) \\
&= \frac{1}{2\sqrt{2}}(|000\rangle(\alpha|0\rangle + \beta|1\rangle)_B + |001\rangle(\alpha|0\rangle - \beta|1\rangle)_B + |100\rangle(\alpha|0\rangle - \beta|1\rangle)_B + |101\rangle(\alpha|0\rangle + \beta|1\rangle)_B \\
&\quad + |010\rangle(\alpha|1\rangle + \beta|0\rangle)_B + |011\rangle(-\alpha|1\rangle + \beta|0\rangle)_B + |110\rangle(\alpha|1\rangle - \beta|0\rangle)_B + |111\rangle(-\alpha|1\rangle - \beta|0\rangle)_B).
\end{aligned} \tag{2.27}$$

In this way is very easy to see that bob now posses on his side the amplitudes of input state, and with some unitary transformations will be able to recover the input state. This is used to rotate his qubit to a suitable basis, before his perform a measurement, which will be eventually sent to Bob.

If Charlie has decided not participating in the protocol, that is equal to do not apply any operation on his qubit, and do not shared any information about his measurements. Then, equation 2.26 can be reorganized as:

$$\begin{aligned}
& \frac{1}{\sqrt{6}}(|000\rangle(\alpha|0\rangle)_B + |100\rangle(\alpha|0\rangle)_B + |011\rangle(\alpha|1\rangle)_B + |111\rangle(\alpha|1\rangle)_B \\
& \quad + |010\rangle(\beta|0\rangle)_B + |110\rangle(-\beta|0\rangle)_B + |001\rangle(\beta|1\rangle) + |101\rangle(-\beta|1\rangle)_B).
\end{aligned} \tag{2.28}$$

As we see, we have not been able to obtain the coefficients of the superposition of the input qubit on the Bob station if the controller has decided to do not participate in the teleportation.

**Step 4.** Now, Alice through the classical communication channel, shares her information of the BSM, again she transmits 2 bits of information. Also, it is important that Charlie shares his bit of information regarding his measurement, to complete the protocol by Bob applying the necessary recovery operations. The unitary recovery operations by Bob are needed in following way:

Alice 1	Alice 2	Charlie	Bob
0	0	0	$\hat{I}$
0	0	1	$\hat{Z}$
0	1	0	$\hat{X}$
0	1	1	$\hat{X}\hat{Z}$
1	0	0	$\hat{Z}$
1	0	1	$\hat{I}$
1	1	0	$\hat{X}\hat{Z}$
1	1	1	$\hat{X}$

Table 2.3: Recovery Operations dependence on the BM for CQT using GHZ entangled state.

## 2.4 Fidelity of States - Quantifier of Efficiency and its Bounds for Quantum Teleportation

Once that both protocols of teleportation which we are going to deal have been introduced, an important question arrives regarding its performance, how much accurate was our quantum device teleporting or transmitting the information we have sent. Then, an important calculation needs to be mention, and is the Average Fidelity of States (AVF), which basically, provides a way to compare the similarities between input and output states, then very easily, it can be computed as:

$$F(\theta, \phi) = |\langle \psi_{in} | \psi_{out} \rangle|^2 = \langle \psi_{in} | \psi_{out} \rangle \langle \psi_{out} | \psi_{in} \rangle = \langle \psi_{in} | \hat{\rho}_{out} | \psi_{in} \rangle. \quad (2.29)$$

Given that the performance of quantum teleportation comes from fidelity of states, a stronger measure of the success is the average of local fidelities. This average will consider the contribution of each possible state on the surface of the Bloch sphere, evolved by the gates that define the protocol, throwing the output state needed in equation 2.29.

We can obtain this result by considering that we are going to have continuous angles, it means, a continuous set of vectors, as:

$$F_{avg} = \frac{1}{\Omega} \int_0^\pi \int_0^{2\pi} F(\theta, \phi) R^2 \sin(\theta) d\theta d\phi = \frac{1}{4\pi} \int_0^\pi \int_0^{2\pi} F(\theta, \phi) \sin(\theta) d\theta d\phi. \quad (2.30)$$

It is important to introduce a variation of equation 2.29, given that it just considers pure states, and as in our process of real computation, our open system will be noisy by different sources, then we are going to use the fidelity of states which takes as input density matrices, and it throws back again a scalar quantity, defined as:

$$F(\theta, \phi) = \text{Tr}(\sqrt{\sqrt{\hat{\rho}_{in}} \hat{\rho}_{out} \sqrt{\hat{\rho}_{in}}})^2. \quad (2.31)$$

### Standard Quantum Teleportation

We have still as arguments  $\theta$  and  $\phi$  because we want to keep the initial and output state as arbitrarily defined by its angles. As we have seen, entanglement in the channel is actually what exhibits quantum behavior, making the protocol able to teleport a quantum state.

Then, as we have a way to test the improvement of quantum regime, let's see how much better is with respect to a classical behavior. To answer this, let's compute the average fidelity according to equation 2.30 with a classical channel, it means without any kind of entanglement between Alice and Bob. Then, initially our systems is:

$$|\phi_{in}\rangle = |\psi\rangle_1 \otimes |00\rangle_{23} = (\alpha|0\rangle + \beta|1\rangle) \otimes |00\rangle, \quad (2.32)$$

where the matrix representation of  $|\phi\rangle$  is:

$$\hat{\rho}_{in} = |\psi\rangle_1 \langle\psi| = \begin{bmatrix} |\alpha|^2 & \alpha\beta^* \\ \alpha^*\beta & |\beta|^2 \end{bmatrix} = \begin{bmatrix} \cos^2(\frac{\theta}{2}) & \cos(\frac{\theta}{2})e^{-i\phi} \sin(\frac{\theta}{2}) \\ \cos(\frac{\theta}{2})e^{i\phi} \sin(\frac{\theta}{2}) & \sin^2(\frac{\theta}{2}) \end{bmatrix}. \quad (2.33)$$

As any input state can be defined by its amplitudes of superposition to get  $\hat{\rho}_{out}$ , we just need to evolve  $|\phi_{in}\rangle$  under the protocol gates and then trace out  $\{1, 2\}$  subsystems, where in the first step we just prepare input qubit. We can include all operator in a superoperator  $\hat{U}_s$ :

$$\hat{U}_s = (\hat{C}X_{23})(\hat{C}Z_{13})(\hat{H}_1 \otimes \hat{I}_2 \otimes \hat{I}_3)(\hat{C}X_{12} \otimes \hat{I}_3). \quad (2.34)$$

So,  $\hat{\rho}_{out}$  becomes:

$$\begin{aligned} \hat{\rho}_{out} &= \text{Tr}_{12}[\hat{U}_s|\phi_{in}\rangle\langle\phi_{in}|\hat{U}_s^\dagger] = \text{Tr}_{AB}[(\alpha|000\rangle + \beta|111\rangle)(\alpha^*\langle 000| + \beta^*\langle 111|)] \\ &= \begin{bmatrix} |\alpha|^2 & 0 \\ 0 & |\beta|^2 \end{bmatrix} = \begin{bmatrix} \cos^2(\frac{\theta}{2}) & 0 \\ 0 & \sin^2(\frac{\theta}{2}) \end{bmatrix}. \end{aligned} \quad (2.35)$$

We are just missing to compute the fidelity according to equation 2.30 and then integrate. Something to mention is that  $\hat{\rho}_{out}$  has become a mixed state. Let's see how the fidelity becomes:

$$F(\theta, \phi) = \begin{bmatrix} \alpha^* & \beta^* \end{bmatrix} \begin{bmatrix} |\alpha|^2 & 0 \\ 0 & |\beta|^2 \end{bmatrix} \begin{bmatrix} \alpha \\ \beta \end{bmatrix} = |\alpha|^4 + |\beta|^4 = \cos^4\left(\frac{\theta}{2}\right) + \sin^4\left(\frac{\theta}{2}\right) = \frac{1}{4}(3 + \cos(2\theta)). \quad (2.36)$$

And finally, we can integrate under each possible contribution coming from each possible vector.

$$\begin{aligned} F_{avg} &= \frac{1}{4\pi} \int_0^\pi \int_0^{2\pi} \frac{1}{4}(3 + 2\cos(2\theta)) \sin(\theta) d\theta d\phi = \frac{1}{8} \int_0^\pi (3 \sin(\theta) + 2\cos(2\theta) \sin(\theta)) d\theta \\ &= \frac{1}{8} \left( \frac{2}{3} - \left(-\frac{2}{3}\right) \right) = \frac{2}{3}. \end{aligned} \quad (2.37)$$

This is an important result given that it is the classical limit, and it means that if the quantum channel that is used to transmit information is not entangled, then the maximum value that the fidelity can achieve is  $\frac{2}{3}$ .

Now, let's explore what happens in the quantum regime, where the best would it be the maximal entanglement, which could be thought as our upper limit. For this, let's compute again the elements for average fidelity. Our input  $|\psi_{in}\rangle$  again is random and we will use  $|\Phi^+\rangle$ .

Then the system initially is  $|\phi_{in}\rangle_{123} = |\psi_{in}\rangle_1 \otimes |\Phi^+\rangle_{23}$ , let's evolve again this state under the protocol gates, and trace out the  $\{1, 2\}$  subsystems to get the outcome state on the third station.

$$\hat{\rho}_{out} = \text{Tr}_{12}[\hat{U}_s|\phi_{in}\rangle_{123}\langle\phi_{in}|\hat{U}_s^\dagger] = (\alpha|0\rangle + \beta|1\rangle)(\alpha^*\langle 0| + \beta^*\langle 1|) = \begin{bmatrix} |\alpha|^2 & \alpha\beta^* \\ \alpha^*\beta & |\beta|^2 \end{bmatrix}. \quad (2.38)$$

We see that this Bell state allows the perfect transference of information according equation 2.21. Then the state in the Bob station is exactly the input state. Now, we have everything, so, let's compute the fidelity.

$$\begin{aligned} F(\theta, \phi) &= [\alpha^* \ \beta^*] \begin{bmatrix} |\alpha|^2 & \alpha\beta^* \\ \alpha^*\beta & |\beta|^2 \end{bmatrix} \begin{bmatrix} \alpha \\ \beta \end{bmatrix} = |\alpha|^4 + |\alpha|^2|\beta|^2 + |\beta|^2|\alpha|^2 + |\beta|^4 \\ &= \cos^4\left(\frac{\theta}{2}\right) + \sin^4\left(\frac{\theta}{2}\right) + 2\sin^2\left(\frac{\theta}{2}\right)\cos^2\left(\frac{\theta}{2}\right) = 1. \end{aligned} \quad (2.39)$$

And, finally the average fidelity:

$$F_{avg} = \frac{1}{4\pi} \int_0^\pi \int_0^{2\pi} \sin(\theta) d\theta d\phi = \frac{1}{2} (1 - (-1)) = 1. \quad (2.40)$$

As we mentioned, the average fidelity reaches its maximum value 1, when the the channel is maximally entangled. In addition, it can be understood that there exist a transition, from the classical limit 2/3 to 1, while the entanglement grows between Alice and Bob, which shows that quantum description and properties of subsystems can provide the perfect media for effective transmission of information.

### Controlled Quantum teleportation

In previous section we described quantum teleportation protocol using three-partite entangled states as GHZ and Werner states<sup>17</sup>. An interesting feature born when the channel of transmission has more than 2 parties and is the Controlled teleportation. As its name indicates, a third parti in the entangled channel can control the success of the protocol, making it possible to transmit the information in the most efficient way or in the other reaching just the limit of non permission.

So, let's explore, how the fidelity changes depending on the decision of Charlie of allowing or not the perfect teleportation.  $F_{CQT}$  is what denotes fidelity of controlled quantum teleportation, then, as was said, the controller or Charlie, performs a orthogonal measurement on his qubit or parti 4 with a outcome t, and for this purpose let's say that the tripartite entangled channel is  $\hat{\rho}$ , then, just after the measurement, the state for channel subsystems {2,3} are:

$$\hat{\rho}'_{2,3} = \frac{\text{Tr}_4[\hat{U}_4^\dagger |t\rangle\langle t| \hat{U}_4 \otimes \hat{I} \hat{\rho} \hat{U}_4^\dagger |t\rangle\langle t| \hat{U}_4 \otimes \hat{I}]}{\langle t| \hat{U}_4 \hat{\rho}_4 \hat{U}_4^\dagger |t\rangle}. \quad (2.41)$$

This state has the projection of the measurement performed on Charlie subsystem  $\hat{U}_4$ , its outcome t, the  $\hat{I}$  operator is the identity matrix of dimension  $4 \times 4$  to satisfy the dimension of the whole system, and the term  $\langle t| \hat{U}_4 \hat{\rho}_4 \hat{U}_4^\dagger |t\rangle$ , is the normalization factor for the subsystems state, coming from the probability of having as result t in the measurement, where  $\hat{\rho}_4 = \text{Tr}_{23}(\hat{\rho})$  is the density matrix for the reduced Charlie state. With this, we can define the fidelity as:

$$F_{CQT}(\hat{\rho}) = \max_{U_4} \left[ \sum_{t=1}^{t=0} \langle t| \hat{U}_4 \hat{\rho}_4 \hat{U}_4^\dagger |t\rangle F(\hat{\rho}'_{2,3}) \right]. \quad (2.42)$$

The term  $F(\hat{\rho}'_{2,3})$  is the faithfulness of the standard teleportation trough the residual state of subsystems {2,3} according to<sup>18</sup>. Using the fully entangled fraction (FEF) quantity as  $f(\hat{\rho}) = \max_e \langle e| \hat{\rho} |e\rangle$ , the fidelity can be defined as  $F(\hat{\rho}) = \frac{2f(\hat{\rho})+1}{3}$ . This expression provides the chance to write non-conditioned and controlled (conditioned) fidelities in a very useful way:

$$F_{CQT}(\hat{\rho}) = \frac{2\max_U [\sum_{t=0}^{t=1} \langle t| \hat{U}_4 \hat{\rho}_4 \hat{U}_4^\dagger |t\rangle f(\hat{\rho}'_{2,3})] + 1}{3}. \quad (2.43)$$

This allows to define very clearly the non-conditioned fidelity, given that Charlie decides do not participate, then, he does not apply the  $\hat{U}$  operation, and obviously do not shared anything regarding his state, then  $F_{NC}(\rho)$  becomes:

$$F_{NC}(\hat{\rho}) = \frac{2f(\hat{\rho}_{23}) + 1}{3}, \quad (2.44)$$

where  $\hat{\rho}_{23} = \text{Tr}_2(\hat{\rho})$ . An intuitive way of thinking about controlled limits, is to measure standard teleportation fidelities for each possible unitary operation on Bob's qubit, and then the maximal fidelity will define the operation we have full participation of Charlie.

Also, we can note, for example in the  $|GHZ\rangle$  state, that if Charlie state is projected into one of its bases states, the remaining state is separable, then it means that we are going to be placed on the classical regime getting a fidelity less or equal to  $2/3$ . On the other hand, if Charlie, for example, applies a  $\hat{H}$  operation, and shares his bit regarding his measurement, the teleportation efficiency reaches its maximum fidelity of 1.

In this sense, we have a new quantity that helps us to define the strength of the controller by the parameter called the **control power**, defined by:

$$P(\hat{\rho}) = F_{CQT}(\hat{\rho}) - F_{NC}(\hat{\rho}). \quad (2.45)$$

It is important to mention that controlled protocol of teleportation is just valid for the regions where the non-conditioned fidelity does not exceed the classical regime  $F_{NC} \leq 2/3$  and the controlled (conditioned) fidelity  $F_{CQT} > 2/3$ , then the power control gets appropriate values.

## 2.5 Causality Problem

The development of entanglement<sup>6</sup> during its initial moments have attracted a lot of attention, because of it was thought that special relativity was violated by entangled parties and that information could travel instantaneously, faster than the speed of the light. We have established that the Einstein theory of special relativity was not violated in the standard and controlled protocol of teleportation because Alice needs to share her outcomes making use of any kind of classical channel, in order to Bob recover the input state.

So, an important question takes place when we push the idea of entanglement and remote transmission of information without an intermediate processes, "how information is transmitted without violating special relativity using entanglement and Bell measurement".

To explore the temporal behavior Holger Hofman<sup>3</sup> has developed a precise formalism, where the causality can be treated due to special properties that the entangled channel possess, and how noisy environments could alter the information transmitted from the Alice Station. To start, let's write our maximal entangled quantum state, the Bell State that is shared between Alice and Bob, in the following way:

$$|\psi\rangle_{A,B} = \frac{1}{\sqrt{2}} \sum_{n=0}^{n=1} (\hat{U}_0|n\rangle)_A \otimes |n\rangle_B. \quad (2.46)$$

Here, we are using common computational basis where  $|n=0\rangle = |0\rangle$  and  $|n=1\rangle = |1\rangle$ , as described in the previous section. It is important to notice that the Unitary operator  $\hat{U}_0$  defines the properties of the entangled channel, because it is used to relate the action of an operator (observable)  $\hat{O}_A$  on the Alice's parti, and an operator (observable) on the Bob's parti  $\hat{O}_B$ , by the following relation  $\hat{U}_R = \hat{U}_0 \hat{U}_A^T \hat{U}_0^{-1}$ .

Following the protocol, created the input state  $|\Psi\rangle_{in}$  and  $|\psi_{max}\rangle_{A,B}$ , the next step is the Bell measurement between input and A, and can be seen with the following relation. Initially, joining the three members, we have:

$$\frac{1}{\sqrt{2}} \sum_n |\psi_{in}\rangle_{A_{in}} \otimes (\hat{U}_0|n\rangle)_A \otimes |n\rangle_B. \quad (2.47)$$

Then, the Bell measurement in the sub Hilbert space of  $A_{in}$  and A is introduced by:

$$\sqrt{\frac{\chi(m)}{2}} \sum_{n'} (\langle n' | \hat{U}^{-1}(m) \rangle_{A_{in}} \otimes \langle n' | \hat{U}_0^{-1} \rangle_A). \quad (2.48)$$

This projects the parties that are in possession of Alice to maximally entangled Bell state, where the  $\hat{U}(m)$  and  $\hat{U}_0$  now define the properties of the state in which  $A_{in}$  and A have been projected to, with  $m$  as an outcome, and the normalization factor  $\chi(m)$  to accomplish a quantum state in concordance with a probability distribution. The conditioned output state, then can be seen, on the Bob station as:

$$\sqrt{\frac{\chi(m)}{2}} \sum_n \langle n | \hat{U}^{-1}(m) | \psi_{in} \rangle |n\rangle_B. \quad (2.49)$$

As can be noticed, the sandwich between the basis and the input state to the unitary operator  $\hat{U}$  will provide the amplitudes of the superposition of the initial state, into the Bob state, finally getting the following state for Bob:

$$\hat{U}^{-1}(m) \frac{\sqrt{\chi(m)}}{2} |\psi_{in}\rangle_B. \quad (2.50)$$

The only missing part, is the classical communication carry out by Alice, sharing her  $m$  result, then giving a value to  $\chi(m)$  and designing an recovery operation to  $\hat{U}(m)$ .

The development of this suitable and simple formalism helps a lot at the moment of introducing any kind of extra source. According to this definition, the existing entanglement between the two parties, provides the chance to know how the outcome (at the Bob station) at the end of the protocol is affected by any kind of noisy source, not just directly on the receiving station, but also in the other two, it means that any action on the sending station will alter the teleported state.

In order to introduce external sources, let's suppose that in the bipartite entangled channel, each parti will be affected by some operator  $\hat{E}_A$  and  $\hat{F}_B$ , respectively. Then, let's see how the system is initially:

$$\frac{1}{\sqrt{N}} \sum_n |\psi_{in}\rangle_{A_{in}} \otimes (\hat{E} \hat{U}_0 |n\rangle)_A \otimes (\hat{F} |n\rangle)_B. \quad (2.51)$$

For the next step, the Bell measurement works in the same way as in equation (1.19), acting on  $A_{in}$  and B, and the output state on Bob station is:

$$\hat{U}^{-1}(m) \frac{\sqrt{\chi(m)}}{N} \hat{U}(m) \hat{F}_B (\hat{U}_0^{-1} \hat{E}_A \hat{U}_0)^T \hat{U}^{-1}(m) |\psi_{in}\rangle_B. \quad (2.52)$$

It is important to highlight that the coefficients of the superposition of the input state now become given by the  $\langle n' | \hat{U}^{-1}(m) | \psi_{in} \rangle$  and  $\langle n' | \hat{U}_0^{-1} \hat{E}_A \hat{U}_0 | n \rangle$ , which depend on the action of  $\hat{U}$  and  $\hat{E}$  acting on first and second qubit. Also, it is important to notice that we can summarize the operators in a  $\hat{T}_{out}$  operator, which acts directly on the output state on the Bob qubit, by the special property of entanglement, translating every action on A to B. Then:

$$\hat{T}_{out} = \frac{\sqrt{\chi(m)}}{N} \hat{U}(m) \hat{F}_B (\hat{U}_0^{-1} \hat{E}_A \hat{U}_0)^T \hat{U}^{-1}(m) = \frac{\sqrt{\chi(m)}}{N} \hat{U}(m) \hat{F}_B \hat{E}_B \hat{U}^{-1}(m). \quad (2.53)$$

Now, we have the option to check the causality in output state depending on the affection on the quantum channel, the operations on Bob have an order, first  $\hat{E}$  and then  $\hat{F}$ , even if they happened in a reverse order in time. It shows

how the past of qubit A is connected to B. If we push to this idea, we can formulate this operator depending on results of  $\hat{E}(l)$ , which is a measurement performed by an eavesdropping trying to extract information of our system and  $l$  the outcome dependence (0 or 1), by the minimal backaction measurement in the A parti in entangled channel.

According to the author, the study of this effect becomes interesting, due to the extraction of information, by the Quantum Non demolition measurement followed by the minimal backaction which, in fact, could produce some perturbation to the measured quantity, letting the state variant under that kind of transformation, and according to our formalism is what defines the  $l$  dependence.

To check how the information is preserved during the protocol of teleportation, we are going to use, as explained, the quantum fidelity, which allows to make a comparison of similarity between the teleported state at the beginning and the output state in the B station. To achieve this, let's make use of the  $\hat{T}$  operator with a variation on the dependence of  $l, m$  results. Then:

$$\hat{P}(l, m) = \frac{\sqrt{\chi(m)}}{N} \hat{U}(m) (\hat{U}_0^{-1} \hat{E}_A(l) \hat{U}_0)^T \hat{U}^{-1}(m), \quad (2.54)$$

where, the result of a measurement like, gets a probability of:

$$p(l, m) = \langle \psi_{in} | \hat{P}^2(l, m) | \psi_{in} \rangle = \frac{\chi(m)}{N^2} \langle \psi_{in} | \hat{U}(m) (\hat{U}_0^{-1} \hat{E}_A^2(l) \hat{U}_0)^T \hat{U}^{-1}(m) | \psi_{in} \rangle. \quad (2.55)$$

So, if some measurement is made on the quantum channel, then some of information is extracted, and the resulting quantum state becomes, which obeys normalization:

$$|\psi_{out}\rangle_B = \sqrt{p(l, m)^{-1}} \hat{P}(l, m) |\psi_{in}\rangle_B. \quad (2.56)$$

With information of the outcome state of the teleportation, we can then compute quantum fidelity of states  $F(l, m)$  as:

$$F(l, m) = |\langle \psi_{in} | \psi_{out} \rangle|^2 = p(l, m)^{-1} |\langle \psi_{in} | \hat{P}(l, m) | \psi_{in} \rangle|^2. \quad (2.57)$$

Which in fact is bounded between 0 and 1. In addition, it is important to note and check that the unitary operators conserve the unitary of the whole quantum state, which can be seen in term of the density matrix accomplishing  $\hat{\rho}_i = \hat{U}_i \hat{\rho}_i \hat{U}_i^\dagger$ .

**Time-Reversal Treatment in Quantum Teleportation:** According to M. Laforest and R. Laflamme<sup>19</sup>, where a theoretical formalism is develop and, in addition, an experimental exploration of maximal bipartite entanglement is done, a time-reversal process must occur. To clarify this idea, let's see the protocol carefully.

We have said that at first we need to prepare our input states (init state plus entangled state), then we move to the stage, where a Bell measurement is performed between Alice's parties. Before moving to the next step, let's check equation 2.29. At the end of the Bell measurement there are four states in a superposition, and one of them is the input state, the other three possess the amplitudes of the input states, but in a different basis or with an additional phase.

It will mean that there exists  $\frac{1}{4}$  of probability of getting the input state without the need of Alice's classical communication. Then, the question is born, "how information is being transmitted without breaking the special relativity, if we carefully look again to the components of the protocol, the only choice of the transmission of the information is the moment of the creation of the entangled state, and if we see this happens before the Bell measurement, it means that the carrier of the Alice's information should have traveled back in time until Bell state creation and transmits what happened to the state during the Bell measurement, connecting two steps of the protocol.

This is what define the time reversal causality in a protocol of quantum teleportation, and considering the situation where there is one of four chances to get the correct state, the situation is known as "conditional time travel". In

addition, Coecke<sup>20</sup> argues that in any of the four situation, the information is send backward in time, it is just the Alice's measurement on her side that affects the final state, providing that Bob could end up with the desired information or with a state with variations.

Finally, the causality problem in the time reversal treatment is addressed by E. Kiktenko and S. Korotaev<sup>21</sup>, where by computing entanglement entropies can study the causal order in teleportation.

## 2.6 Problem Statement

The temporal causality idea becomes relevant when we try to understand how the transmitted information could be preserved by the quantum channel, when it is exposed to the environment, which could induce decoherence. Then, as we saw, the  $\hat{T}$  operator encloses possible noisy operators acting on the entangled parties, as a minimal backaction, being able to produce a decrease in the fidelity value.

Given that physical systems are supposed to do not have local interactions, it means they are separated in space, then the causality is important when we try to describe the connecting events on A to the output at B. As fidelity of states gives us the chance to quantify the success of the the protocol, and as we already have described what could reduce this value, then some attractive thoughts arrive with this formalism, and they are the main motivation of our study.

At first, let's suppose we know which are the noisy operators (E and F), then the first question comes: Are these operators going to produce the same effects on the fidelity value, if they are being applied in different orders? And, second question: given that we know which are the exact relations connecting the events between each party, for example, in the entangled channel the connection coming from the  $\hat{U}_0$  operator for A and B, and then the Bell measurement connecting  $A_m$  and A, is there going to be any difference in fidelity of states if we place our noisy operator in different qubits?

Summarizing, the main aim of this job is represented by the study of the causal effects on the output state, when we know which are the noisy operators, making different configurations, by applying them at different stages of the protocol and to different carriers of information, computing the fidelity quantifier, when each protocol is finished.

### General and Specific Objectives

According to the previously formulated two questions, our general objective is to study the success of standard and controlled quantum teleportation under noisy environments, applying three approaches, the first one is a theoretical model, then making use of "qiskit" python package to study our theoretical model by the use of simulators and with these two previous results, to test our models in real public IBM's quantum processors. We will realize numerical integration, given that we can just take a finite number of input states. We will compute average fidelities with discrete set of angles, and then we will compare experimental results trying to exhibit the performance of IBM's quantum processors.

For: **SQT - CQT**

- Theoretical model test using  $F_{avg}$  quantity.
- Simulation test, execution on qiskit simulators using  $F_{avg}$  quantity.
- Experimental test, execution on IBMQ's devices, to corroborate the two previous items.



## Chapter 3

# Methodology

In the previous chapter, we have mentioned that we will be facing two types of protocols of quantum teleportation, each of them is gonna be explored using quantum circuit models. For this purpose we will make use of the "Qiskit python package". In addition, given that we want to compute average fidelities, the mathematical model should be discretized, as we can only consider a finite set of input states, which indeed breaks the continuity of previous developments.

Therefore, the approach we are going to use at each protocol is:

$$F_{avg} = \frac{1}{4\pi} \sum_{\theta_i}^{n\theta} \sum_{\phi_i}^{n\phi} \Delta\theta\Delta\phi F(\theta_i, \phi_i) \sin(\theta_i). \quad (3.1)$$

We know each angles bound that defines the deltas as,  $\Delta\theta = \frac{\theta_f - \theta_i}{n_\theta}$  and  $\Delta\phi = \frac{\phi_f - \phi_i}{n_\phi}$ , and what we just need is to find the local fidelities  $F(\theta, \phi)$  and modulate them by  $\sin(\theta)$ . Each angle can be computed by  $\theta_i = \Delta\theta * i$  where  $i$  will be the counter labeling each  $\theta$ , and the same for  $\phi$  angles.

### 3.1 Standard Quantum Teleportation

As we already made a distinction, the Standard Quantum Teleportation (SQT), is the study of transmission of information, through bipartite entangled quantum state, represented by Bell states. Given that our approach needs to employ quantum circuits, then let's explore each step in detail.

Using Qiskit, we need to define our quantum circuit, which needs as inputs the quantum register (qubits) and classical register (bits).

```
qrA = QuantumRegister(2, 'alice')
qrB = QuantumRegister(1, 'bob')
crA1 = ClassicalRegister(1, 'crA1')
crA2 = ClassicalRegister(1, 'crA2')

circuit_sqt = QuantumCircuit(qrA, qrB, crA1, crA2)
```

where, A and B are related to Alice and Bob, including both the quantum and classical registers. We have to remember that at the beginning the fiducial state of initialization is defined as  $|000\dots\rangle$

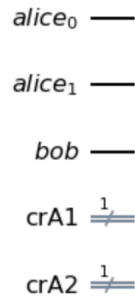


Figure 3.1: Initial circuit with quantum and classical registers. Classical registers are used to store the results of BSM.

**Step 1.** We have to prepare our initial state, the one that is going to be teleported or input state and entangled state, Einstein-Podolsky-Rosen (EPR) pair. To parametrize the input state  $|\psi\rangle = \alpha|0\rangle + \beta|1\rangle$ , Bloch Sphere (BS) angles are utilized, then what we need is just to set the angles that will define the position of the unit vector on the surface.

In this particular example we are going to use  $\theta = \pi$  and  $\phi = 0$ , which is the  $|1\rangle$  state, the entangled state will be implemented as said, by first applying the Hadamard gate ( $\hat{H}$ ) and then controlled-not gate ( $\hat{C}X$ ). The implementation then becomes:

```
a = np.cos(theta/2)
b = np.exp(1j * phi) * np.sin(theta/2)
circuit_sqt.initialize([a,b],0)
circuit_sqt.h(qrA[1])
circuit_sqt.cx(qrA[1],qrB[0])
```

We can see that the quantum register possesses a index depending on the number of register, in case of Alice [0] or [1], then the circuit looks like:

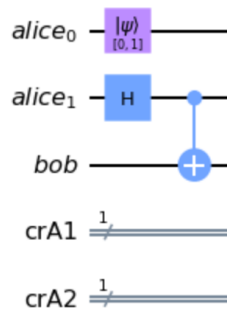


Figure 3.2: First step of teleportation, preparation of input states ( $Alice_0$ ) and the entangled state ( $Alice_1$  and  $Bob$ ).

**Step 2.** In the next step, we need to perform a Bell State Measurement (BSM), which for our purpose is implemented by the controlled-not ( $\hat{C}X$ ) gate and the Hadamard ( $\hat{H}$ ) gate:

```
circuit_sqt.cx(qrA[0],qrA[1])
circuit_sqt.h(qrA[0])
```

In order to distinguish the steps of teleportation, we are going to place barriers between each two steps, as showed in the following circuit. They just make simpler graphical representation, without any effect on qubits.

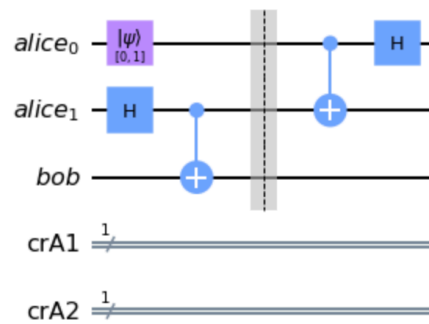


Figure 3.3: Second step of SQT represented by the BSM performed by Alice. The barrier is marked by the dotted line.

**Step 3.** In this step Alice performs measurements on her two qubits and the results are transmitted to Bob via classical communication. Given that we want to simulate the classical communication of Alice, we can measure her quantum registers, and then she will communicate a pair of classical bits to Bob.

Then, Bob with these outcomes will perform conditioned unitary operations, as already explained in the section one.

```

circuit_sqt.measure(qrA[0], crA1)
circuit_sqt.measure(qrA[1], crA2)
circuit_sqt.z(qrB).c_if(crA1, 1)
circuit_sqt.x(qrB).c_if(crA2, 1)

```

With this, we have already finished the protocol of SQT and our full circuit has become:

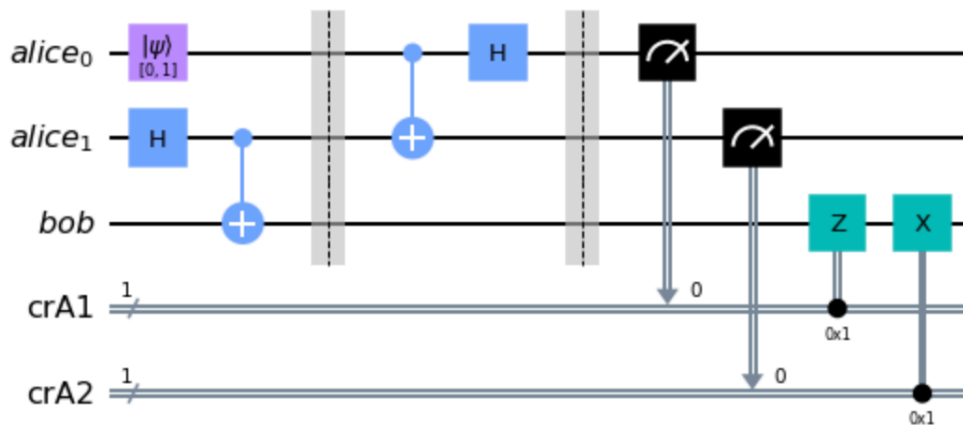


Figure 3.4: Third step of SQT, with the Alice results transferred to Bob via classical registers, and he applies the corrective unitary gates based on the obtained two bits.

If, everything has been successful, without the appearance of noisy sources and decoherence in the outcome qubit or the Bob parti, using another copy of the input state, we can validate the performance of our approach.

As it was mentioned, one can also use the Deferred Measurement Principle (DMP) and instead of classically conditioned operations, quantum ones are used, like  $\hat{C}X$  and  $\hat{C}Z$ , then the measurements can be done at the end. This is useful specially if classical registers are not available.

```

circuit_sqt.cz(qrA[0], qrB[0])
circuit_sqt.cx(qrA[1], qrB[0])

```

And the circuit looks like this:

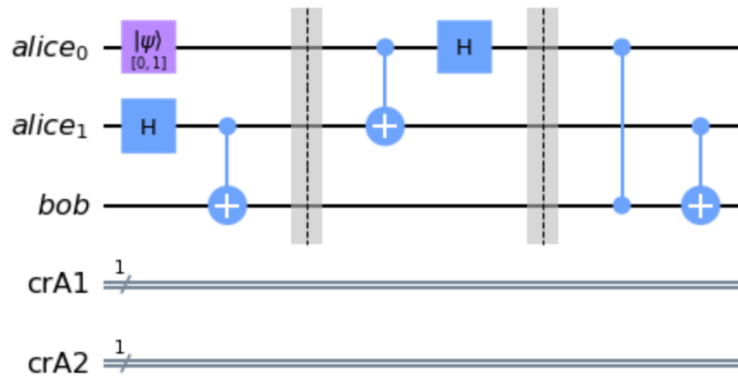


Figure 3.5: SQT circuit with the principle with deferred measurement. The recovery operations are controlled gates.

This last circuit, is the one we will use for the purpose of executing our experiment.

### SQT Interpretation via the Bloch Sphere

We can visualize the protocol of teleportation by using the BS for each single qubit, and see how they evolve when each gate is applied, starting by setting the input qubit state as a random state. It starts with the fiducial state, where all qubits are place in the  $|0\rangle$  state (see Figure 2.6),

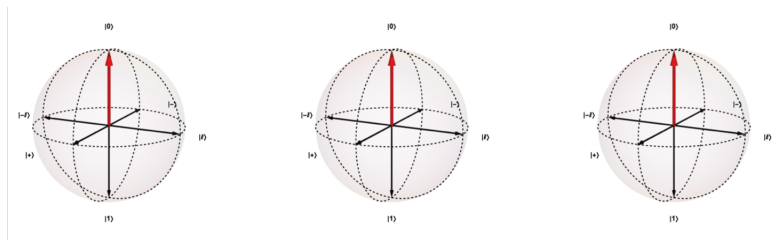


Figure 3.6: Fiducial state in SQT composed of 3 qubits, all set to the state  $|0\rangle$ . In this plot, as well in following ones, the order of qubits is:  $Alice_0, Alice_1, Bob_0$ .

followed by the initialization of input state (to be teleported) and application of H gate on the qubit  $Alice_1$ , and then, the CX operation with  $Alice_1$  as a controller and  $Bob_0$  as a target, as shown in the Figure 2.7.

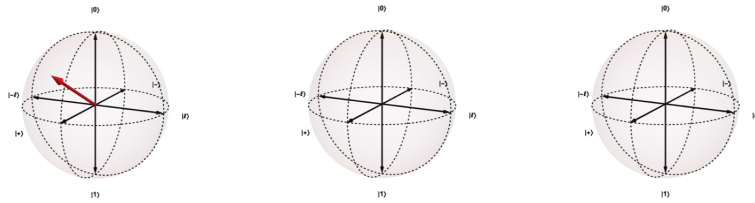


Figure 3.7:  $Alice_0$  is input state,  $Alice_1$  and  $Bob_0$  are used to form an entangled channel, implementing on the Bell State.

Jumping into the second stage, where the BSM is done, the  $\hat{C}X$  gate is applied on  $Alice_0$  and  $Alice_1$ , as target and controller, respectively.

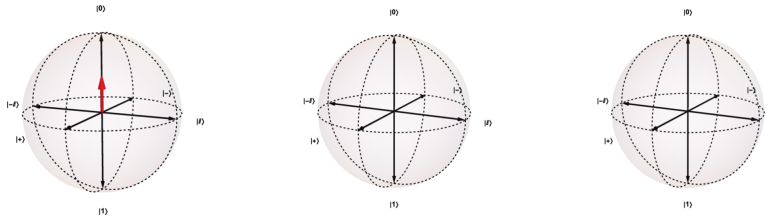


Figure 3.8: The  $\hat{C}X$  gate applied on  $Alice_0$  and  $Alice_1$  qubits.

The  $\hat{H}$  gate is applied on the  $Alice_0$  qubit to conclude with the Bell measurement, see Figure 2.9.

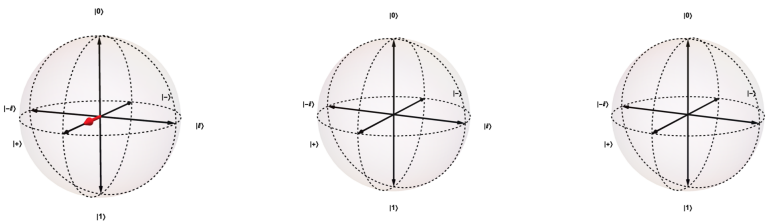


Figure 3.9: The H gate applied on  $Alice_0$  qubit to conclude the Bell state measurement.

Moving to the third stage, the CZ gate controlled by  $Alice_0$  is applied on  $Bob_0$ , using the deferred measurement principle.

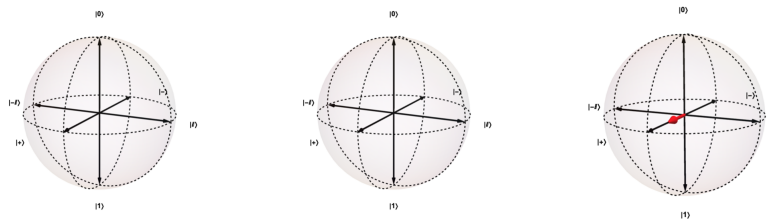


Figure 3.10: Recovery CZ operation on  $Bob_0$ .

And to conclude the CX gate between Alice1 and Bob, as controller and target, respectively, is applied. The final states of each qubits are presented in the Figure 2.11. As we can observe, the Bob qubit contains the teleported input state.

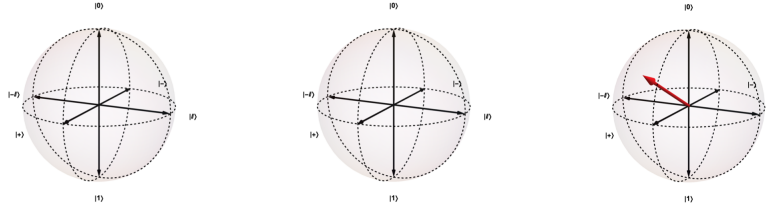


Figure 3.11: Output state of the SQT protocol. The *Bob* qubit represents the teleported state.

### Temporal Causality in SQT

In the section 1.5 related to Temporal Causality problem, we have established the dependence of the fidelity of states and how it is going to variate. So, we will try to explore this, by implementing a noisy source and checking that effectively the fidelity of states can variate, e.g. decreases.

We inserted noise in the input qubit or the qubits forming the entangled channel, and by varying its strength, we observe resulting effects. We will use a simple model, which implements this noisy source, making use of an extra qubit, on which we will first apply Hadamard operation to create a superposition of  $|0\rangle$  and  $|1\rangle$  states, and then it will be used to control the  $\hat{C}(\hat{U})$  applied on the qubit one in which we want to produce the decoherence.

In order to make it very simple, we can implement  $U$  as the rotation around x-axis-operator ( $\hat{R}_x$ ), then it becomes  $\hat{C}(\hat{R}_x)$ , which writes:

$$\begin{aligned} \hat{C}(\hat{R}_x)(\theta) &= |0\rangle_C \langle 0| \otimes \hat{I}_T + |1\rangle_C \langle 1| \otimes \hat{R}_x(\theta)_T \\ &= \begin{pmatrix} 1 & 0 & 0 & 0 \\ 0 & 1 & 0 & 0 \\ 0 & 0 & \cos \frac{\theta}{2} & -i \sin \frac{\theta}{2} \\ 0 & 0 & -i \sin \frac{\theta}{2} & \cos \frac{\theta}{2} \end{pmatrix}. \end{aligned} \quad (3.2)$$

As we saw in the section one, where we have treated the formalism of single qubits. Finally, our operator has a dependence on angle  $\theta$ , which will allow us to produce small rotations in a quasi-continuous way. This piece of code can be implemented, as:

```
nr = 21
alpha = pi / nr
#Stage of S. teleportation
circuit_sqt.h(qrN)
circuit_sqt.crx(alpha, qrN, qrA)
#Stage of S. teleportation
```

First, we have defined the extra register (noisy) as "qrN" and introduced it in the circuit\_sqt. We have set as an example the target state  $Alice_0$ , but we have to do it with all qubit.

The number of rotations is  $nr = 21$  and the angle of rotation  $\theta$  is bounded by  $0 \leq \theta < 2\pi$ , but we want to let it go just until  $\pi$ , given than the other second half of the sphere is going to produce the same effects as the first half.

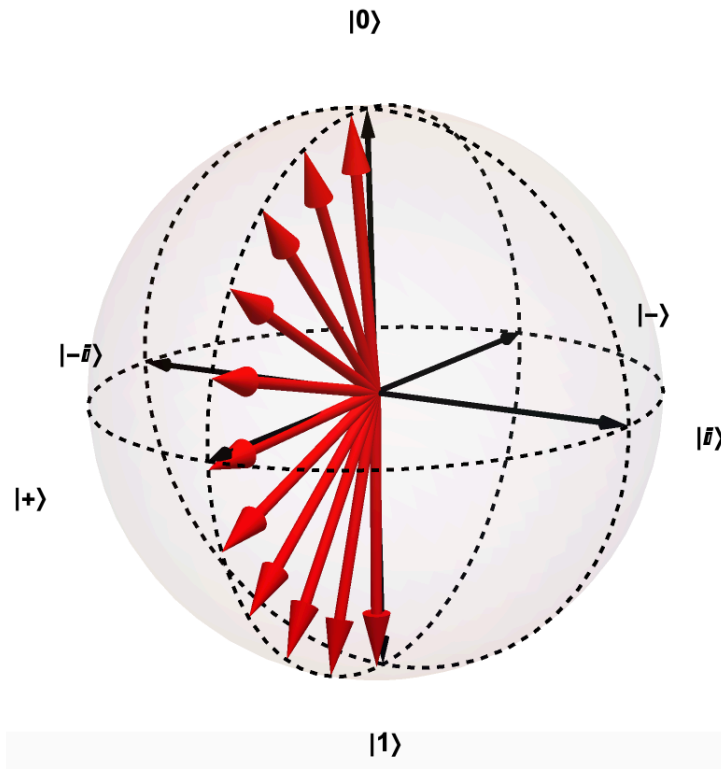


Figure 3.12: Evolution of a single qubit state under  $R_x$  rotation-gate. Adapted from<sup>1</sup>.

Then, we can achieve all the possible scenarios, illustrated with quantum circuits, in the following figures 2.13 - 2.18.

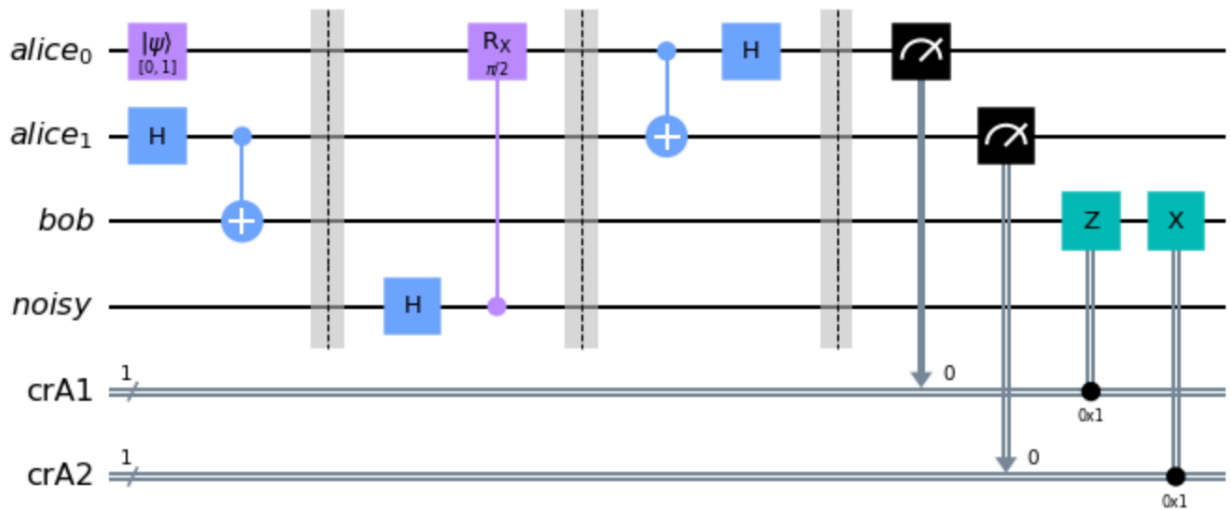


Figure 3.13: Noise acting after the first step on first qubit of Alice,  $Alice_0$ .

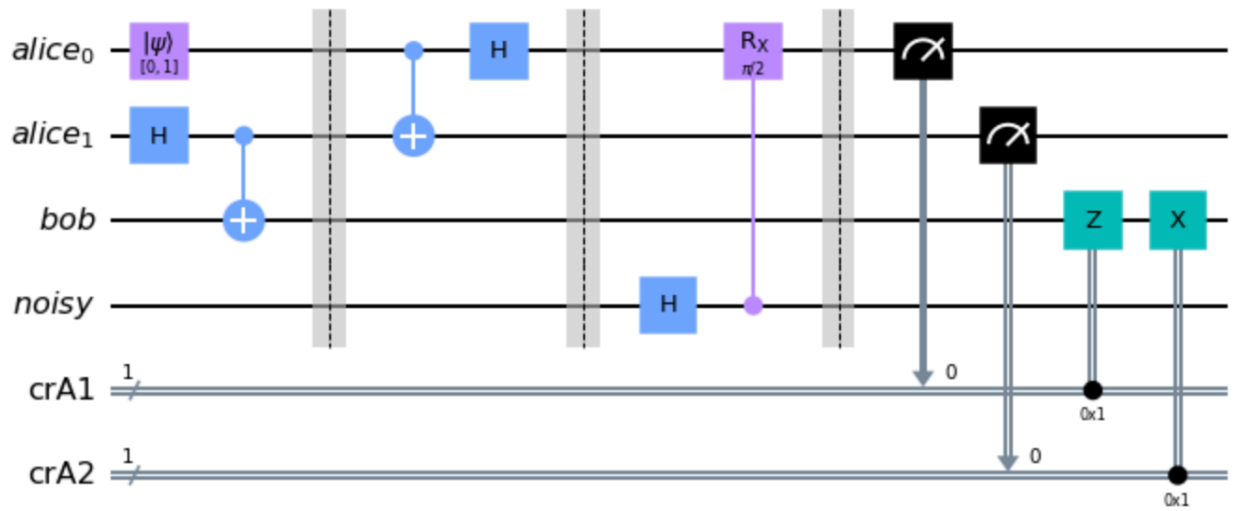


Figure 3.14: Noise acting after the second step on first qubit of Alice, *Alice*<sub>0</sub>.

When the noise is acting on the *Alice*<sub>0</sub> qubit, as an example we have used theta set to  $\pi/2$ . We can also compare circuits and check that the noise affections are placed in different stages of the SQT protocol. In the following example, noise is inserted to the *Alice*<sub>1</sub> qubit.

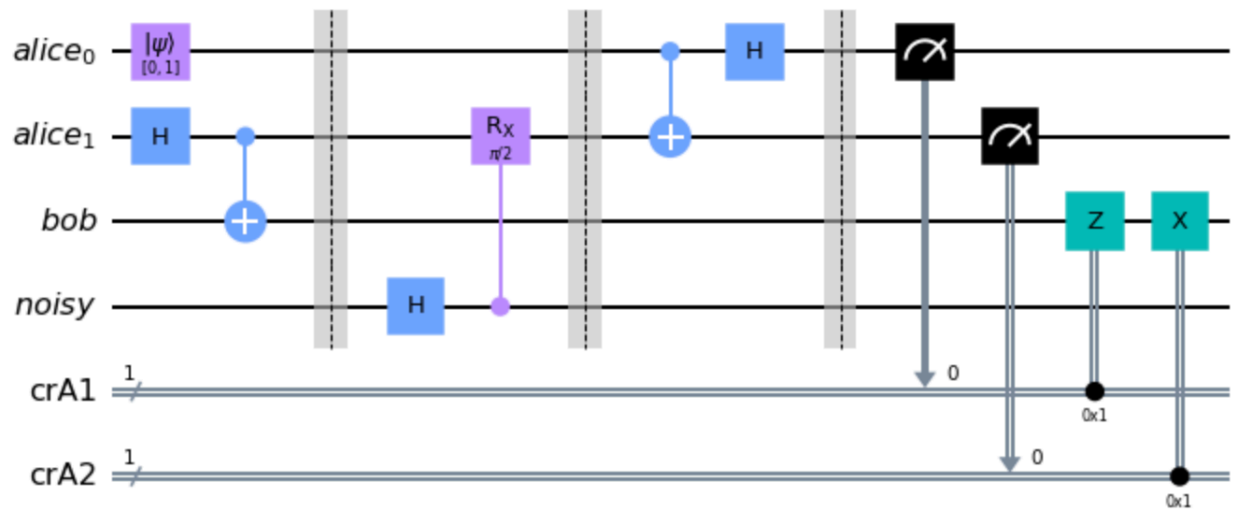


Figure 3.15: Noise acting after the first step on the second qubit of Alice, *Alice*<sub>1</sub>.

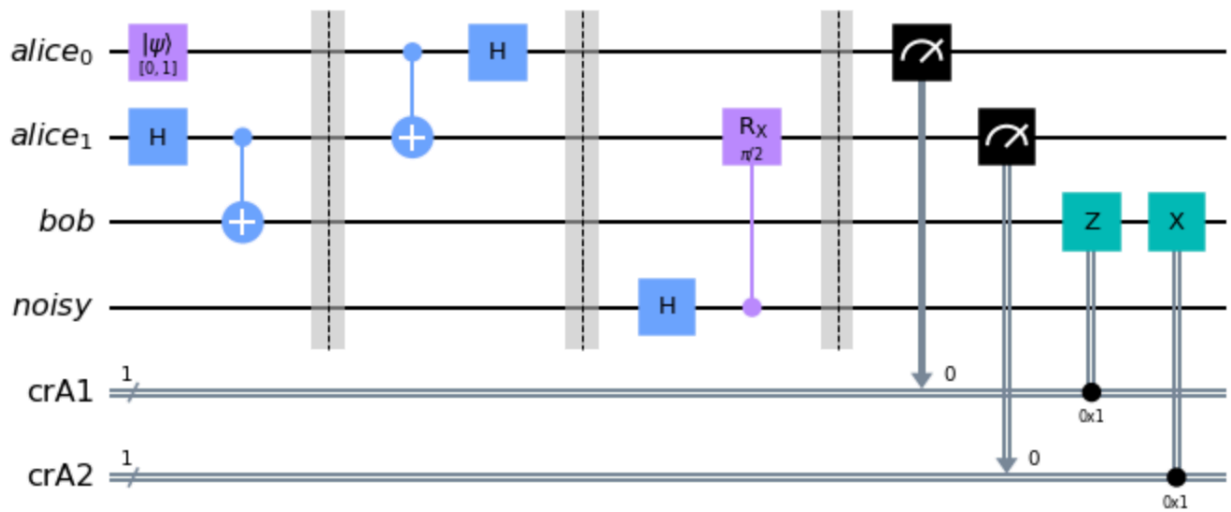


Figure 3.16: Noise acting after the second step on the second qubit of Alice,  $Alice_1$ .

Our final option will be the noise affecting the qubit of Bob.

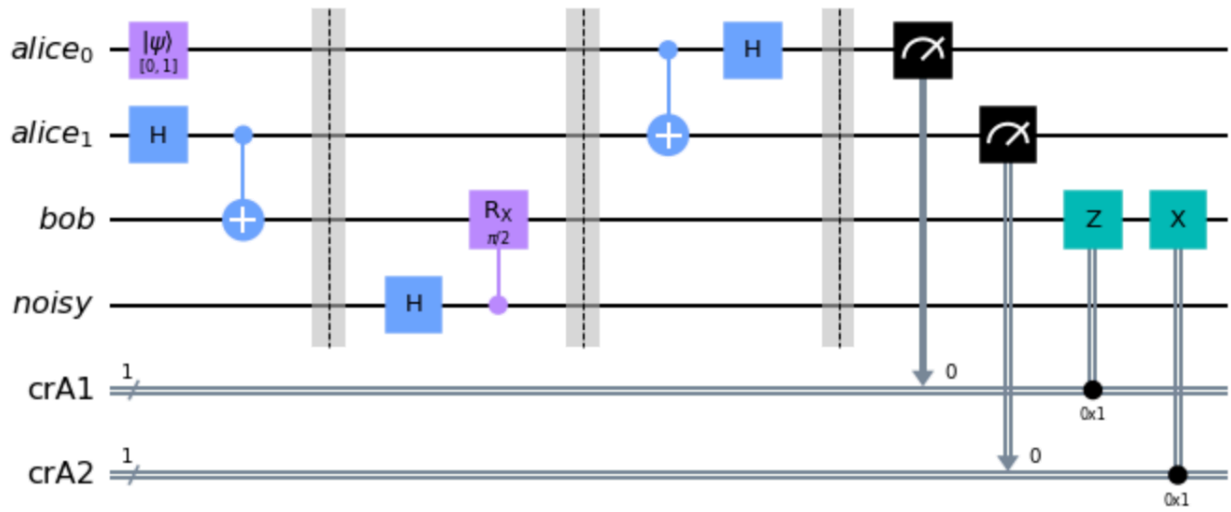


Figure 3.17: Noise acting after the first step on the qubit of Bob,  $Bob_0$ .

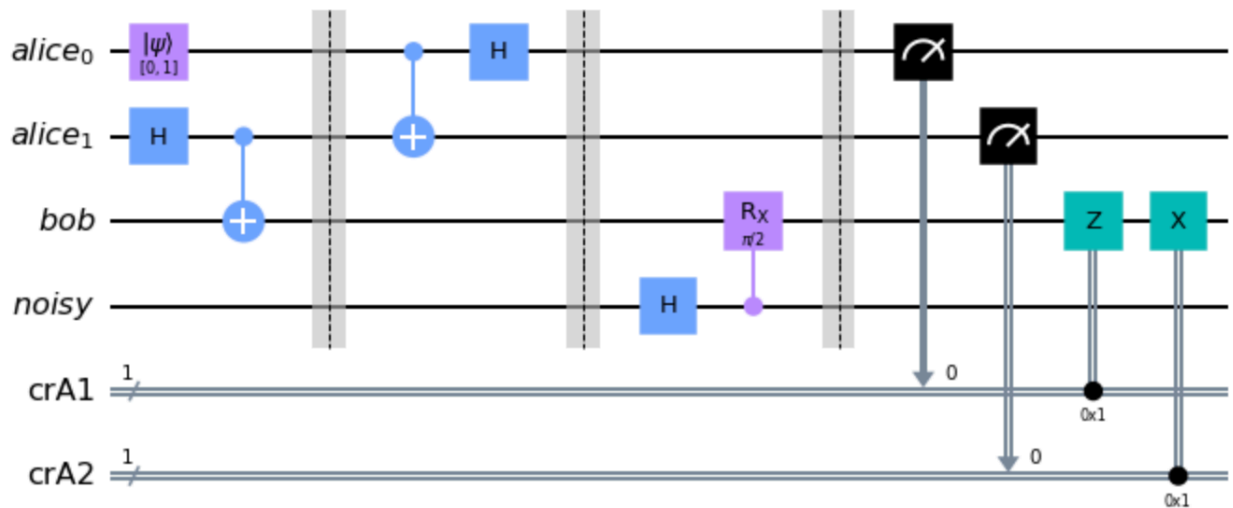


Figure 3.18: Noise acting after the second step on the qubit of Bob,  $Bob_0$ .

All the above examples can be compared using the average fidelity. Exactly the same approach will be applied for the execution in IBM's processor, just as explained using the deferred measurements, using CZ and CX gates.

## 3.2 Controlled Quantum Teleportation

As we have already introduced in previous section, we will mainly focus on the tripartite teleportation using the  $|GHZ\rangle$  state. Also, it is important to remember that the new qubit is gonna be distributed to the Charlie station, which will be considered as the Controller of the teleportation.

Then, at first, let's define the teleportation using the Greenberger-Horne-Zeilinger (GHZ) entangled state.

**Step 1.** We need to prepare the input states, as in SQT, but now the GHZ-state will be implemented by using the Hadamard and two CX gates. All is applied on the fiducial state is  $|0000\rangle$ , as follows:

```
qrA = QuantumRegister(2, 'alice ')
qrB = QuantumRegister(1, 'bob ')
qrC = QuantumRegister(1, 'charlie ')
crA = ClassicalRegister(3, 'crA ')

circuit_cqt = QuantumCircuit(qrA, qrB, qrC, crA)

a = np.cos(pi/2)
b = np.sin(pi/2)exp(1j*0)
circuit_cqt.initialize([a, b], 0)

circuit_cqt.h(qrA[1])
circuit_cqt.cx(qrA[1], qrB)
circuit_cqt.cx(qrA[1], qrB)
```

We are going to use the same input state as previously, and also we are going to define a single classical register with contains three bits. The measurements will give a 3 bit-string. The initial circuit look like as follows, in the Figure 2.19.

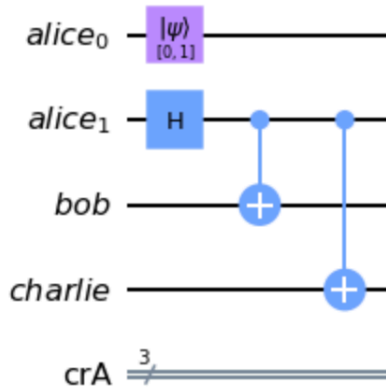


Figure 3.19: First step of CQT, preparation of initial states.

**Step 2.** Again, as previously, we perform a Bell measurement using the CX and H gates.

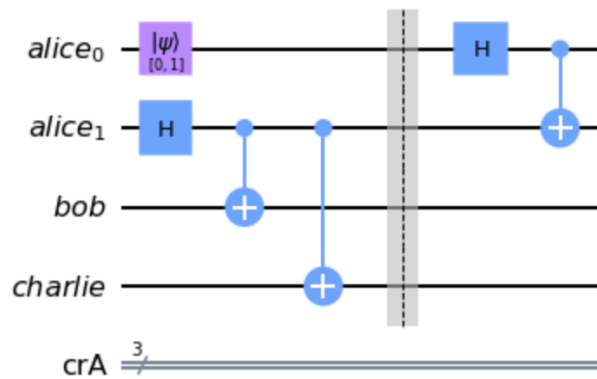


Figure 3.20: Second step of CQT, which corresponds to the Bell Measurement.

**Step 3. Non-conditioned Teleportation Scenario:** As described previously, we will apply recovery operations, depending on the result of the measurements obtained by Alice of her qubits and ignoring the measurement result of Charlie of his qubit. Only she will transmit to Bob her two bits as a bit-string.

In this point, we will just exemplify the situation where there is not knowledge about the collaboration of Charlie, reflecting that he is not communicating his result. We will make a clear distinction in the following part. We also will make a slightly change in the classical registers just for simplicity of this example.

```
circuit_cqt.measure([0,1,3],[0,1,2])
circuit_cqt.z(qrB).c_if(crA1,1)
circuit_cqt.x(qrB).c_if(crA2,1)
```



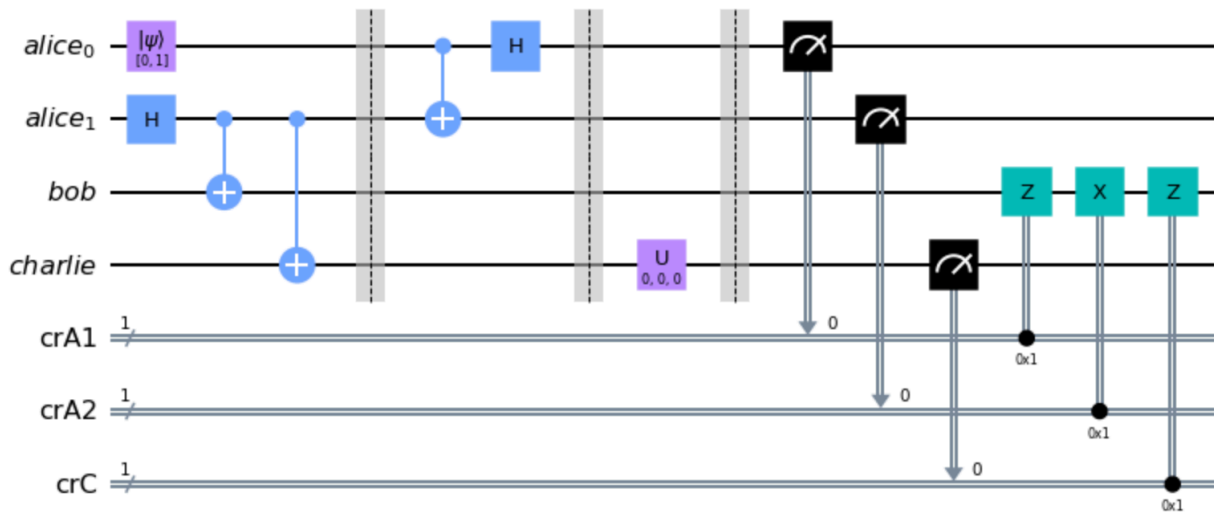


Figure 3.22: Circuit implementing the Controlled conditioned teleportation.

Bob is effectively able to recover the input state, and to complete successfully the teleportation protocol. As it was commented in the formalism development, the operation that produces the maximal fidelity is for values of  $\theta = \pi/2$ ,  $\phi = 0$  and the contribution of  $\lambda$  will not change the fidelity value.

We have placed the controller operation after the second step, without any kind of preferences, but it is important to comment that it needs to be between the second and the final stage. The controller operation now opens and a new stage of the teleportation. Also, the circuit applying the principle of deferred measurement is:

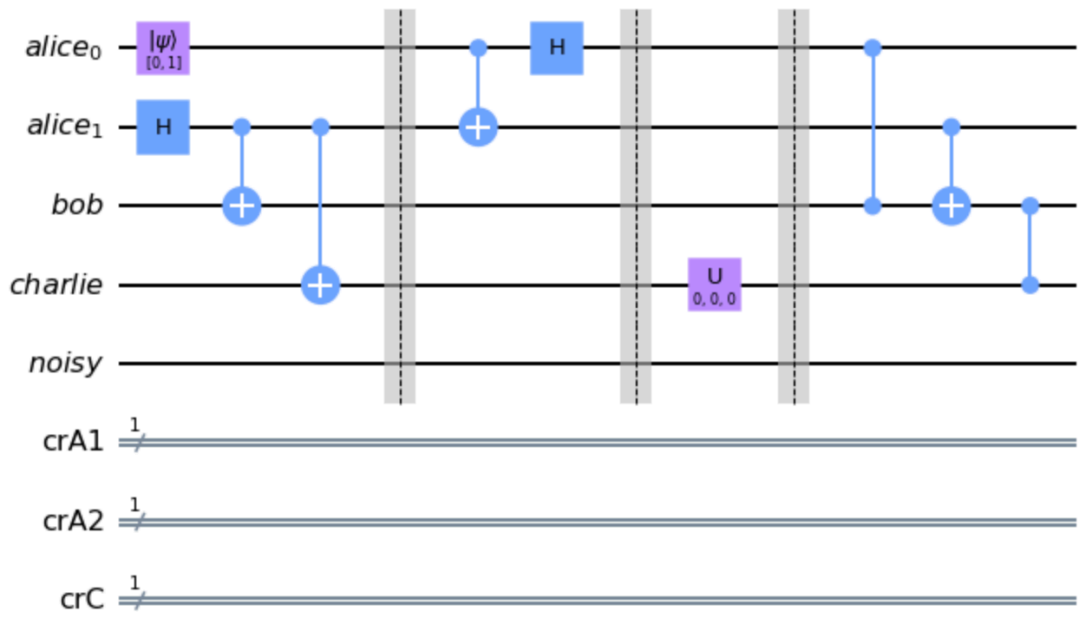


Figure 3.23: CQT with the deferred measurements applied on it by using controlled gates.



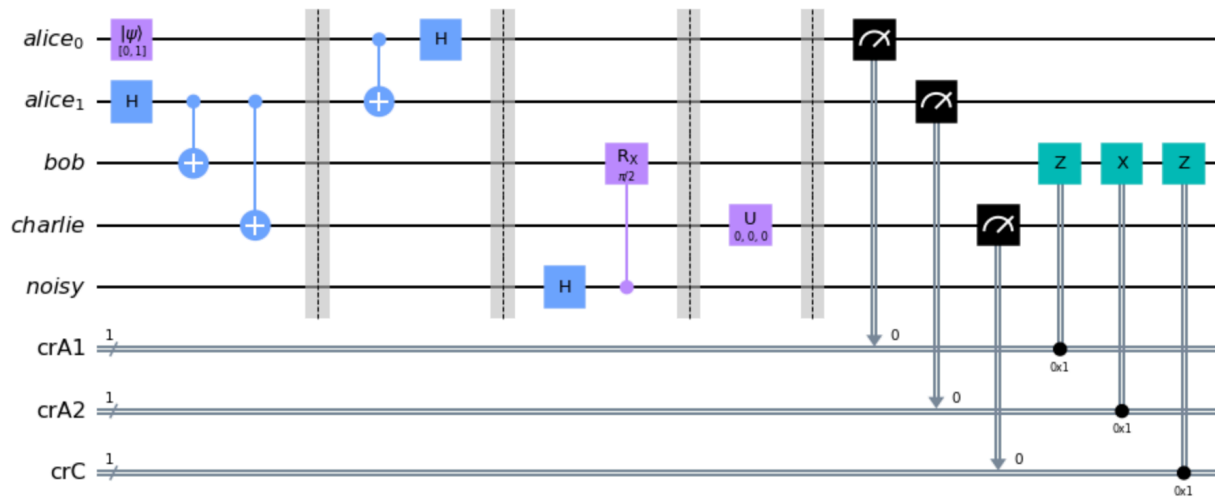


Figure 3.26: Noise implementation after the second step on Bob side ( $Bob_0$ ).

We will see in the next circuit, how the order of the noise implementation will affect the fidelity, even more, when it is affecting the Charlie station, considered as a controller.

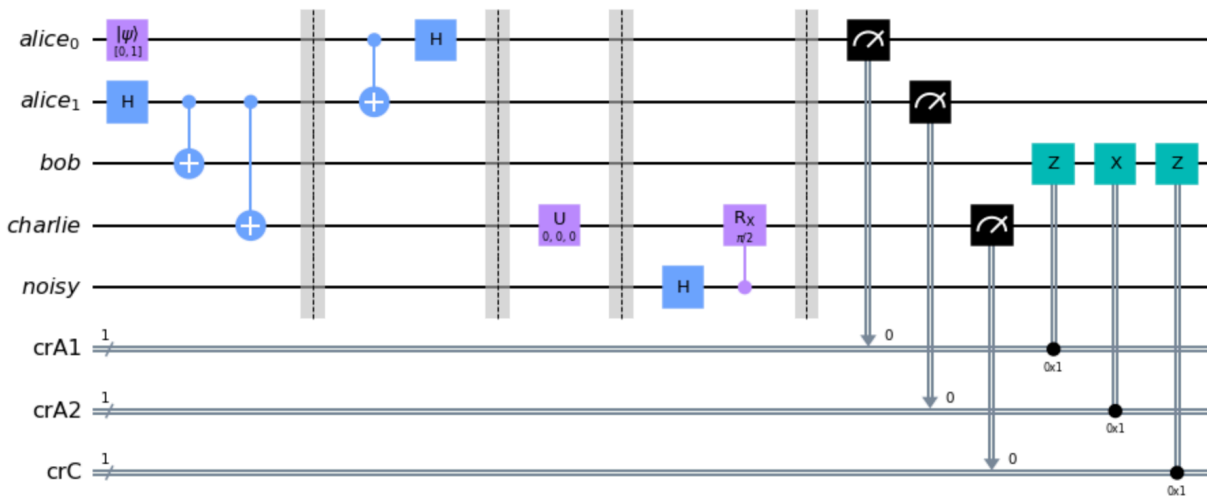


Figure 3.27: Noise implementation after the third step on Charlie side,  $Charlie_0$ .

### 3.3 Quantum State Tomography

One of the most important implementations, when we execute our code in real quantum processors, is the ability to reconstruct a desired unknown quantum state<sup>22</sup>. We can accomplish this task by using the Quantum State Tomography (QST), which works by first considering the unknown state in its density matrix representation  $\rho$ , and that we have a source of them with large enough number of copies.

It can be thought, that the state is always the product of a determined process, then by just reproducing the dynamics of such a process we could have the desired states as many times as needed. Qiskit has already developed this

tool, which is part of the modules of *ignis.verification.tomography* by importing *state\_tomography\_circuits* and also *StateTomographyFitter*, which is going to be very useful to get the most accurate state.

In order to exemplify this, we can check how state tomography works by describing the simple scenario, the single qubit quantum state tomography. First, as commented, supposing that we have enough samples of the desired state, then we can use a simple way to rewrite  $\rho$  by using the Pauli group operators. They will allow to perform measurements in different bases of our system:

$$\hat{\rho} = \frac{1}{2}(\hat{I} + x\hat{\sigma}_x + y\hat{\sigma}_y + z\hat{\sigma}_z) = \frac{1}{2}(\hat{I} + \vec{r} \cdot \vec{\sigma}), \quad (3.3)$$

where  $\vec{r} = (x, y, z) \in \mathbb{R}^3$  is the Bloch vector, then it is non-negative and  $\vec{\sigma} = (\hat{\sigma}_x, \hat{\sigma}_y, \hat{\sigma}_z)$ . Considering this kind of representation, the eigenvalues of  $\rho$  are:  $\lambda^\pm = 1 \pm \sqrt{x^2 + y^2 + z^2}$ .

Given that the Pauli group operators form a set of orthonormal matrices, and can expand the density matrix of each state by a superposition of them. Amplitudes of superposition will give exactly what is needed to place each vector on the unitary sphere. Then, the matrix representation of the states is expressed as following, making use of the trace operator:

$$\hat{\rho} = \frac{1}{2}(\text{Tr}(\hat{\rho})\hat{I} + \text{Tr}(\hat{X}\hat{\rho})\hat{X} + \text{Tr}(\hat{Y}\hat{\rho})\hat{Y} + \text{Tr}(\hat{Z}\hat{\rho})\hat{Z}). \quad (3.4)$$

Perhaps, to present this, it could be nice to show a plot, of a current density matrix. We have used as an example a state placed in perfect superposition by using Hadamard gate on it, then the state is exactly overlapping the  $\hat{x}$  axis. The plot has been made by using *plot\_state\_city*, which shows both the real and the imaginary part of the state.

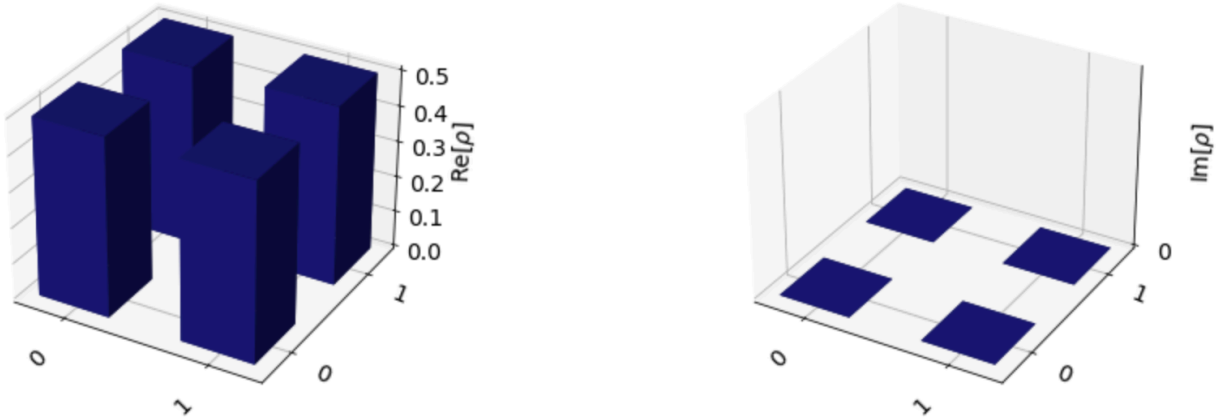


Figure 3.28: Density matrix plot for the  $|+\rangle$  state, representing real and imaginary parts.

As each trace represents an expectation value of it, and comparing it with equation (2.3), we can notice that they will provide the scalars that reconstruct  $\vec{r}$ . In our formalism each trace can be computed as, setting the  $\rho$  matrix arbitrarily as  $\alpha|0\rangle + \beta|1\rangle$ :

$$\begin{aligned} \text{Tr}(\hat{\rho}) &= |\alpha|^2 + |\beta|^2, \\ \text{Tr}(\hat{\rho}\hat{X}) &= \alpha\beta^* + \alpha^*\beta, \\ \text{Tr}(\hat{\rho}\hat{Y}) &= i(\alpha\beta^* - \alpha^*\beta), \\ \text{Tr}(\hat{\rho}\hat{Z}) &= |\alpha|^2 - |\beta|^2. \end{aligned} \quad (3.5)$$

We can see the change of bases using the  $\hat{H}$  gate in the following way:

$$\hat{H}(\alpha|0\rangle + \beta|1\rangle) = \alpha \left( \frac{|0\rangle + |1\rangle}{\sqrt{2}} \right) + \beta \left( \frac{|0\rangle - |1\rangle}{\sqrt{2}} \right) = \alpha|+\rangle + \beta|-\rangle. \quad (3.6)$$

But, as our device is designed to produced measurements in the z-axis (or  $|0\rangle$  and  $|1\rangle$  states), then, we can rewrite the last equation as:

$$\alpha|+\rangle + \beta|-\rangle = \frac{\alpha + \beta}{\sqrt{2}}|0\rangle + \frac{\alpha - \beta}{\sqrt{2}}|1\rangle. \quad (3.7)$$

And then, by producing measurements as usual, we will be able to get the probabilities of the superposition of these desired bases, in this example, the x-axis.

Additionally, by producing n number of measurements of one of the basis, for example  $x_i$ , where X-gate has been used, we can take its average value as  $\sum_i \frac{x_i}{n}$ . We show in results section, that the optimal number of samples is needed, which we will call Shots, that produces enough information about the state, with the lower error.

To conclude, it is important that there exist many alternatives to produce QST, and maybe different approaches become better, when the dimension of systems grows given the possible addition of extra qubits, and also, it is very important to consider the efficiency of measurement device, and the possible noisy sources.

### 3.4 Calibration

Quantum states can be very susceptible to errors in the outcomes of performed measurements. For example, we can think that we desire to measure a single qubit that we know, very confidently, is in state  $|0\rangle$ , then, we perform for example  $n_s = 1000$  experiments, which means we prepare  $n_s$  times the  $|0\rangle$  state and measure it  $n_s$  times.

What we expect to get of this experiments is a string with 1000 times 0, but it is an ideal situation, when we are not considering noisy sources or systematic errors produced by the same device. Therefore, if we execute that kind of experiment we are going to observe the imperfections coming from error measurements.

Given that we are now placed in a real situation, we can think that we produce again the same experiment, but now we get as results, like,  $n_{|0\rangle} = 990$  and  $n_{|1\rangle} = 10$ , which means that for any kind of extra contribution, the state was measured in  $|1\rangle$ , but we were very sure that the state was  $|0\rangle$ . Then, we can assume that this 10-times wrong measurements are due to systematic mistakes of the device, no matter which is its source.

This is the main motivation to calibrate our device, assuming the Error-Measurements. A common process of this is called Measurement Error Mitigation (MEM), which can be prepared using quantum circuits, executing them and collecting their information.

Let's exemplify this for a single qubit situation. In order to explain MEM, we are going to use the same  $n_s = 1000$ . We are going to save our measurements in vector as follows:

$$\begin{bmatrix} n_{|0\rangle} \\ n_{|1\rangle} \end{bmatrix}_p, \quad (3.8)$$

which we will call vector of perfect data.

Now, let's produce the following experiments: First, we prepare the  $|0\rangle$   $n_s$  times, measure it, and save its data. Second, let's prepare the state  $|1\rangle$   $n_s$  times, measure it and save its results.

We can create a 2x2 matrix with these results by placing the collected data as: In the first column we will place the measurements coming from 1st experiments, where the first entry is for the number results of measurements made on  $|0\rangle$  and with result 0 and the second entry is for for  $|0\rangle$  with result 1.

We will do the same for the second column taking the results of the 2nd experiment, where the first entry is for the number counts of measuring  $|1\rangle$  and as result 0, and the second entry is for 1 counts. Finally, we will get the Calibration matrix by normalizing it, diving each entry by the total number of shots. The calibration matrix, then will looks like:

$$\frac{1}{n_s} \begin{bmatrix} n_{|0\rangle,0} & n_{|1\rangle,0} \\ n_{|0\rangle,1} & n_{|1\rangle,1} \end{bmatrix}. \quad (3.9)$$

We can notice that while the device would be more accurate, the calibration matrix is going to be more diagonal, given that there will be less chances to return a wrong outcome. Finally, we can perform an experiment where we know we have to measure that qubit in the  $|0\rangle$  state, but due to noise we get now a vector that we will call imperfect  $[\ ]_{iP}$ , which contains, for example, in the first entry  $n_{|0\rangle} = 990$  and in the second entry  $n_{|1\rangle} = 10$ , as in the previous example.

Then, we now do the following:

$$\begin{bmatrix} 990 \\ 10 \end{bmatrix}_{iP} = \frac{1}{n_s} \begin{bmatrix} n_{|0\rangle,0} & n_{|1\rangle,0} \\ n_{|0\rangle,1} & n_{|1\rangle,1} \end{bmatrix} \begin{bmatrix} n_{|0\rangle} \\ n_{|1\rangle} \end{bmatrix}_P. \quad (3.10)$$

As example, we can say that perfect-vector has 1000 and 0 entries, and we can say the calibration matrix is also filled with same results as the experiment one, we can multiple the system and solve, as:

$$\begin{aligned} 990 &= \frac{n_{|0\rangle,0}}{n_s} n_{|0\rangle} & ; & \quad 10 = \frac{n_{|1\rangle,1}}{n_s} n_{|0\rangle}, \\ \Rightarrow 990 &= \frac{990}{1000} n_{|0\rangle} & ; & \quad 10 = \frac{10}{1000} n_{|0\rangle}. \end{aligned} \quad (3.11)$$

and, as a solution we get what was expected.

In practice, we are going to be able to collect all the data that reconstruct the c-matrix and the imperfect-vector. And last though has brought us exactly where we wish to point out, how to correct our data from C-matrix and iP-vector.

For this, we are going to call another vector called the corrected-vector  $[\ ]_{cD}$ , which will be very similar to the perfect-vector, but given that the retrieved data in experiments of calibration, can fluctuate at the moment of collecting the iP-vector, then there is a chance that our data would be very good, but still with some little imperfections.

The system is gonna be the same as previously  $i\vec{P} = \hat{C} \cdot c\vec{D}$ . Given, that what we wish is the vector of corrected data, then we finish with the following system:

$$c\vec{D} = \hat{C}^{-1} \cdot i\vec{P}, \quad (3.12)$$

where once that we get the calibration matrix, we need to invert it and them multiple it with the imperfect data vector.

It is important to comment, at this moment, that sometimes this kind of systems produces wrong solutions, given that it could give back a cD vector with negative entries, which has not physical meaning given that they are probability-density vectors, they still sum to one, but with wrong entries. To fix this kind of situations, we can use, for example, the least-squares method, or a minimize method of a function  $f$  given by:

$$\|(\hat{C}^{-1} \cdot i\vec{P}) - c\vec{D}\|^2 = f, \quad (3.13)$$

where we need to set the bounds,  $\|c\vec{D}\|^2 = 1$  and  $c\vec{D}_i \geq 0$ ,  $i$  is used to denote the entries of the vector, which can be implemented in *Mathematica* by using first *minimize*, *Thread* function, and we can write the whole system using the dot product  $(\hat{C}^{-1} \cdot i\vec{P} - c\vec{D}) \cdot (\hat{C}^{-1} \cdot i\vec{P} - c\vec{D})$ , as an input function to be minimized.

There could be an extra source of noise that we can try to mitigate and it is coming from imperfections of gates used for our experiments. We can think on this, for example, in the X-gate, which takes the  $|0\rangle$  to the state  $|1\rangle$ .

This kind of systematic noise will affect the whole process, in our case the whole protocol of teleportation. A good way check if our gates are doing what we wish can be implemented by using the Hermitian conjugate gate.

As we saw in the first section, we just work with unitary operators that fulfil  $\hat{U}^\dagger \hat{U} = \hat{I}$ . If we apply to a qubit in  $|0\rangle$  the  $\hat{X}$  gate and again  $\hat{X}$  gate, the compose action will be the identity, producing an invariance on the state.

If there exist some noise coming from the gates, the state in not going to be anymore in the suppose state, and we can measure those variations. In order to provide an example to this, let's check the following circuit.



Figure 3.29: Circuit for calibration of the  $\hat{H}$  gate, using the  $|0\rangle$  state.

As we see, we have used Hadamard gates, for which the hermitian conjugate operator and the operator are the same. With this, we can record the information for the first column of our calibration matrix, for the other column we need to test with the  $|1\rangle$  state, as:



Figure 3.30: Circuit for calibration of the  $\hat{H}$  gate, using the  $|1\rangle$  state.

where, we have placed the state in  $|1\rangle$  state by using the X-gate and then we produce the identity operation with a combination of  $\hat{H}$  and  $\hat{H}^\dagger$ . With this, we have the requested information for the calibration matrix.

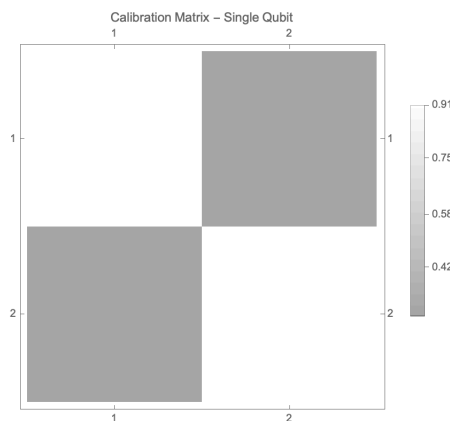


Figure 3.31: Calibration matrix for a single qubit. Lateral bar show the density number scale. Adapted from<sup>23</sup>.

As it has been pointed in<sup>23</sup>, the calibration of our circuit can be implemented by diving the number of gates of the circuit in halves, if the depth of the circuit is too much large, then we will produce two circuits, where each one will

need to possess its hermitian conjugate part. At the end, we are going to end up with two calibration matrices, that then will be averaged, and the average is going to be the Calibration matrix used for the whole calibration, as  $C = \frac{C_1 + C_2}{2}$ .

We are now just missing how to produce the calibration matrix for one of our experiments. To achieve this, we can focus on the SQT. We have to take each gate, even the gates that create the input and Bell states. For this, let's check the following circuit.

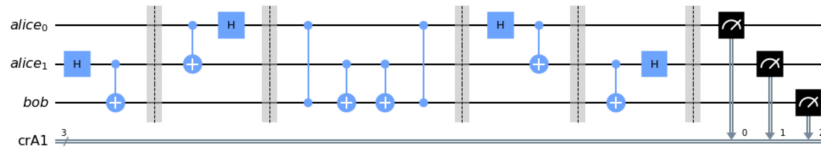


Figure 3.32: Calibration Circuit for the  $|000\rangle$  state section.

We can notice that in this case the calibration matrix is gonna have a bigger dimension, given that we have 3 qubits involved in our protocol, then the calibration matrix has the dimension  $2^N \times 2^N$ , for our case is  $2^3 \times 2^3$ . To finish the circuit that will expand the whole information for C, we need to place X-gates before the corrected gates, in order to produce the 8 possible states for corrections.

Additionally, there are many things that we could do for improving the corrections, for example, the calibration matrix can be changed by usage of the Hamming Distance.

It is also an implementation of MEM in Qiskit, in the Ignis module, where we can import from *qiskit ignis mitigation measurement* each calibration circuit as *complete\_meas\_cal* and *CompleteMeasFitter*, where the fitter will help exactly to produce correct results.

To conclude, it is important to check the correct hermitian conjugate representation of each gate used and in the mitigation section it is important to always be sure about the dimension of the systems, given that it could result in and incorrect mitigation.

# Chapter 4

## Results & Discussion

We are going to focus on running our experiments by the simulator and then by real quantum processors, where the first experimental realization of Quantum teleportation was realized by D. Bouwmeester<sup>24</sup>. Let's see what has been possible to observe for us, in both stated scenarios, SQT and CQT. Additionally, let's check if using IBM's devices, can probe the quantum advantage for quantum information transmission making use of entangled channels.

### 4.1 Standard Quantum Teleportation

#### 4.1.1 Simulated Implementation - Qiskit Simulators

If we remember, the number of shots (repetitions) is something that should be established firstly, in order to produce very accurate fidelities coming from QST.

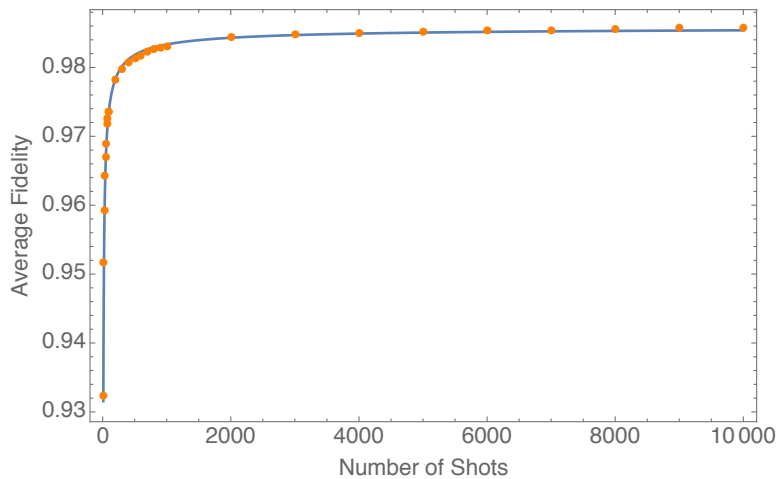


Figure 4.1: Average Fidelity of SQT protocol dependence on the number of shots, using QASM.

This behavior of the average fidelity depending on the number of shots, showed in figure 4.1, effectively exhibits that the large number of shots is important in order to achieve a very accurate Average Fidelity of States (AVF). We can check that with less than  $n_s = 1000$  the average fidelity is not good at all, producing fidelities lower than 0.98.

Our choice needs to be placed significantly above this value. We have chosen for each experiment at least  $n_s = 2048$ . It seems that the average fidelity does not vary significantly above this number. In each experiment it will be clarified to avoid uncertainties about calculations. It is important to mention that this result has been obtained by using QASM simulator. Also, we have characterized the number of shots, which effectively shows entanglement in the quantum channel due to the average fidelities above the classical limit ( $2/3 \approx 0,67$ ).

Regarding temporal causality, we have used, as explained before, the controlled rotation around x-axis, getting following results:

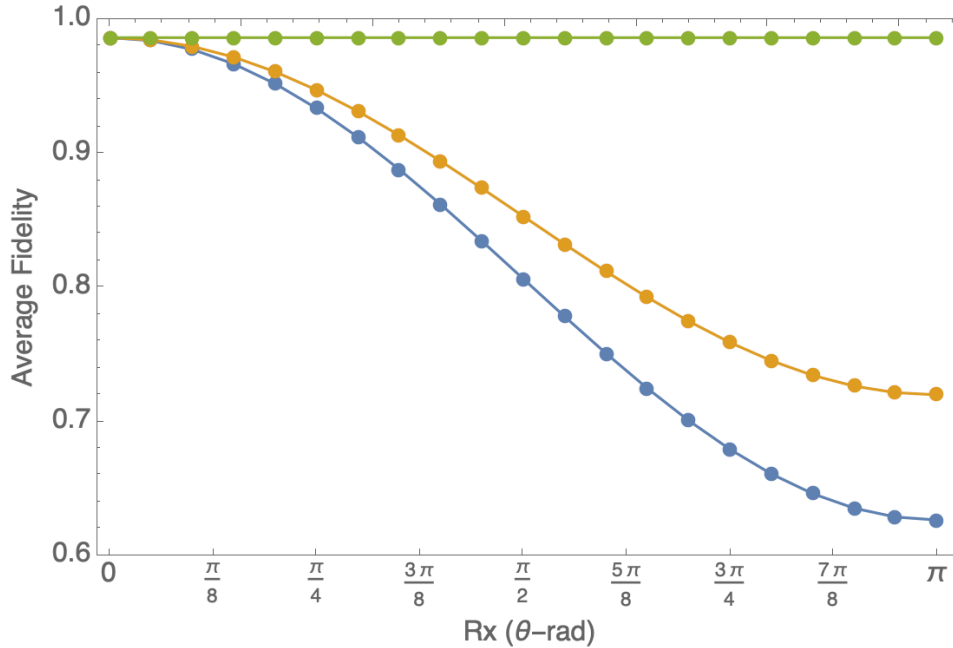


Figure 4.2: Dependence of  $F_{avg}$  when a noisy source affects  $Alice_0$  qubit. Blue-curve indicates a noise inserted after the stage 1, the orange-curve when noise is inserted after the stage 2, and the green-curve when noise is inserted after the stage 3.

In Figure 4.2, we can see that the affection of noise on Alice input qubits can decrease the fidelity, more than the other two scenarios, when the noisy source has been applied after the first stage of the protocol. It could mean that the information is better preserved when the noise affects the qubit after the second stage or the BSM, it could be given that Bell Measurement already has projected the input state into the entangled channel, achieving the transmission of information faster than the affection of the noise, in that way, preserving it better than in other scenario.

We can observe that the qubit has achieved its maximally entanglement with the noisy source when the minimal fidelity has been reached, stating that the information is better dissipated to the noisy source when the entanglement is maximal, as it was expected.

Bob's qubit noise affection does not happen in the same way, given that the noisy source is affecting directly to the qubit, then it is not necessary to search for non-local correlations, given that the qubit will be always rotated in the same way. As we have commented, the rotation will take place only until  $\theta = \pi$  given that the other half is going to provide a symmetric curve to the one we already have, recovering the fidelity until to be as much close to 1. All scenarios mentioned are presented in the Figure 4.3.

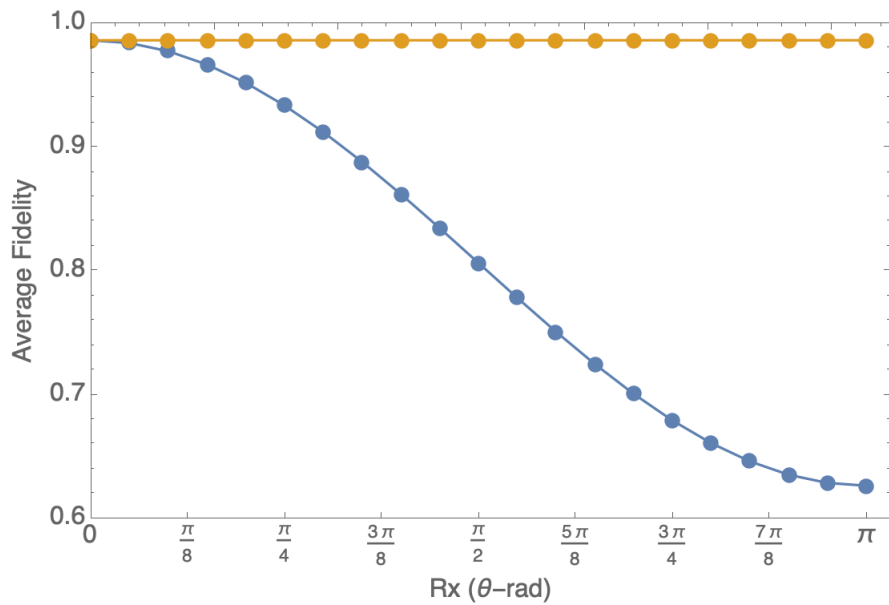


Figure 4.3: Dependence on  $F_{avg}$  when a noisy source is inserted in the *Bob* qubit. Blue-curve when noise is inserted after the stage 1 and also after the stage 2, orange-curve when noise is inserted after the stage 3.

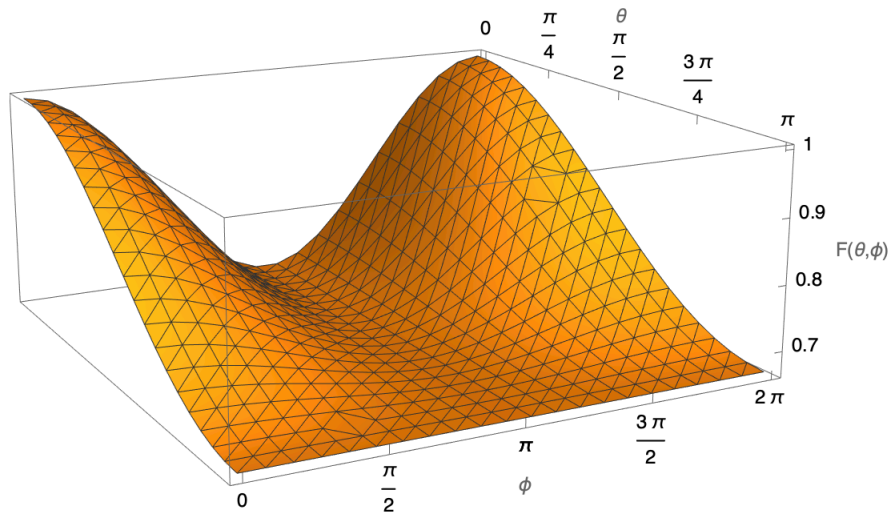


Figure 4.4: Average fidelity for noise acting on *Alice*<sub>0</sub> input qubit by using the CU-gate.

#### 4.1.2 Experimental Implementation - IBM's Quantum Devices.

There exist many limitations in executing a circuit implementation on a real quantum processor, which returns a noisy data with imperfections. The state of the art of quantum computing at this moment is actually placed in solving this kind of imperfections, some that comes from the same nature of the qubits implementation or just because the processors are open quantum systems, which by interactions with its environments, get entangled, losing purity of their states, spreading its information, producing defects in resulting data.

Despite of the deepest mechanism in which our systems could get mixed, as we saw in the last chapter, we can make use of MEM to improve our calibration, by previous executions of it. At the moment of the development of this thesis, most of public quantum processors are 5-qubits computers, and we can see a calibration matrix of the whole systems in the following figure:

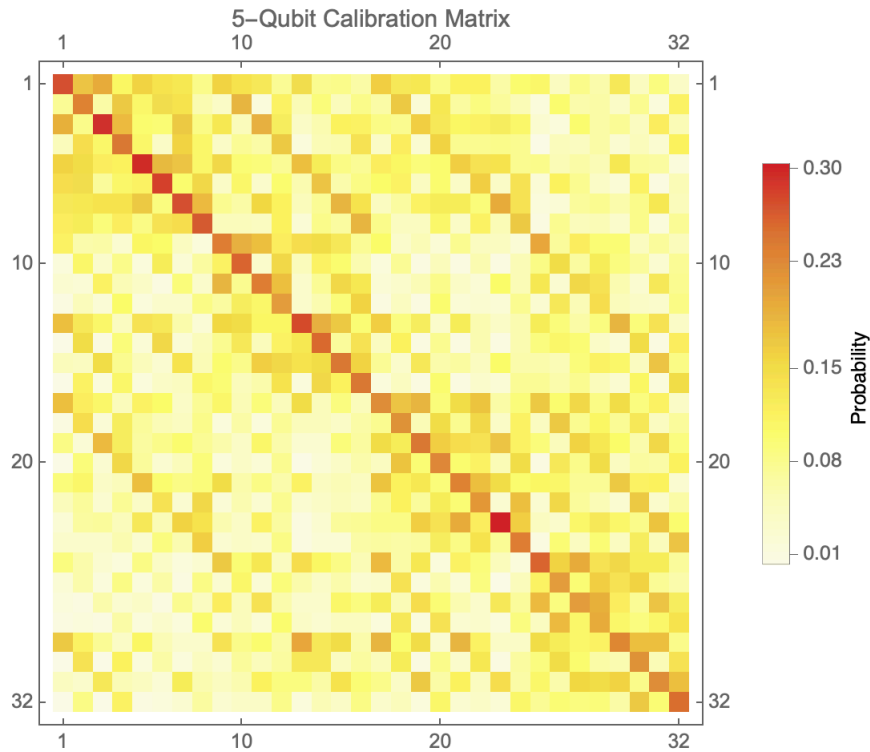


Figure 4.5: Five qubits calibration matrix for the `ibmq_quito` processor.

The C-matrix of the Figure 4.5 is a calibration matrix, where the frames have been changed to decimal form plus one. It means that for example, the 1 is the representation of  $|00000\rangle$  and 32 is  $|11111\rangle$ , which takes into account the "General measurement error mitigation", which considers state preparations and measurements, and as it was explained it has the gates that are part of the teleportation circuit, using its hermitian conjugate gate in order to always apply just the Identity matrix.

Something important from the calibration matrix is its diagonally, which shows that the device is actually doing what we previously thought it should do.

Once that we have calibrated our circuit, we can execute our circuits to test the temporal causality by using the average fidelity. Given that the connection with our quantum processors is time consuming because the circuits needs to be compiled and sent to the devices, and additionally these devices are public and other researchers are making use of them too, it is quite problematic to make our calculations with a big set of input qubit states, and there is also a limitation in our classical device, given that the depth size of the sending circuit will need to respect the Ram memory available.

For this reason our calculations of average fidelity are going to be made by using  $25 \times 25$  input states, and a total number of shots per circuit of  $n_s = 10000$ , which can produce good statistic in our outcome states after teleportation.

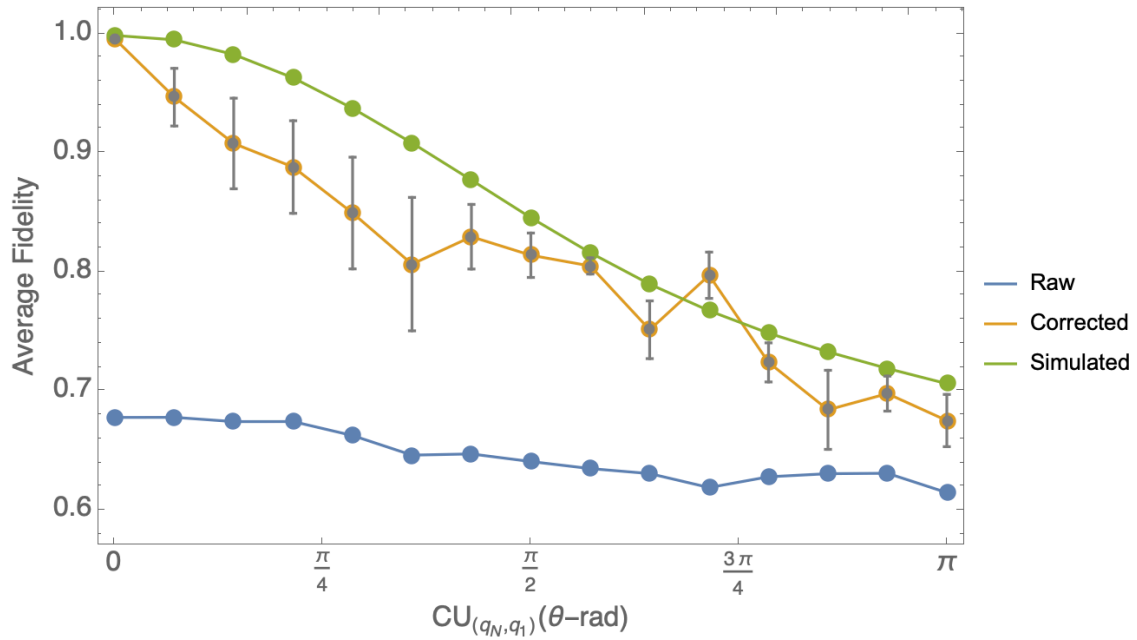


Figure 4.6: Temporal Causality of noisy source inserted in  $Alice_0$  qubit - stage 1, by applying H and CU gates. Here simulated means by run QASM.

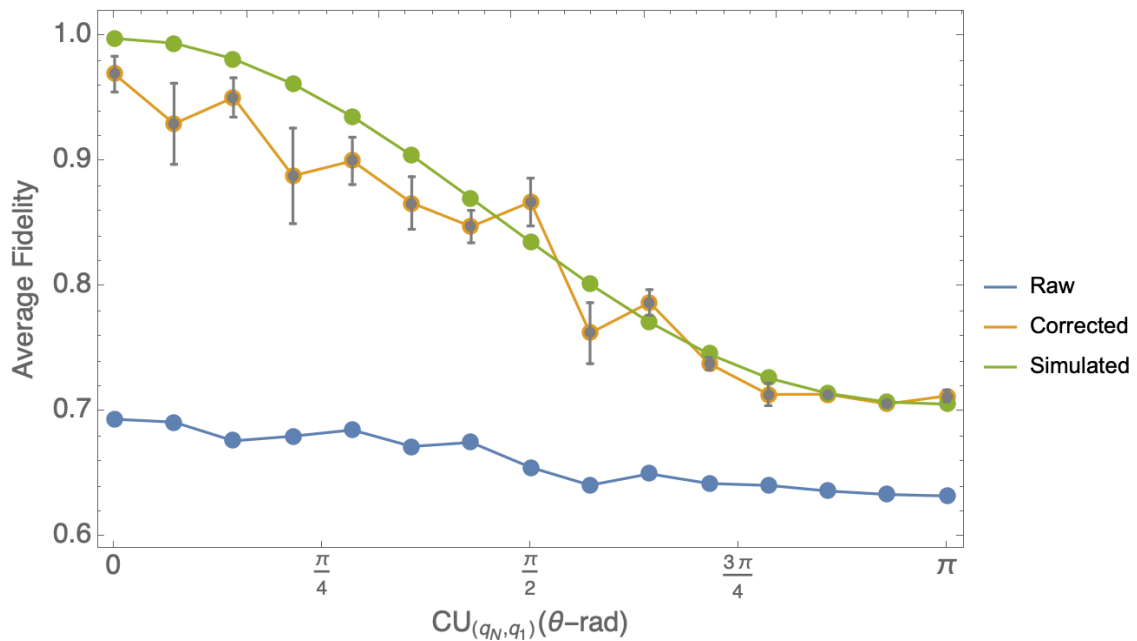


Figure 4.7: Temporal Causality of noisy source inserted in  $Alice_0$  qubit - stage 2, by applying H and CU gates.

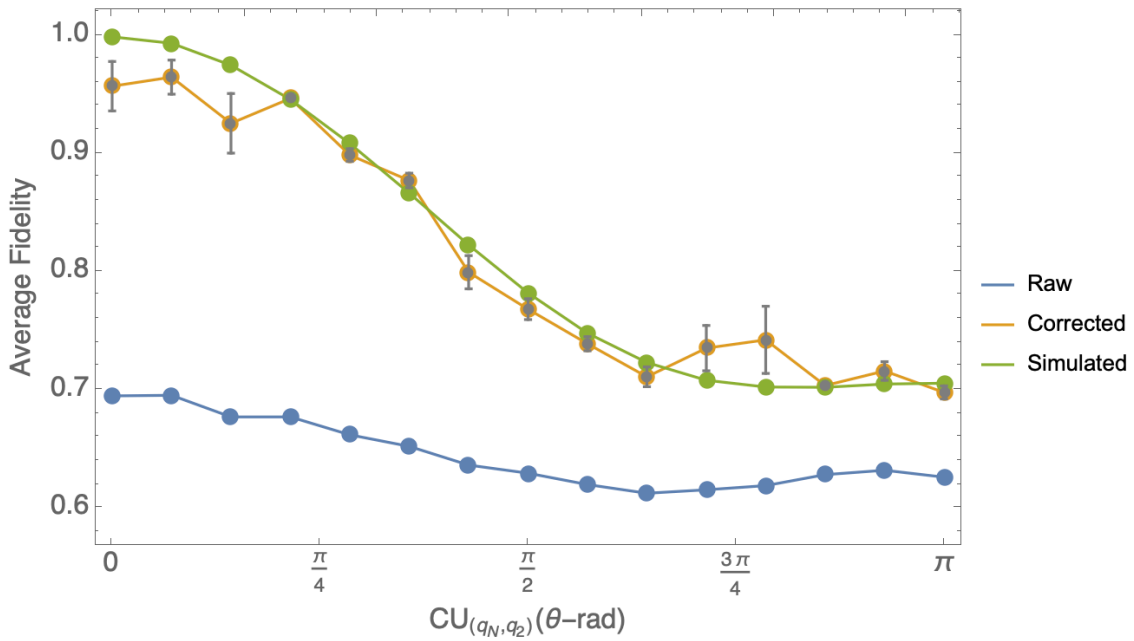


Figure 4.8: Temporal Causality of noisy source inserted in  $Alice_1$  qubit - stage 1, by applying H and CU gates.

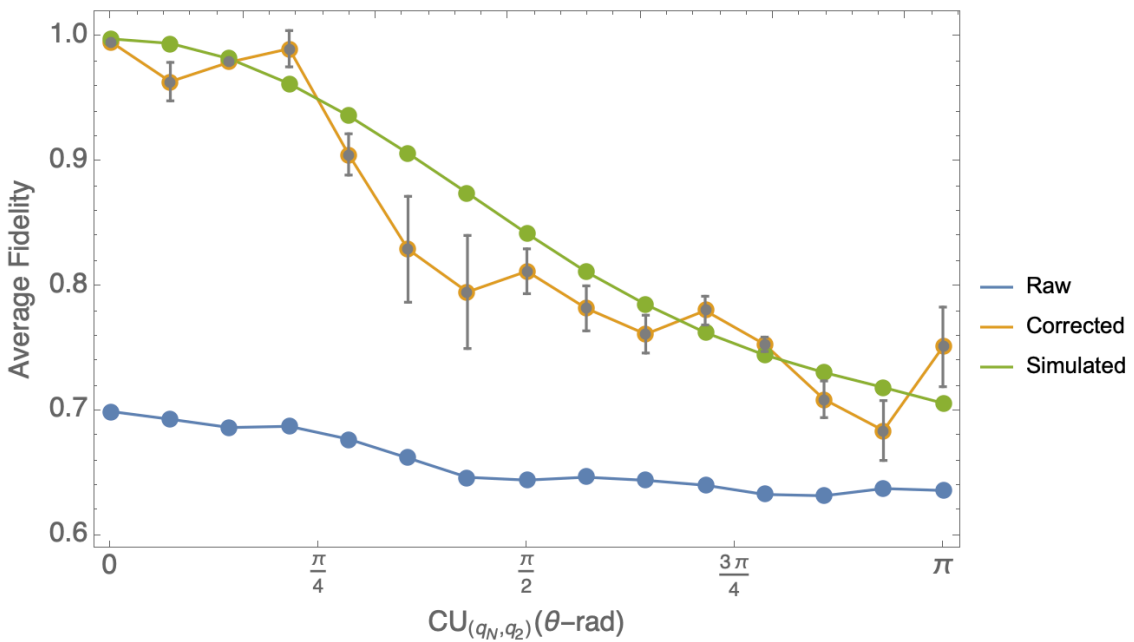


Figure 4.9: Temporal Causality of noisy source inserted in  $Alice_1$  qubit - stage 2, by applying H and CU gates.

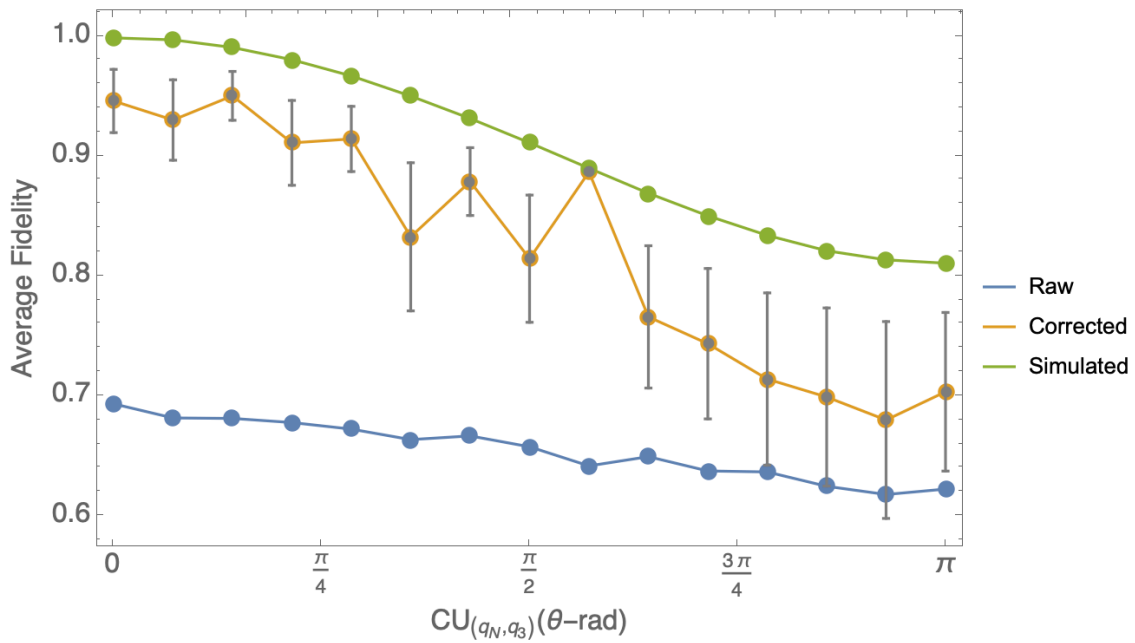


Figure 4.10: Temporal Causality of noisy source inserted in  $Bob_0$  qubit - stage 1, by applying H and CU gates.

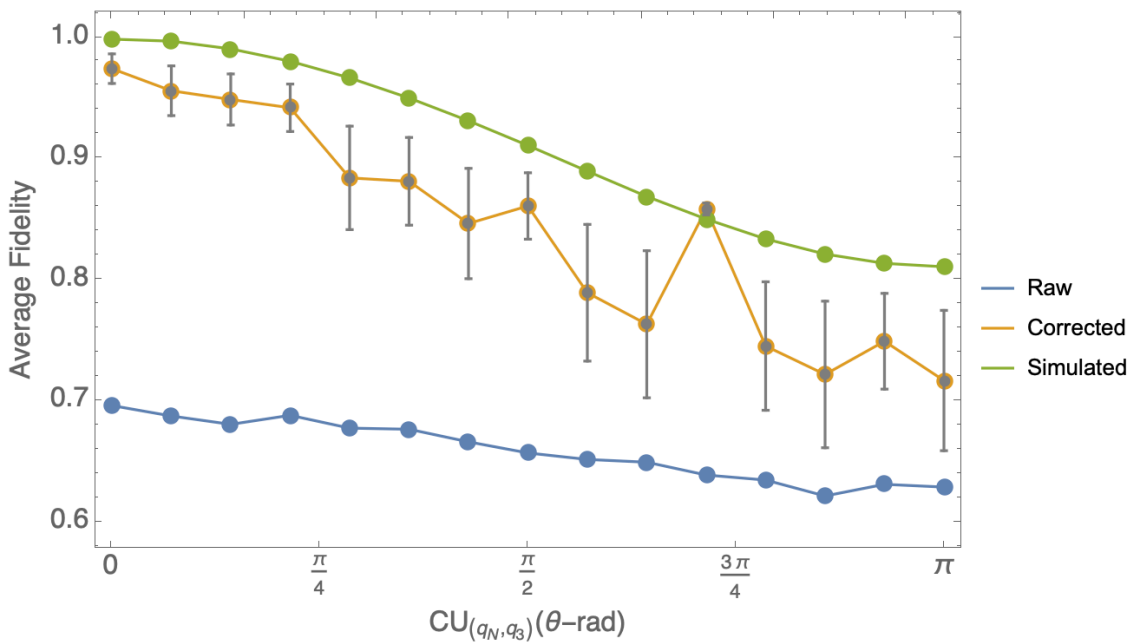


Figure 4.11: Temporal Causality of noisy source inserted in  $Bob_0$  qubit - stage 2, by applying H and CU gates.

To obtain this data, we have used the `ibmq_quito` quantum processor which is a quantum device with 5-qubits, Quantum Volume=16, and its architecture looks like a t shape. As with most public devices, it possesses a maximum number of shots equal to 20000 and a maximum of circuit execution equal to 100 circuits per execution.

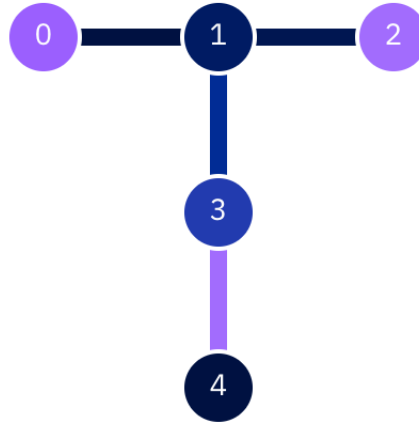


Figure 4.12: Ibmq\_quito device's architecture. Adapted from<sup>15</sup>.

The Figure 4.12 has been taken from the IBM quantum experience platform, showing the architecture of the device which is known as Falcon r4T. Additionally, its decoherence times can be seen in the following Table 4.1, where the relaxation time T1 and the dephasing time T2 have been provided IBM in the quantum experience platform, where the information about any device can be found at real time.

	T1(ns)	T2(ns)
Q0	53.8	122.78
Q1	143.35	171.87
Q2	101.99	130.13
Q3	103.69	12.2
Q4	149.8	238.74

Table 4.1: Coherence times (T1-T2) of ibmq\_quito quantum processor provided by Quantum Experience platform.

In addition, IBM services share information related to CX gates for example, and their respective error rates. Additionally, the basis gates that the device has implemented given that combinations of them can expand any other gate needed. The basis gates that this device realizes are: CX, ID, RZ, SX, X, and at the platform, its error rates can be found.

## 4.2 Controlled Quantum Teleportation

### 4.2.1 Simulated Implementation - Qiskit Simulators

We are going now to characterize CQT and its optimal number of shots. For the following plot, we have chosen the GHZ-state as a channel with permission of the controller. We can observe a similar behavior in the curve, then we have selected again for each experiments at least  $n_s = 2048$  for the QST that will return us the outcome state.

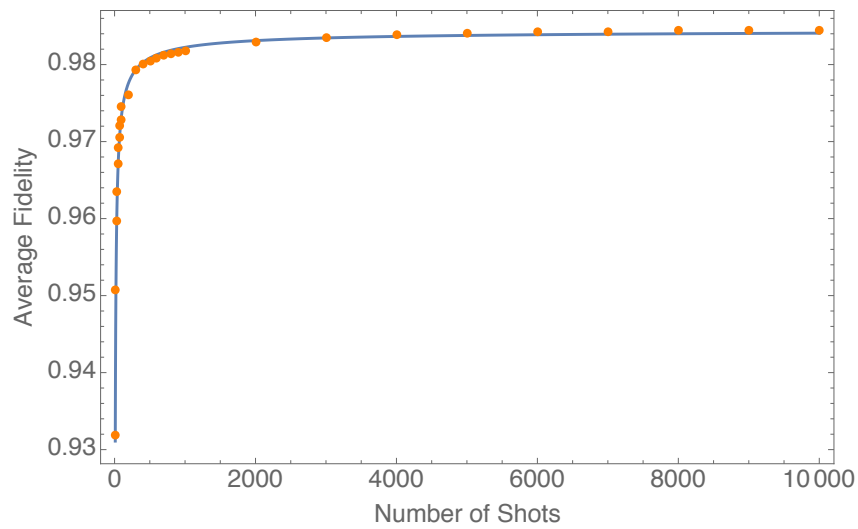


Figure 4.13: Average Fidelity of CQT protocol dependence on the number of shots, the  $|GHZ\rangle$  is considered.

We also produce for this scenario, rotations around the  $x$ -axis, but we have included scenarios where we applied noisy sources in different stages at once, in order to explore what happens when there is more than one contribution to the decoherence.

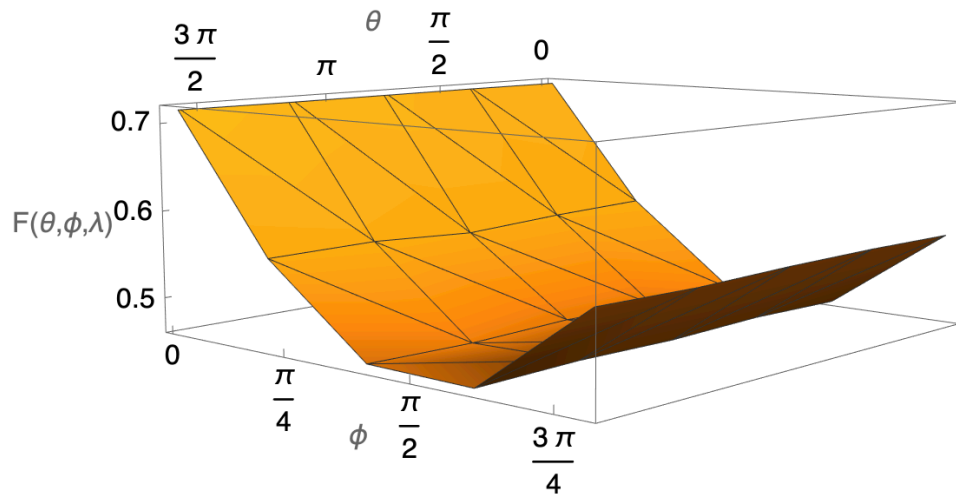


Figure 4.14: Conditioned average fidelity as a function of  $U(\theta, \phi)$  operator dependence.

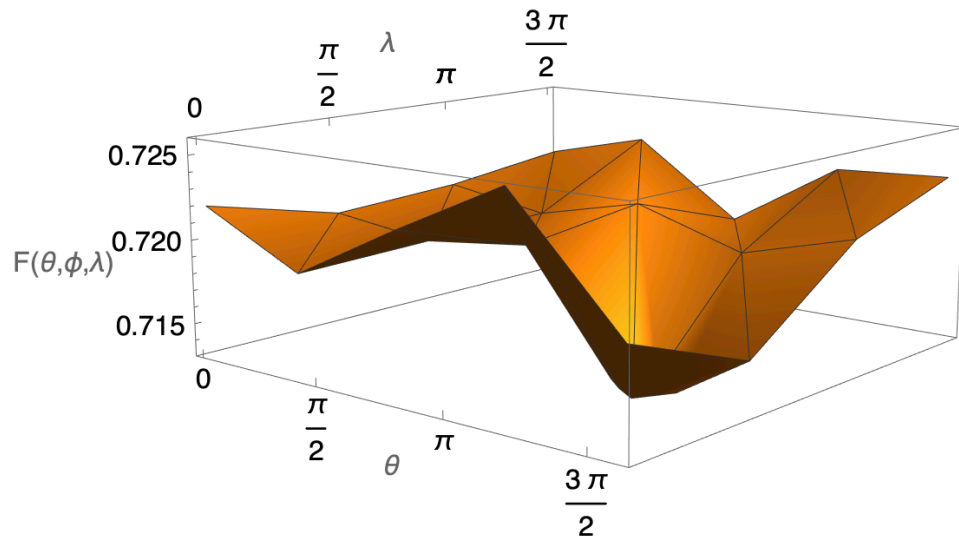


Figure 4.15: Conditioned average fidelity as a function of  $U(\theta, \lambda)$  operator dependence.

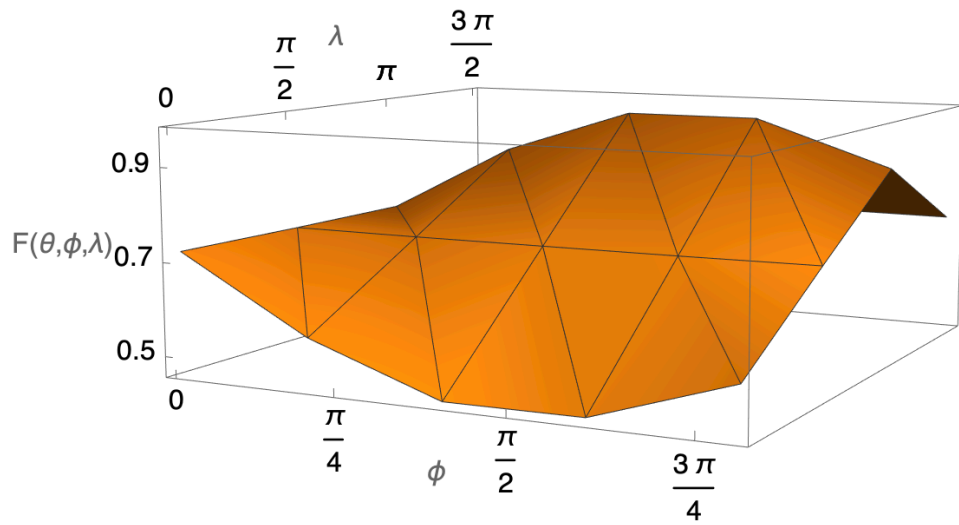


Figure 4.16: Conditioned average fidelity as a function of  $U(\phi, \lambda)$  operator dependence.

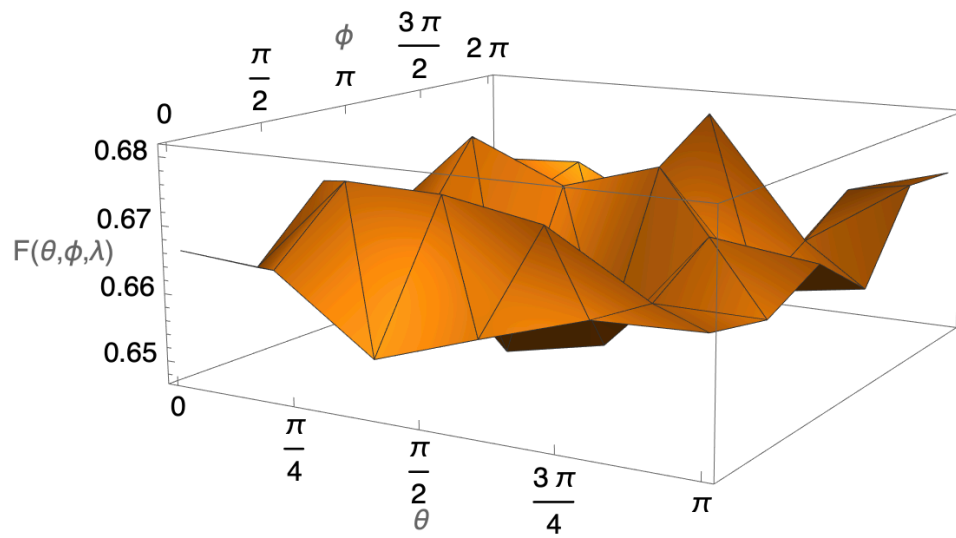


Figure 4.17: Non-Conditioned average fidelity as a function of  $U(\theta, \phi)$  operator dependence.

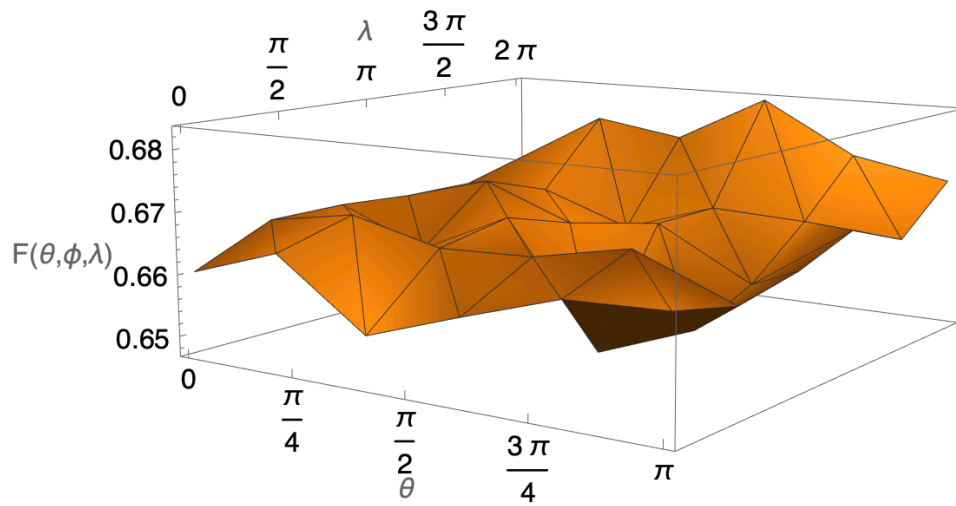


Figure 4.18: Non-Conditioned average fidelity as a function of  $U(\theta, \lambda)$  operator dependence.

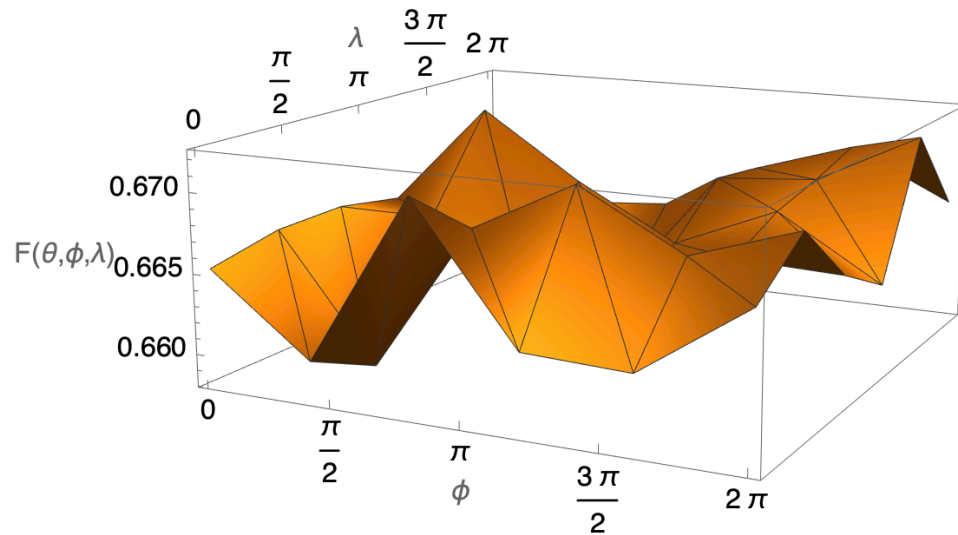


Figure 4.19: Non-Conditioned average fidelity as a function of  $U(\phi, \lambda)$  operator dependence.

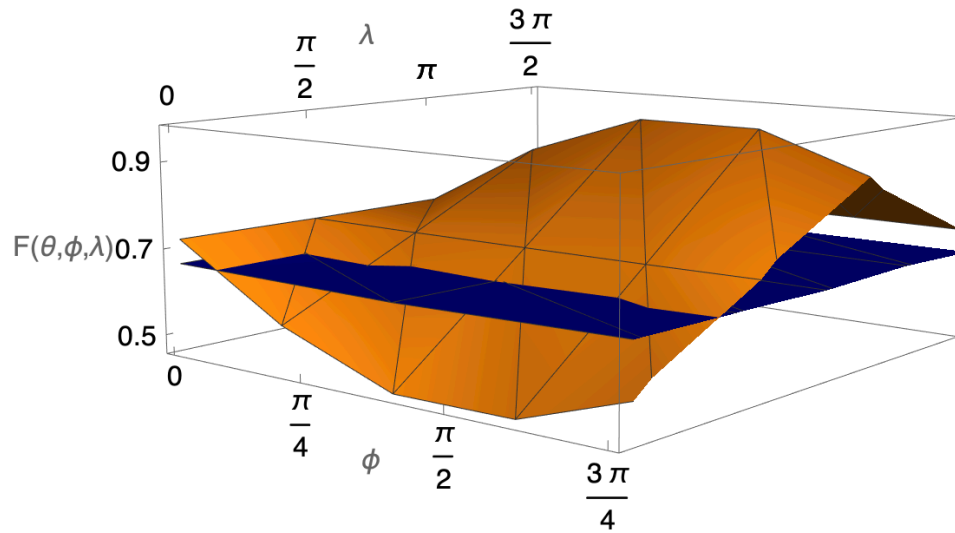


Figure 4.20: Overlap between the regions where the control power works with  $U(\phi, \lambda)$  operator dependence.

Finally, we can see at figure 4.20 perfect regions, where the control power works very good, given that the conditioned fidelity exceeds the classical limits, achieving the maximal fidelity value, and the non conditioned fidelity, induced by Charlie non-sharing result, never exceeds the classical limits  $2/3$ .

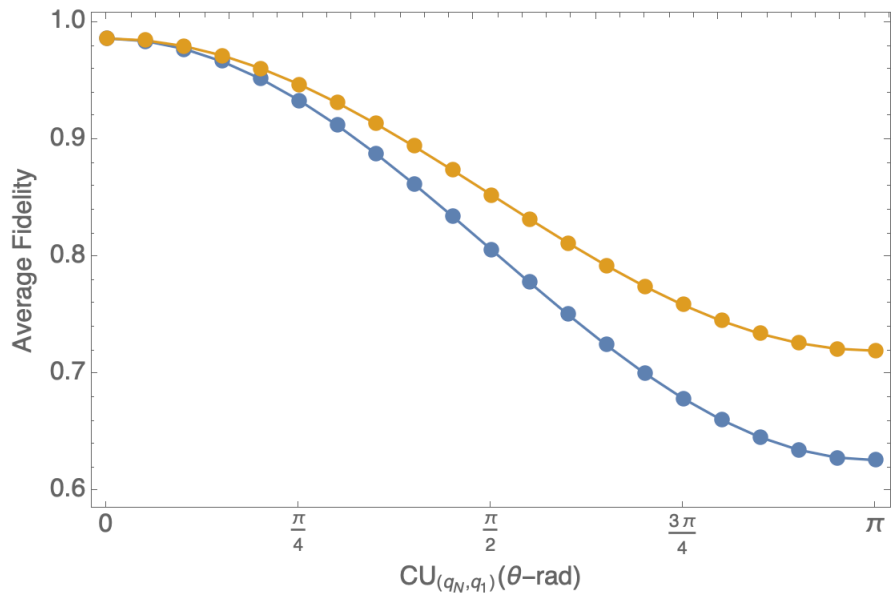


Figure 4.21: Dependence of  $F_{avg}$  when a noisy source is inserted in the  $Alice_0$  qubit. Blue-curve when a noise is inserted after the stage 1, orange-curve when a noisy is inserted after the stage 2 and 3.

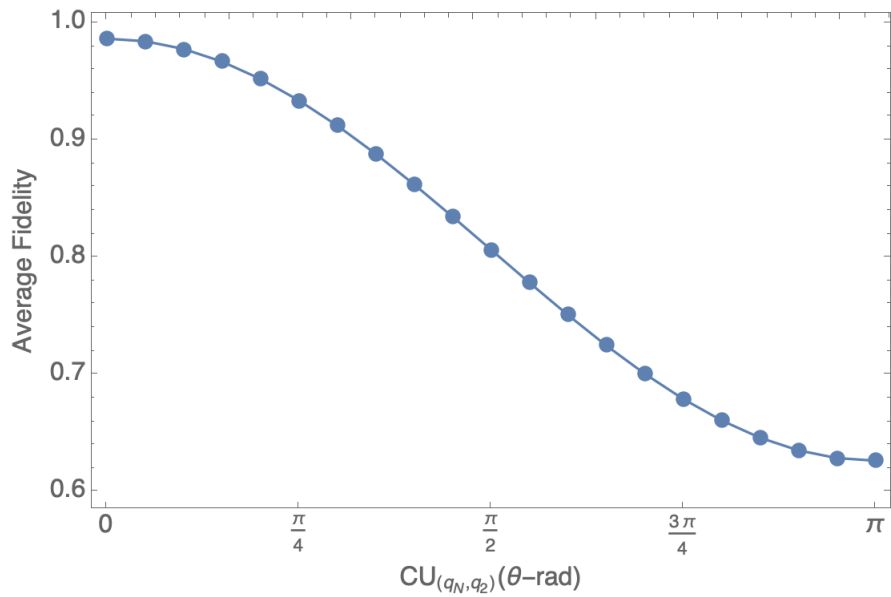


Figure 4.22: Dependence of  $F_{avg}$  when a noisy source is inserted in the  $Alice_1$  and  $Bob_0$  qubits. Blue-curve when a noise is inserted after the stages 1, 2 and 3.

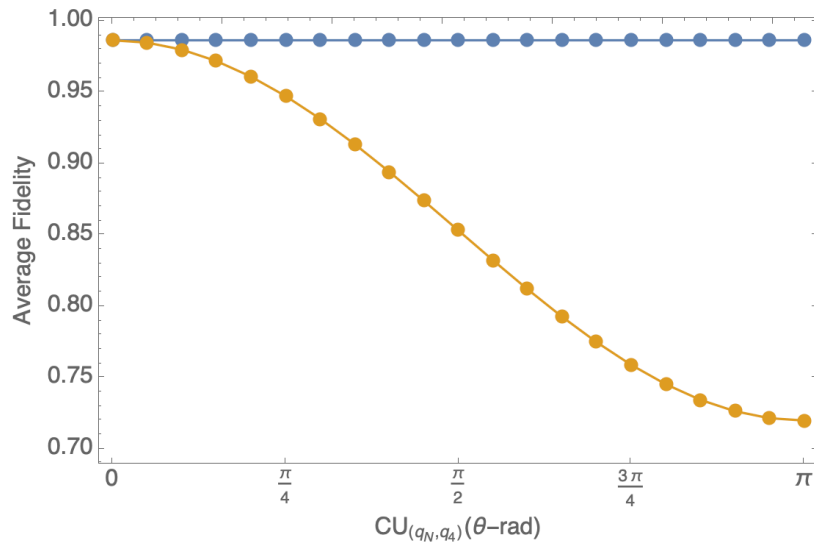


Figure 4.23: Dependence of  $F_{avg}$  when a noisy source is inserted in the  $Charlie_0$  qubit. Blue-curve when a noise is inserted after the stages 1, 2 and orange-curve after the stage 3.

#### 4.2.2 Experimental Implementation - IBM's Quantum Devices

With previous results about the optimal number of shots and the region where controlled quantum teleportation is indeed conditioned, we are going to test the temporal causality. We are always taking for granted that Charlie will share his information of its local measurements on his party.

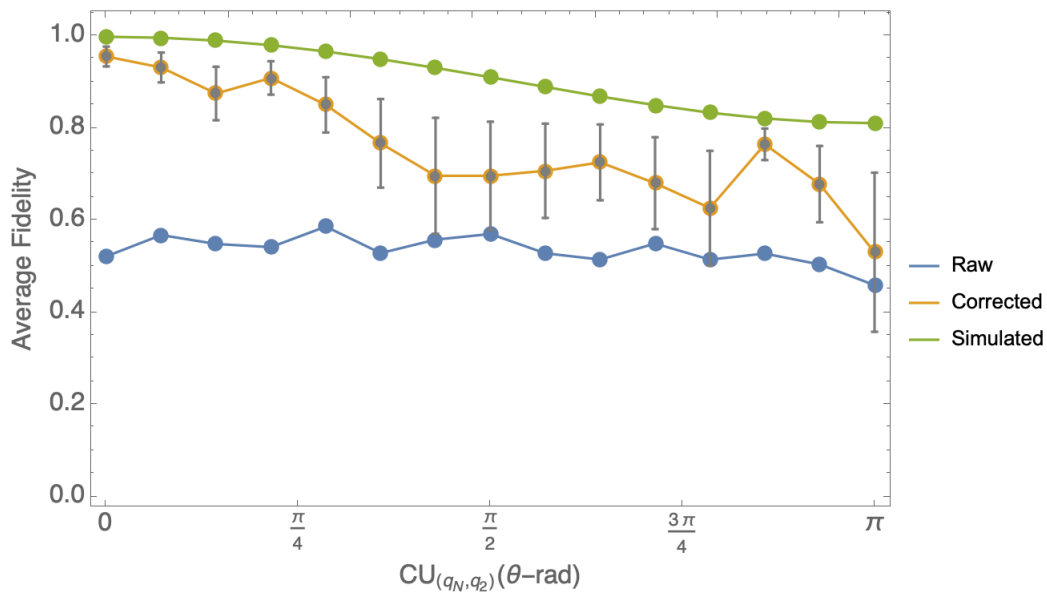


Figure 4.24: CQT - Temporal Causality of noisy source when is inserted in  $Alice_0$  qubit - stage 1.

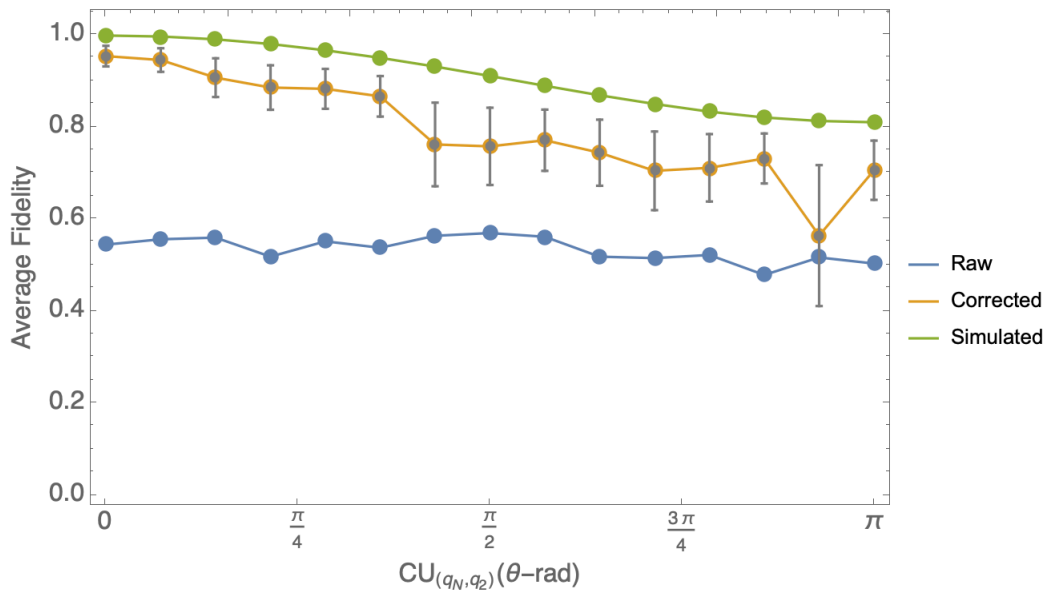


Figure 4.25: CQT - Temporal Causality of noisy source is inserted in  $Alice_1$  qubit - stage 2.

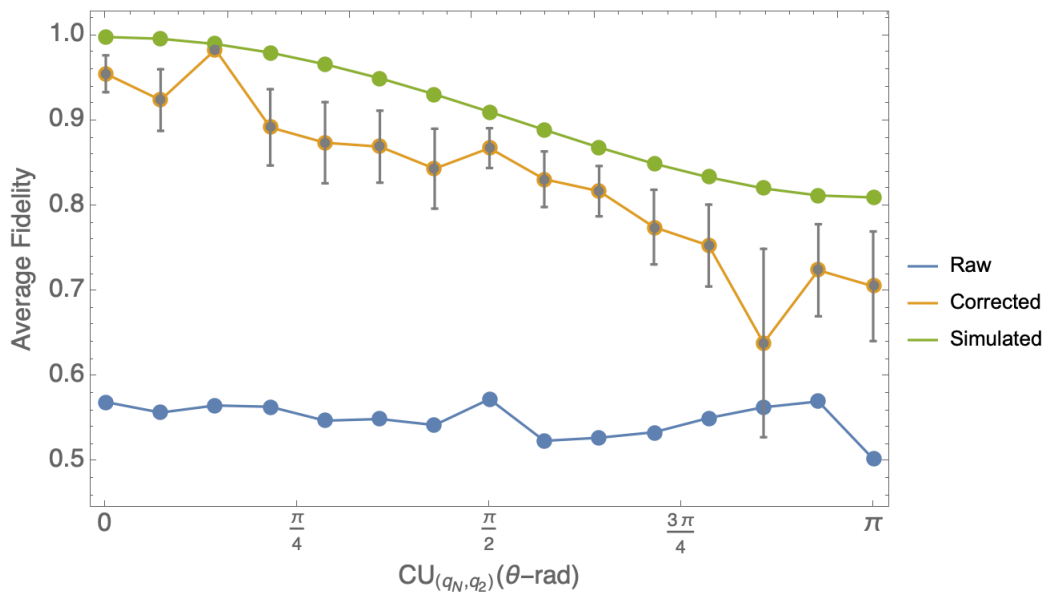


Figure 4.26: CQT - Temporal Causality of noisy source is inserted in  $Charlie_0$  and  $Bob_0$  qubits - stage 3.

We have only placed these three scenarios, which actually are pretty similar between all of them, and this could be given that three-partite quantum states creation could be noisier, and for example, we can not observe the differences in the fidelity curves produces by temporal affection of noisy sources.

Again, to obtain this data, we have tested our circuit using many public devices, but this particular data comes

from the `ibmq_manilla` quantum processor, which is a quantum device with 5-qubits, quantum volume=32, and its architecture is horizontal. As `ibmq_quito` and other public devices, it possesses maximum number of shots equal to 20000 and maximum of circuit execution equal to 100 circuits per execution.



Figure 4.27: `ibmq_manilla` device's architecture. Adapted from<sup>15</sup>.

The figure 4.27, has been taken from the IBM quantum experience platform, showing the architecture of the device which is known as Falcon r5.11L. Additionally, its coherence times can be seen in the following Table 4.2, where as for the case of `quito` device, we present the relaxation time  $T_1$  and the dephasing time  $T_2$  for each qubit, provided by IBM in the quantum experience platform, where the information about any device can be found at real time.

	$T_1(\mu\text{s})$	$T_2(\mu\text{s})$
Q0	212.27	105.22
Q1	189.26	70.98
Q2	163.81	25.04
Q3	128.2	50.59
Q4	83.25	32.44

Table 4.2: Coherence times ( $T_1$ - $T_2$ ) of `ibmq_manilla` quantum processor provided by Quantum Experience platform.

The Quantum experience platform shows the qualities of the device, for example, the error rates for each basis gates (CX, ID, RZ, SX, X), for this purpose, and as it is constantly being updated due to calibration, it is important to check the data before executions.

## Chapter 5

# Conclusions & Outlook

Quantum teleportation, even in its simplest scenarios as the standard quantum teleportation, hides unknown behaviors of the universe we are living in. However, we still lack a complete understanding of it, when the questions go even deeper, including more basic ingredients in its universal description, where such a task could actually demand a full understanding of quantum mechanics and possibly its relation with space-time. In this thesis, we have observed by using very simple models, how the interconnection of the system with its environments can break the quantum advantage provided by quantum entanglement, pushing the system to a classical description of physics and information theory. In addition, we have explored the usefulness of the research of a higher number of parties, given that the addition of more subsystems could lead to extra behaviors, which are mandatory to be understood if these kind of systems are pretended to be of common use of the public.

Additionally, we have successfully tested the universality of Qiskit simulating quantum mechanics. The huge advantage that it provides for research focused on quantum computation and by consequence for this thesis is the chance to study any implementation of quantum teleportation prior to its execution on quantum devices. For example, given that the execution on real devices can take long time, which is the case for the computation of average fidelity. Now, having a principal idea of how the system will behave based on simulations, could be very relevant in producing optimal executions on Quantum Computer (QC).

Considering the purpose of this research thesis, we have successfully proved how the temporal causality works in each teleportation scenario, and that the information shared by the real system could be spread into its environment, by simply applying an extra qubit noisy source, which produces decoherence. In each scenario, the teleportation produces a different curve of fidelity due to rotations of this extra party. It has been shown very well using the "QASM" simulator, but also doing executions on IBM's processors. This constitutes real evidence of this behavior that has not been clear at all, until now.

We have also incorporated advanced error correction schemes, in order to minimize different kinds of errors, caused by the measurement device, state preparation, and individual quantum gates. The process of generalizing error mitigation has been developed and successfully utilized to correct the data with a high level of noise. This has helped us to observe quantum behavior even on real quantum devices.

Regarding quantum computation, it seems there is still a big gap from a research point of view of quantum computers, and the purpose targets that are public quantum computers. The experimental realization that could exhibit quantum behaviors has been highly explored since the first days of quantum mechanics, and nowadays there is a lot of investment in public and private research centers, that work towards materializing the dream of perfect Quantum Computers.



# Bibliography

- [1] Nielsen, M. A.; Chuang, I. Quantum computation and quantum information. 2002.
- [2] Bennett, C. H.; Brassard, G.; Crépeau, C.; Jozsa, R.; Peres, A.; Wootters, W. K. Teleporting an unknown quantum state via dual classical and Einstein-Podolsky-Rosen channels. *Physical review letters* **1993**, *70*, 1895.
- [3] Hofmann, H. F. Causality in quantum teleportation: Information extraction and noise effects in entanglement distribution. *Physical Review A* **2002**, *66*, 032317.
- [4] Terhal, B. M. Bell inequalities and the separability criterion. *Physics Letters A* **2000**, *271*, 319–326.
- [5] Bell, J. S. On the einstein podolsky rosen paradox. *Physics Physique Fizika* **1964**, *1*, 195.
- [6] Einstein, A.; Podolsky, B.; Rosen, N. Can quantum-mechanical description of physical reality be considered complete? *Physical review* **1935**, *47*, 777.
- [7] Huang, Y.; Duan, X.; Cui, Y.; Lauthon, L. J.; Kim, K.-H.; Lieber, C. M. Logic gates and computation from assembled nanowire building blocks. *Science* **2001**, *294*, 1313–1317.
- [8] Khaing, S.; Nopparatjamjomras, S.; Nopparatjamjomras, T.; Chitaree, R. Development of Arduino-based logic gate training kit. 2018.
- [9] Arrazola, J. M.; Bergholm, V.; Brádler, K.; Bromley, T. R.; Collins, M. J.; Dhand, I.; Fumagalli, A.; Gerrits, T.; Goussev, A.; Helt, L. G. Quantum circuits with many photons on a programmable nanophotonic chip. *Nature* **2021**, *591*, 54–60.
- [10] Haroche, S.; Brune, M.; Raimond, J. From cavity to circuit quantum electrodynamics. *Nature Physics* **2020**, *16*, 243–246.
- [11] Blakestad, R.; Ospelkaus, C.; VanDevender, A.; Wesenberg, J.; Biercuk, M.; Leibfried, D.; Wineland, D. Near-ground-state transport of trapped-ion qubits through a multidimensional array. *Physical Review A* **2011**, *84*, 032314.
- [12] Laflamme, R.; Knill, E.; Cory, D. G.; Fortunato, E. M.; Havel, T. F.; Miquel, C.; Martinez, R.; Negrevergne, C.; Ortiz, G.; Pravia, M. A.; Sharf, Y.; Sinha, S.; Somma, R. D.; Viola, L. Introduction to NMR Quantum Information Processing. *arXiv: Quantum Physics* **2006**,
- [13] Josephson, B. D. Possible new effects in superconductive tunnelling. *Physics letters* **1962**, *1*, 251–253.
- [14] Devoret, M. H.; Wallraff, A.; Martinis, J. M. Superconducting qubits: A short review. *arXiv preprint cond-mat/0411174* **2004**,

- 
- [15] Abbas, A. *et al.* Learn Quantum Computation Using Qiskit. 2020; <http://community.qiskit.org/textbook>.
- [16] Koch, J.; Terri, M. Y.; Gambetta, J.; Houck, A. A.; Schuster, D. I.; Majer, J.; Blais, A.; Devoret, M. H.; Girvin, S. M.; Schoelkopf, R. J. Charge-insensitive qubit design derived from the Cooper pair box. *Physical Review A* **2007**, *76*, 042319.
- [17] Karlsson, A.; Bourennane, M. Quantum teleportation using three-particle entanglement. *Physical Review A* **1998**, *58*, 4394.
- [18] Barasiński, A.; Svozilík, J. Controlled teleportation of qubit states: Relation between teleportation faithfulness, controller's authority, and tripartite entanglement. *Physical Review A* **2019**, *99*, 012306.
- [19] Laforest, M.; Baugh, J.; Laflamme, R. Time-reversal formalism applied to maximal bipartite entanglement: Theoretical and experimental exploration. *Physical Review A* **2006**, *73*, 032323.
- [20] Coecke, B. *Horizons of the Mind. A Tribute to Prakash Panangaden*; Springer, 2014; pp 250–267.
- [21] Kiktenko, E.; Korotaev, S. Causality in quantum teleportation. **2013**,
- [22] Schmied, R. Quantum state tomography of a single qubit: comparison of methods. *Journal of Modern Optics* **2016**, *63*, 1744–1758.
- [23] Jattana, M. S.; Jin, F.; De Raedt, H.; Michielsen, K. General error mitigation for quantum circuits. *Quantum Information Processing* **2020**, *19*, 1–17.
- [24] Bouwmeester, D.; Pan, J.-W.; Mattle, K.; Eibl, M.; Weinfurter, H.; Zeilinger, A. Experimental quantum teleportation. *Nature* **1997**, *390*, 575.

# Abbreviations

**AVF** Average Fidelity of States 27, 55

**BS** Bloch Sphere 5, 6, 24, 36, 38, 46

**BSM** Bell State Measurement 24–26, 36, 37, 39, 56

**CQT** controlled quantum teleportation iii, 25, 33, 46, 55, 62

**DMP** Deferred Measurement Principle 25, 37

**EPR** Einstein-Podolsky-Rosen 24, 36

**GHZ** Greenberger-Horne-Zeilinger 25, 26, 29, 44, 62

**JJ** Josephson Junction 18, 19, 21, 23

**MEM** Measurement Error Mitigation iii, 51, 54, 58

**QC** Quantum Computer 22, 25, 71

**QHO** Quantum Harmonic Oscillator 21

**QST** Quantum State Tomography 49, 51, 55, 62

**SQT** Standard Quantum Teleportation iii, 23, 25, 26, 33, 35, 37, 38, 42, 55

**Transmon** Transmission line shunted plasma oscillation 21, 22